HYDROTHERMAL LIQUEFACTION OF WILD-HARVESTED CYANOBACTERIAL BLOOM FROM HYPEREUTROPHIC LAKE TAINTER, WISCONSIN

BY

MEGAN SWOBODA

THESIS

Submitted in partial fulfillment of the requirements
for the degree of Master of Science in Agricultural and Biological Engineering
in the Graduate College of the
University of Illinois at Urbana-Champaign, 2018

Urbana, Illinois

Master's Committee:

Professor Yuanhui Zhang, Chair
Assistant Professor Paul Davidson
Clinical Assistant Professor Neslihan Akdeniz

ABSTRACT

This study demonstrates the potential of Harmful Algae Blooms (HABs) as a feedstock for generating biofuels hydrothermal liquefaction (HTL) and asserts that HTL is a uniquely practical technology for use of this biohazardous material. Using a wild-harvested cyanobacteria HAB from Lake Tainter, Wisconsin as a low-cost feedstock for HTL, the projected Minimum Fuel Selling Price of reformed biocrude produced from the Lake Tainter HAB is 18-29% lower than biocrude produced from cultivated algae. The biocrude produced is of sufficient yield and quality to realize a net energy profit making HTL an important environmental remediation strategy for air and water quality.

HTL reactions were conducted over a range of reaction temperatures (280-350°C), holding times (30-60 min), and feedstock total biomass solids content (10%-25%TS) using fresh and aged biomass. Bulk biocrude properties (e.g., yield, elemental analysis, high heating value (HHV)), energy balances, and nutrient recovery in the products were compared from each condition.

Using HTL, at 340°C and 50 min retention time with 20%TS, 41.8±6.1% daf biocrude yield is possible with this feedstock. The biocrude produced has an HHV of 32.5 MJ/kg, recovering 73.9% of the energy in the biomass and 1:3.3 ratio for energy input for heating to energy recoverable in the crude. Promisingly, this biocrude has a low sulfur content (0.07% wt.) and 60% wt. of the crude is in the light and medium molecular weight fractions (volatile<350ºC). However, high nitrogen (5.93% wt.) and oxygen (16.74% wt. by calc.) contents, and probable acidic nature of the biocrude indicate upgrading is needed pre-refinery. At this temperature, 47% of the nitrogen in the feedstock is recoverable in the post-hydrothermal processing wastewater (HPW), with 55.8% of it as ammoniacal nitrogen.

ACKNOWLEDGEMENTS

Firstly, I would like to thank my benefactors, the JBT Wright Fellowship, without their generous support I would not be able to be a part of this research group.

My heartfelt thanks are extended to Dr. Yuanhui Zhang, for his advice and patient direction, for the example he sets as a leader, and for the decades of hard work he and his teams have put into this research. Thank you for making it possible for me to study this. There is no greater gift anyone could have given me, but to let me explore this solution to our sick lakes. I am very grateful to be part of your team.

Thank you Wan-Ting (Grace) Chen, Peng Zhang, Aersi Aierzhati, Steve Ford, Buchun Si, Chi-Ting Kuo, Libin Yang, Rowie Carpio, and Michael Stablein, members of the Environment-Enhancing Energy Group. Your expertise is much appreciated. Thank you for being so open and welcoming.

Thank you to Lance Schideman and Joseph Pickowitz for the experience with the pilot scale reactor. It has changed my perspective on this project and colors the way I think about every part of this process.

Thank you to the good people of Menomonie for the schooling I had growing up, for your diligent efforts to monitor and clean the lake, and for the enthusiastic support I have received in this project.

Access to the equipment at UIUC Materials Research Lab (MRL) was imperative to my work. The MRL Shared Experimental Facilities are supported by the MRSEC Program of the NSF under Award No. DMR 1720256; a member of the NSF-funded Materials Research Facilities Network

To my parents, Montgomery and Lucinda Morse, husband, Lucas Swoboda, and the rest of my enthusiastically supportive family.

TABLE OF CONTENTS

TABLE OF ABBREVIATIONS

Acronym	Definition
AD	Aged Dried
ADF	Acid Detergent Fiber
AW	Aged Wet
CC	Cyclic Hydrocarbons
CCL	Ceiling Concentration Limit
CHN	Carbon, Hydrogen, and Nitrogen (% mass)
daf	dry, ash free
DCM	Dichloromethane
DOE	U.S. Department of Energy
ECR	Energy Consumption Ratio
ER	Energy Recovery
FD	Fresh Dried
FW	Fresh Wet
GC-MS	Gas Chromatography-Mass Spectrometry
GHG	Greenhouse Gas
HAB	Harmful Algae Bloom
HC	Linear or Branching Hydrocarbons
HHV	High Heating Value
HR	Heat Recovery
HT	Holding Time
HTL	Hydrothermal Liquefaction
ICP	Inductively Coupled Plasma
LSD	Least Squares Difference
LT916	Lake Tainter Algae collected September 2016
LT917	Lake Tainter Algae collected September 2017
MFSP	Minimum Fuel Selling Price
MC	Microcystin
MWL	Midwest Laboratories
NC	Nitrogen, Heterocyclic
NDF	Neutral Detergent Fiber

Acronym	Definition
NX	Nitrogenous Compounds
OC	Oxygen, Heterocyclic
OX	Oxygenates
PCL	Pollution Concentration Limit
PHE	Phenols
PO	Phosphorus containing compounds
HPW	Post-Hydrothermal Waste Water
PNNL	Pacific Northwest National Laboratory
RT	Reaction Temperature
SCS	School of Chemical Sciences laboratory
TEA	Technoeconomic Assessment
TGA	Thermogravimetric Analysis
TN	Total Nitrogen
UIUC	University of Illinois-Urbana Champaign
TS	Total Solids in (d.b.)

CHAPTER 1: INTRODUCTION

1.1. Background and Challenges

Like many lakes around the world, Lake Tainter in Menomonie, WI is in poor condition, hyper-eutrophic and hyper-hypoxic. The lake is man-made, a wild rice stand that was flooded in the 1800's to move timber. The lakes are shallow, slow-moving, bottom draining, and eutrophic, all conditions leading to algae growth. The algae blooms turn the lakes to pea soup in the summer. The lakes are hyper-hypoxic and labeled as impaired waterways. Some residents even leave their homes part of the year or sequester themselves inside due to illnesses and reactions to the strong odor from the lake (Gaumnitz, 2010). Despite considerable community effort to curb anthropomorphic nutrient sources, the nitrogen and phosphorus levels in the lakes remain hypertrophic, as shown in Figure 1, partially due to phosphorus laden rock and sediment in the watershed (TMLIA, 2016; TMLIA, WI DNR, & UW extension, 2013). Further, in recent decades, the anoxic conditions and abundant nutrient inflow have encouraged the growth of a toxic cyanobacteria (Lyon, 2004). The bloom is no longer just a noxious nuisance, the toxins produced by the bloom cause skin rashes, sicknesses, and pet deaths (Lyon, 2018; WQOW, 2016). The lake needs an immediate mitigation and radical shift to be healthy.

Removing the bloom from the lakes could help curb the problem, if done on a large enough scale (Guo et al., 2015). Harmful Algal Blooms (HABs) grow exponentially; harvesting the population regularly can keep the microalgae population from entering the explosive growth range of a population curve. Additionally, removing the bloom helps condition the water to support a heathier ecosystem. If left to grow in the water, the HAB grows to maximum capacity and dies,

decaying on the lake bed, absorbing oxygen from the water, releasing the cyanotoxins and nutrients back into the lake (WHO, 2003).

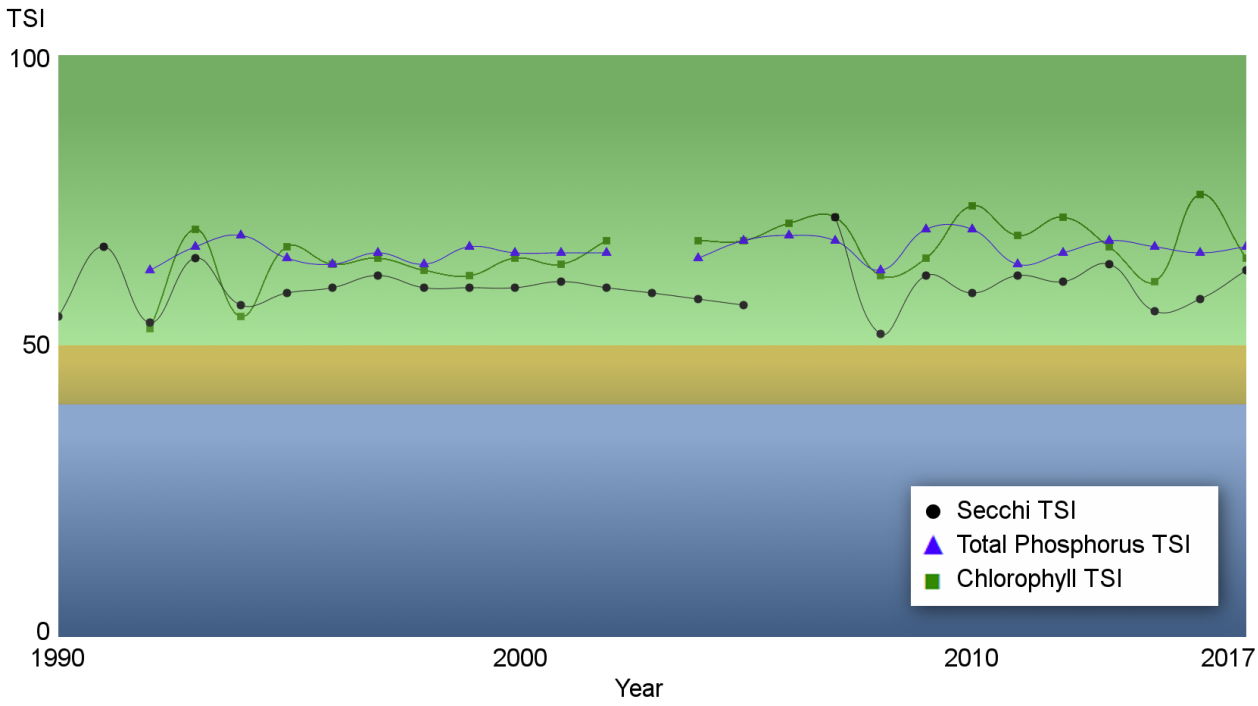

Figure 1: The Trophic State Index (TSI) for Middle Basin (Site 2) of Tainter Lake over the years 1991-2017. Despite community efforts to change the nutrient loading in the lake, there are hypereutrophic levels in the lake with little improvement over time,. Chart modified from WI DNR (2018).

There are some considerations in removing the bloom. The HAB has limited utility and is a danger ecologically if released to the environment with the cyanotoxins untreated (EPA, 2014; Tian et al., 2015; WHO, 2003). HTL is a thermochemical conversion technique with unique advantages for this feedstock which is a wet, low-lipid, toxic biomass. For wet feedstocks, 70% water or more by weight, HTL is energetically more favorable than other processes that require drying the biomass (Changi, Faeth, Mo, & Savage, 2015). HTL converts proteins, a major component of this biomass, as well as carbohydrates and lipids, into fuel (Biller & Ross, 2011;

Elliott et al., 2013). Perhaps most paramount to this feedstock, the extreme conditions of the reaction are severe enough to destroy the cyanotoxins (WHO, 2003).

Currently, the price of HTL derived biocrude is not cost competitive with harvesting petroleum crude resources. Wild-harvesting a bloom instead of raising algae, would produce a substantial cost savings, by reducing the costs associated with feedstock acquisition (Barlow, Sims, & Quinn, 2016; Patel, Tamburic, Zemichael, Dechatiwongse, & Hellgardt, 2012).

Using the biocrude from HTL of an HAB, as a fuel source, could have other positive environmental impacts beyond lake health. Replacing petroleum derived fuel sources with biocrude from algae could remove carbon and nitrogen from the air. Microalgae have high photosynthetic efficiencies and act as an atmospheric carbon and nitrogen sink (Biller & Ross, 2011; Singh & Ahluwalia, 2013). Not all the carbon or nitrogen in the feedstock is transmitted to the combustible product, biocrude (Yu, Zhang, Schideman, Funk, & Wang, 2011), so the net effect is carbon sequestration. HTL may also prevent greenhouse gas (GHG) production by coupling it with other renewable energy sources, as a scalable energy storage mechanism. This offers a solution to difficulties with intermittent supply from wind and solar installations and could encourage more widespread use of these low GHG technologies. Many studies have shown a net positive energy return is possible with HTL (Biller & Ross, 2011; Elliott, Biller, Ross, Schmidt, & Jones, 2015), something traditional batteries are not able to boast, the energy density of biocrude is higher than our most sophisticated batteries, and the energy stored in the fuel is ready on demand.

1.2. Thesis Project

The purpose of this investigation was to apply HTL to the Harmful Algal Blooms from Lake Tainter, to demonstrate HTL's effectiveness with this feedstock and determine if using this is

a suitable feedstock to improve HTL process economics. Many studies of HTL of microalgae show promising results, but the yield and quality of biocrude produced varies widely from species to species. Demonstration is needed to evaluate the bloom as an HTL feedstock. Different biochemical compositions and different cell structures in microalgae have different optimal HTL conditions. The wild-harvested bloom was subjected to a spectrum of operating conditions, described later, to determine trends in product mass distribution and the operating conditions that maximize biocrude yield. The viability of the feedstock was determined using the economic sensitivity analysis of a combination HTL and upgrading plant in the Pacific Northwest National Laboratory (PNNL) document distributed by the U.S. Department of Energy (DOE), "Process Design and Economics for the Conversion of Algal Biomass to Hydrocarbons: Whole Algae Hydrothermal Liquefaction and Upgrading" (Jones et al., 2014).

The effect of aging on the feedstock was considered because of the seasonality of dense algae blooms. An HTL plant sized to meet the daily supply of feedstock during the peak of the bloom, would need supplemental feeds in the winter months. Drying and storing algae for the winter months is an energy intensive operation. A small processor could eventually work its way through stored harvested blooms and which could prove to be more energy effective if the yield or quality of the biocrude is comparable. The aged feedstock was subjected to the same HTL conditions as the fresh feedstock and the same analyses were used to compare yield and quality of the products.

Using the information from these experiments, an expectation for biocrude quality and yield were determined. Once the conditions for maximum biocrude yield were determined for each feedstock, the products from those runs were further characterized by GC-MS to determine

major compounds in them. The biocrude was also measured by thermogravimetric analysis (TGA) as another indication of quality.

1.3. Objectives and Approach

The purpose of this investigation was to apply HTL to a fast-growing, wild-harvested bloom, from Lake Tainter, to demonstrate HTL's capability with this feedstock and determine whether it would be a profitable feedstock to use. The specific objectives of this study are as following:

1. Product distribution from HTL of the Lake Tainter Bloom including yield and CHN distribution at different operating conditions.
2. Determine the operating conditions for maximum biocrude yield and quality of the biocrude under those conditions.
3. Determine the effect of aging the feedstock on HTL products.
4. Use the results of these studies to estimate the Minimum Fuel Selling Price (MFSP) of biocrude produced from Lake Tainter.

The three most critical operating parameters were varied to determine the effect of operating conditions on HTL products from the Lake Tainter HAB: the mass percentage of algal biomass in the feedstock slurry (%TS), reaction temperature (RT), and reaction holding time (HT) (Jena, Das, & Kastner, 2011; Jones et al., 2014). The effect of %TS was investigated at RT=300°C and HT=60 min, optimum conditions suggested for near-complete decomposition of wastewater algae in Chen (2013). The biocrude yield at this HT has been also been shown to have

fairly consistent yields for RTs 250-400°C (Valdez, Nelson, Wang, Lin, & Savage, 2012). A feedstock slurry of 20%TS was used for the remaining experiments. This %TS strikes a balance between dewatering costs and capital costs for the HTL system (Jones et al., 2014). A feedstock slurry of 20%TS maintains a high energy return and yet allows for complete mixing of the dried biomass with water in the reactor. This value is also typical for many papers, allowing for easy comparison with other types of algae in the literature. Product yields were measured as RT was increased from 280°C to 350°C, while %TS and reaction HT were held constant. A reaction holding time of 50 min was selected based on the findings of Guo et al. (2015). This temperature range begins below the temperature at which MCs are destroyed (300°C), spans the HTL spectrum, and includes temperatures on both sides of the peak temperature for yield. The effect of HT was observed using the peak temperature for biocrude yield determined previously (RT=340°C).

The products from each operating condition were measured for yield and characterized. The biocrude composition was measured using elemental analysis (CHN) to estimate the quality of the fuel. Nutrient recovery in the aqueous and solid products was determined using HACH test n' tube kits and elemental analysis, respectively. The chemical composition of the liquid products from the conditions producing the best biocrude yield were characterized further using GC-MS and the biocrude was also analyzed for sulfur content and mass percentage of fuel fractions as further indications of quality.

As an appraisal of the Lake Tainter HAB as an HTL feedstock, the production characteristics were compared against the base case scenario in the Jones et al. Technoeconomic assessment (TEA) to determine the MFSP for an HTL plant using these wild-harvested blooms. The techniques described above were used to define the yield and characteristics of the biocrude

produced. An estimate for capacity of the plant was based on an estimate of the amount of biomass recoverable from the lake.

CHAPTER 2: LITERATURE REVIEW

2.1. Harmful Algal Blooms as a Feedstock

The harmful algae blooms (HABs) in Lake Tainter are not an isolated problem. HABs are occurring at an increasing rate due to the declining health of freshwater lakes and streams (Gągała & Mankiewicz-Boczek, 2012; Lone, Koiri, & Bhide, 2015). Worldwide, lakes and rivers are trapped in a cycle of deterioration that encourage toxic blue-green algae blooms and drive out the other aquatic life. Removing blooms from the water would remediate the hypoxia and eutrophication of these waterways. The nutrients that were taken up by the harvested bloom are captured and not available to cause further eutrophication problems downstream (Guo et al., 2015). The bloom would not decay in the water, remediating the oxygen depletion associated with their decay. However, if the bloom is not properly handled, the release of odors and contamination of drinking water could prove to be an environmental problem (Tian et al., 2015). The biomass that would be collected from an HAB has limited utility and it is not a great feedstock for traditional biofuels. Another approach, HTL, is investigated in this paper as a technology that can help us take advantage of this plentiful biomass.

High levels of persistent cyanotoxins in the biomass complicate disposal or use of the biomass. Microcystins (MCs), just one class of toxin produced by cyanobacteria in the HAB, is found intracellularly and extracellularly. Microcystin-LR (MC-LR) is the most toxic of the MCs (Lone et al., 2015), is the most frequently occurring (Chorus & Bartram, 1999), and is a persistent contaminant. It is very stable in water in a wide range of pH and can withstand temperatures up to 300°C. MC concentrations of almost 2000 μg/g dry biomass and MC-LR concentrations of more than 600 μg/g dry biomass have been reported at numerous locations (WHO, 2003). As a

comparison, the EPA suggests a swimming advisory if the MC-LR level goes above 4 μg/L and little data exist for the risks associated with constant exposure to lower levels or other forms of Microcystin (EPA, 2014). Ninety-five percent of the time, only a small amount of MCs are found extracellularly, but lysis of cyanobacterial cells can lead to high extracellular toxin levels in the water (EPA, 2014; WHO, 2003). If the HAB were harvested, ideally most of the MCs would stay in the biomass. Spreading that biomass on a field would release the MCs contained in it into the food cycle and the water table. MCs are available for uptake into plants. They restrict plant growth and accumulate in roots, leaves, and stalks (Cao, Steinman, Yao, & Xie, 2017; Corbel, Mougin, & Bouaïcha, 2014; Machado, Campos, Vasconcelos, & Freitas, 2017). Drinking water contaminated by MCs can result in toxic injury to the liver, promote tumor growth, and DNA damage leading to cancers(Gągała & Mankiewicz-Boczek, 2012). These toxins can persist for weeks or even years in dark waters, they are chemically stable resisting hydrolysis and oxidation (Chorus & Bartram, 1999; Gągała & Mankiewicz-Boczek, 2012; WHO, 2003). The biomass would have to be treated severely to destroy the persistent cyanotoxins.

Using the wild-harvested blooms as a biofuel can be a great way to use the HAB, but there is only one conversion technique that makes sense. Algal biofuels hold great promise as way to supplement the US energy supply from a plentiful, environmentally friendly source. Replacing fossil fuels with algal bloom-based biofuels could positively impact both air and water quality. Algal bio-fuels are carbon-neutral and algae are able to mitigate more CO_2 per acre than terrestrial feedstocks (Biller & Ross, 2011). Algae can be grown without removing arable land needed for food production and algae have exponential growth rates, doubling in mass every 3.5 hours (Brennan & Owende, 2010). It is not a food crop, so it doesn't drive up food prices (Patel et al., 2012). However, the traditional algae biofuel, biodiesel, requires specialized strains and careful

control of nutrient conditions to produce high-lipid algae. Unfortunately, the low lipid content of an HAB makes it difficult to use HABs as a bio-diesel feedstock. The recalcitrant lignocellulosic portion makes it difficult to use as a fermentable feed for bioethanol or bio-butanol. The tendency of algae to hold water makes it hard to use the bloom for direct combustion. The feedstock can be anaerobically digested, but because of the long time scales and the sheer mass of the feedstock (Yuan et al., 2011), the storage tank capacity needed to clean the growing number of impaired waterways would be prohibitive. However, an energy-dense fuel, biocrude, can be produced from microalgae using hydrothermal liquefaction and valuable agricultural nutrients in the biomass can be recovered as a by-product (Elliott et al., 2013). Not only that, at the right conditions, HTL has a net positive energy balance (Biller & Ross, 2011; Minowa, Yokoyama, Kishimoto, & Okakura, 1995) and energy returns that are on par with conventional biofuels (Elliott et al., 2013). HTL can be used to convert fast-growing, low-lipid algae, like cyanobacteria, to fuel, perhaps opening the way for wild harvest of algal biofuels on an unprecedented scale.

Algae and HTL are a great fit. The algal biomass does not need physical resizing, as other agricultural wastes do, to make a pumpable slurry for continuous flow HTL reactors (Dãrãban, Rosendahl, Pedersen, & Iversen, 2015; Elliott et al., 2013). Since HTL uses water as a catalyst, it is energetically more profitable than drying, whenever the biomass contains more than 30% water (Changi et al., 2015).

Using the HAB may address a problem the algal biofuel community has been facing. The biggest obstacle to widespread HTL adoption is production of fuel at a cost competitive price. In a 2014 analysis by PNNL, costs associated with growing microalgae, harvesting and dewatering the biomass, and optimization of nutrient recycle were identified as critical determiners of fuel price (Jones et al., 2014). Feedstock costs are the single largest determining factor of the price of

biocrude, 80% or more of the MFSP. Of that, fully a third can be attributed to cultivation direct costs (Barlow et al., 2016). Further, construction costs, energy inputs, and nutrient inputs associated with generating algal feedstock can single-handedly determine the net energy ratio of an algal biofuel (Jones et al., 2014; Slade & Bauen, 2013). Cultivation energy inputs (55-65%) can eclipse even the intense energy needs of the HTL processing (32-40%) (Patel et al., 2012). The water use, and the nutrient load for cultivation ponds to grow enough microalgal feedstock to replace the US oil demand, even at 2008 levels, would be a real challenge (Hannon, Gimpel, Tran, Rasala, & Mayfield, 2010). Wild-harvesting algal blooms would address these problems, eliminating the costs and materials needed to raise the biofuel feedstock.

HTL of HABs shows promise as a solution to a multitude of problems: as a bioremediation tool, a method of recovering valuable agricultural nutrients, and a carbon-neutral, renewable, domestic fuel supply that can be integrated into current infrastructure.

2.2. Hydrothermal liquefaction (HTL)

Hydrothermal liquefaction is a method of thermochemical conversion (TCC) of biomass in subcritical water. HTL processing takes place at temperatures of 250°C to 350°C (Changi et al., 2015) or 400°C (Ramirez, Brown, & Rainey, 2015), just below the critical temperature of water. At these temperatures, the properties of water change (Jena et al., 2011), the hydrogen bonding network is disrupted, and small organic molecules become soluble. There is an increase in the number of hydrogen ions in the water, as the temperature of water is increased towards 250°C, cleaving bonds in biomass, catalyzing decomposition reactions. At temperatures greater than 300°C , this effect fades and free radical reactions dominate at critical conditions (Changi et al., 2015). The hydrolysis, depolymerization, and subsequent repolymerization of the biomass in HTL

(Yin, Dolan, Harris, & Tan, 2010) produces a gas phase, a solid phase, and two liquid phases, one that is aqueous and a hydrophobic one, called bio-crude.

Bio-crude is a catch-all term used to describe the non-aqueous liquid portion of HTL products. The biocrude is of special interest because it can be upgraded (Elliott et al., 2013) and used to produce drop-in fuels and other replacements for petroleum products (Biller & Ross, 2011). Like petroleum, it is a very viscous, black tarry substance, a mixture of hydrocarbon compounds. The exact composition of this material can vary widely, depending on the feedstock and process used to produce it (Ramirez et al., 2015). The promise of algal biofuels can be fully realized more quickly and at less capital cost if the bio-crude produced can be integrated into the current petroleum refinery infrastructure (Hoffmann, Jensen, & Rosendahl, 2016; C. U. Jensen, Hoffmann, & Rosendahl, 2016). Therefore, characterizations of HTL biocrudes mimic the characterizations of petroleum crude, as discussed in section 2.2.2.

The aqueous phase, post-hydrothermal processing wastewater (HPW), contains important agricultural nutrients (N and P) though it also contains other toxic compounds. It is the largest fraction of the products, since the feedstock starts as mostly water. Biomass amplification, achieved by recycling the HPW to grow more algae, is possible at dilutions of up to 29% HPW (Zhang et al., 2016) and the biomass can be amplified more than 10 times in this manner (Zhou, Schideman, Yu, & Zhang, 2013). In other studies, precipitation of phosphate and ammonium from the HPW with magnesium as struvite has been demonstrated as a way of recovering the nutrients from HPW for use as a fertilizer (Shanmugam, Adhikari, & Shakya, 2017).

The gas and solid products are minor products, with low quality energy. By the kinetic model discussed below, solids are unreacted biomass not yet coaxed into decomposing. The gases are decomposed biocrude or organics in the HPW.

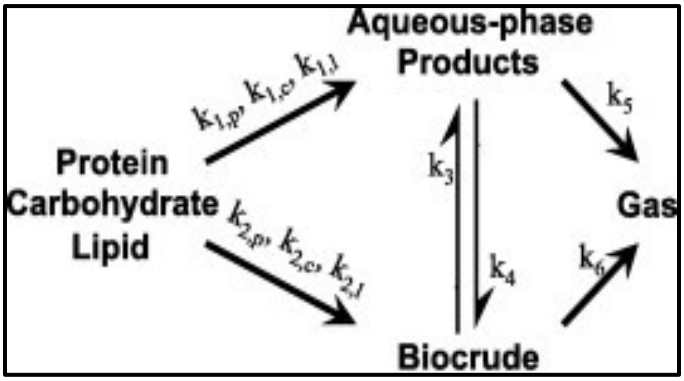

Figure 2: A proposed HTL model where the biomass is solid residue, converted to liquid products, biocrude, HPW, and gases (Valdez et al., 2014).

Predicting the yields from HTL is often done from a biochemical basis. Biller and Ross (2011), used the conversion rates from model lipid, protein, and carbohydrate compounds to formulate a simple predictive model for biocrude yield based on the additive contribution from the mass of each in a feedstock. Valdez, Tocco, and Savage (2014), modified their early kinetic model to include the biochemical distinctions set forth by Biller and Ross (2011) and their model shows better predictive properties for experimental data from three different types of algae. Their model, shown in Figure 2, assumes first order reactions, with temperature-dependent rate constants. According to the model, biocrude and organics in the HPW are formed by decomposition of the solid biomass, mass is exchangeable between the liquid phases, and the liquid phases decompose into gases.

The rate constants from their model, shown on the following pages in Table 1 and in Figure 3(a-c), suggest that the feedstock can be high in lipid or protein content, but high carbohydrate

feedstocks produce the lowest yield for a given reaction time and mass concentration. At any temperature, the rate constants for converting protein or lipid to biocrude are orders of magnitude higher than for carbohydrates. At lower temperatures, 250°C, the biocrude yields from proteins are larger than from the lipids in the feedstock, but the lipid conversion rate is slightly higher than the protein conversion rate at higher temperatures. Other studies have suggested alternative values for these rate constants (Brown, Duan, & Savage, 2010; Leow et al., 2015), but there is a consensus that in order of biocrude yield lipid>protein>carbohydrate for high temperatures, near 350°C (Biller & Ross, 2011; Brown et al., 2010; Teri, Luo, & Savage, 2014; Valdez et al., 2014). The rate constant for carbohydrate conversion to HPW is orders of magnitude higher than for conversion to biocrude (Valdez et al., 2014).

Table 1: Rate constants for the model shown in Figure 2 (Valdez et al., 2014).

	k (min^{-1})			
Reaction	250°C	300°C	350°C	400°C
Protein =>HPW ($k_{1,p}$)	0.095	0.20	0.28	0.33
Lipid =>HPW ($k_{1,l}$)	0.15	0.35	0.35	0.35
Carb =>HPW ($k_{1,c}$)	0.25	0.35	0.35	0.35
Protein => Biocrude ($k_{2,p}$)	0.13	0.13	0.28	0.32
Lipid => Biocrude ($k_{2,l}$)	0.031	0.11	0.33	0.35
Carb => Biocrude ($k_{2,c}$)	0.00010	0.00010	0.00010	0.00320
Biocrude => HPW (k_3)	0.0044	0.14	0.30	0.35
HPW => Biocrude (k_4)	0.003	0.12	0.26	0.26
HPW => Gas (k_5)	0.0010	0.00040	0.0014	0.0014
Biocrude => Gas (k_6)	0.0010	0.00020	0.00090	0.0053

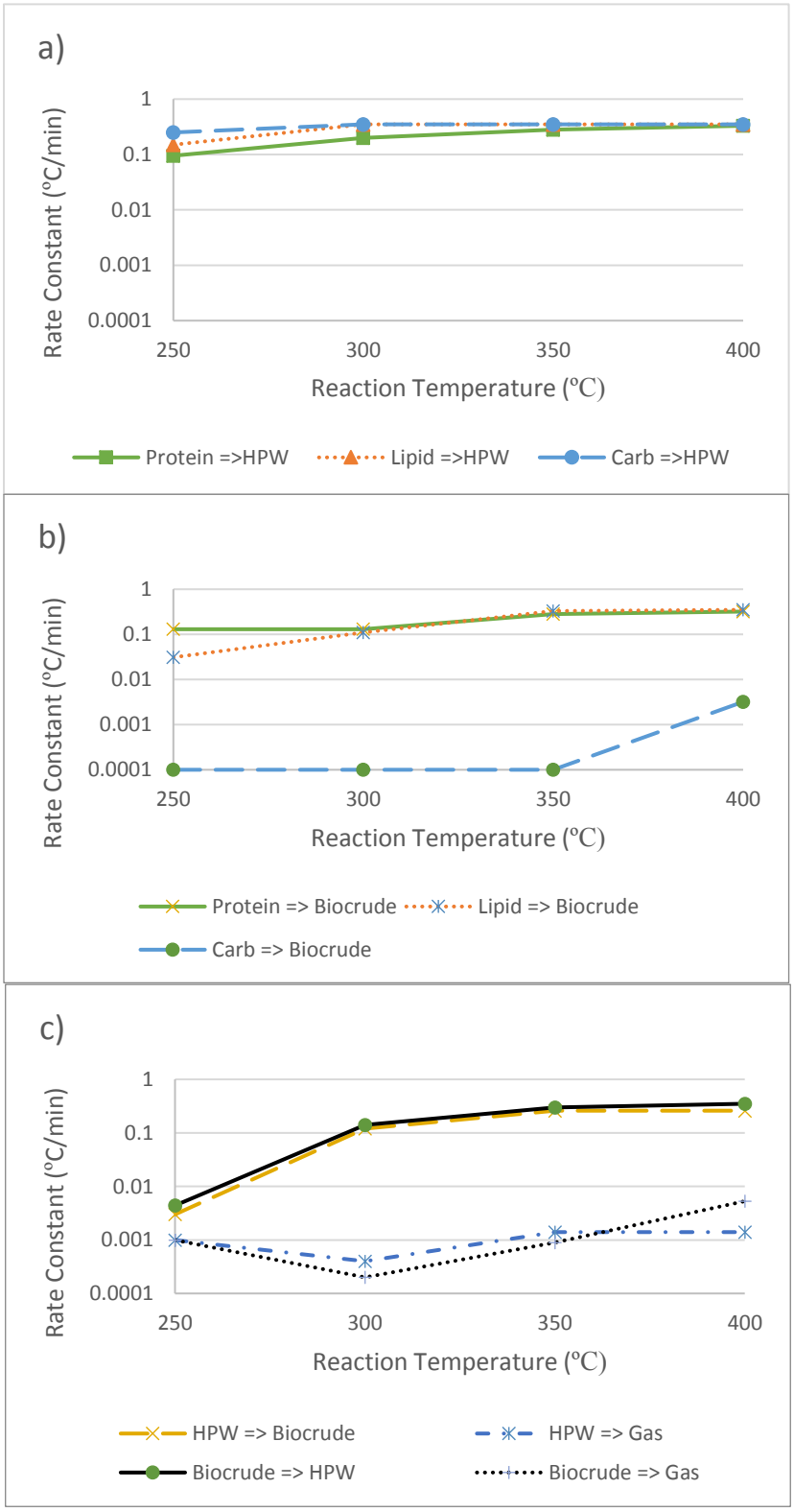

Figure 3: Rate constants for conversion of biomass to HPW (a) and biocrude (b), and for redistribution of mass between liquid and gas phases (c) (Valdez, 2014).

Accurate and detailed modeling is difficult due to the complexity of the natural world and molecular level modeling of HTL is not yet possible (Valdez et al., 2014). The cell wall structure of microalgae can influence the products, especially at lower HTL temperatures (López Barreiro et al., 2013). The types of fatty acids making up the lipid fraction will affect yield (Brown et al., 2010; Leow et al., 2015). Different amino acids and different sugar complexes all have different free energy needs during the melting stage of the decomposition reaction. Hundreds of simultaneous reactions occur during HTL (Raikova et al., 2016). The interactions of the molecular pieces during the condensation phase are complex, with many products formed from the same reactants (Teri et al., 2014). Additionally, many unique compounds are formed during the reaction (Valdez et al., 2014). Although useful comparison can be made between feedstocks, expectations of biocrude quality and yields from a feedstock are best formed from experimental data.

2.2.1. HTL of microalgae

Many studies have been conducted using microalgae as the feedstock for HTL, with the first study conducted by Dote et al. in 1994 (Brown et al., 2010; Elliott et al., 2013). The biochemical composition of the feedstock, HTL processing conditions (temperature, pressure, residence time, heating rate) and their effect on biocrude yield and quality have been documented for a number of species of microalgae (Brown et al., 2010; Shakya et al., 2017). Much of the literature to date uses commercially available algal feedstocks or specially cultivated strains (Elliott et al., 2013) including: *B. braunii* (Dote et al., 1994), *Nannochloropsis* (Brown et al., 2010), *Spirulina platensis* (Jena et al., 2011), *Dunaliella tertiolecta* (Minowa et al., 1995), *Chlorella vulgaris, Porphyridium cruentum* (Biller & Ross, 2011), *Chlorella pyrenoidosa* (Yu et al., 2011), *Tetraselmis* (Eboibi, Lewis, Ashman, & Chinnasamy, 2014), *Scenedesmus* (Vardon,

Sharma, Blazina, Rajagopalan, & Strathmann, 2012), and *Desmodesmus* (Alba et al., 2012). Some work has been published using HPW-cultivated algal feedstocks (Zhou et al., 2013), wastewater feedstocks (Chen et al., 2014; Vardon et al., 2011), and some wild-harvested studies, discussed later, but there is a lack of natural harvested HTL data (Guo et al., 2015). To the author's knowledge, no studies have been published using a feedstock like that collected at Lake Tainter, a wild-harvested, Microcystis Aeruginosa bloom, an extremely low lipid (0.55%), low ash (5.64%) feedstock with nearly equal protein and carbohydrate proportions by wt. (53.7% and 40.1% respectively).

Wild-harvested algae from nitrogen replete conditions, like eutrophic lakes, often have very low levels of lipids. In cultivation settings, algae growers can artificially induce lipid production by restricting nitrogen to the ponds. The fast-growing HAB strains do not have the fat stores that cultivated strains do and conditions that are best for fatty acid growth are not good for biomass growth (Elliott et al., 2013). Often the designation of low-lipid is given to feedstocks with lipid contents as high as 14%(d.b.) (Valdez et al., 2014), though even this small percentage can have a large effect on the products (Leow et al., 2015) and is much higher than the HAB lipid content.

Table 2: Wild harvested microalgae biochemical compositions and biocrude yields documented (%mass d.b.).

Feedstock	Protein	Lipid	Carb	Ash	Biocrude (%daf.)	Reference
LT916 (fresh dried)	53.7	0.55	40.1	5.64	42±6	this study
Taihu Lake HAB	53.69	7.83	20.01	8.11	38.46	Guo et al. 2015
Dianchi Lake HAB	24.8	1.9	73.2	41.6	16.8	Tian et al. 2015

Tian et al. (2015) also used wild-harvested algae from Dianchi Lake, a world-renowned eutrophic lake in China, obtaining a maximum biocrude yield of 18.4%dry, ash-free (daf) at

300°C, 60 min, and 20%TS. As shown in Table 2, the Dianchi feedstock was very low lipid (1.9%daf), though almost 4x higher than the Lake Tainter bloom. The ash content was very high (41.3%d.b.) and the protein content was significantly lower (24.8%daf). The higher protein and lower ash content of LT916 promised better yields than this feedstock.

In another study, optimal conditions for biocrude yield were determined for a wild-type Cyanophyta feedstock from Taihu Lake in China, consisting of "*Microcystis*, Basketballalgae, *Oscillatoria* sp., *Nostoc*, seaweed and other mutant species and toxins." by Guo et al. (2015). The maximum biocrude yield of 39.54%wt. was achieved in this study at 370°C, 50 min, 10%TS. Though this feedstock had lower ash content (8.11%d.b.) than the Dianchi Lake, it also has half the carbohydrate content (20.01%d.b.) and a larger lipid content (7.83%d.b.) than the Lake Tainter feedstock in this study.

At least one study used *Microcystis viridis*, cultivated in a lab from a wild-harvested culture, obtaining 33%daf biocrude yields (Yang, Feng, Inamori, & Maekawa, 2004). This is a closely related species to *M. aeruginosa* (Lópa‐Rodas & Costa, 1997), but there is a lot of variation between *Microcystis* species (Wu, Wei, Tan, Li, & Li, 2017). No biochemical breakdown is reported for the cultivated *M. viridis* in the paper, but nitrogen percent mass values (9.5%N) indicate a higher protein content.

2.2.2. Petroleum crude characterization

Petroleum is processed into a wide range of products, gasoline, road surfaces, plastic, and lubricants to name just a few. Each of these products is made from a special "fraction" of the crude separated from the whole by distillation at increasing temperatures. Although these fractions

are still mixtures of complex hydrocarbons, the chemical properties of the fractions are identifiable from each other because the compounds found in each fraction are sorted according to molecular weight and volatility at distillation (Wauquier, 1995). Crude oil may be characterized as a whole or in terms of these fractions (Hoffmann et al., 2016). Refineries are complex chemical facilities, optimized to specific types of crude feeds. To integrate bio-crude into these facilities, the refinery needs the feed to meet specifications for the type of crude they already process (Jensen et al., 2016)

Physical and chemical properties of the crude or its fractions are measured to evaluate the suitability of a crude for a refinery, determine upgrading processes needed during treatment, and anticipate the products that it can be used for (Ramirez et al., 2015; Wauquier, 1995). Physical properties include viscosity, density and heating value which are measured as both bulk and fractional qualities (Hoffmann et al., 2016; Ramirez et al., 2015; Wauquier, 1995) and flash point, pour point, and total acid number as bulk quantities (Hoffmann et al., 2016). Chemical properties include elemental analysis for oxygen, nitrogen and Sulphur content, carbon residue, molecular chemical composition, H/C and O/C ratios (Hoffmann et al., 2016; Ramirez et al., 2015; Wauquier, 1995).

Eleven different groups of crude oil are defined by the specific densities of their heavy gasoline and residue fractions, which are distilled in the 100-200°C range and at greater than 350°C, respectively. The specific gravity of the fractions is closely related to the H/C ratio of the compounds in the fraction and the boiling point is determined by molecular weight. So, these measurements give some insight into the molecular characteristics of the fractions (Wauquier, 1995). Some fractions of petroleum are more valuable than others, because of the products they can be used for. Gasoline, diesel, and fuel oil are the major petroleum products used in the US

(EIA, 2016). These products are made from the lighter fractions of crude (Landais, 1997). A crude oil with low specific gravity is desirable since it contains more of these valuable light fractions with low boiling points. Crude prices are in part based on the specific gravity of the crude. Specific gravities of petroleum crude generally fall in the 0.800 to 1.000 range (Wauquier, 1995).

Two other crude classifications are used widely. According to ASTM method D86 boiling points are measured for a crude that result in 10, 30, 50, 70, and 90 vol% distilled (Dutton, 2018a). A more general way of classifying the crude fractions is by light, medium and heavy distillates. With a boiling point of 70-200°C, the light fraction, or heavy naphtha, contains the gasoline. The medium fraction, at boiling points of 200-350°C, contains diesel and kerosene. Finally, the heavy fraction, at temps of greater than 350°C, contains the residue, heavy oil, and asphaltenes.

Sulfur content of petroleum crude is generally 0.05-5% by weight. High sulfur content is undesirable, it degrades catalysts used in the refinery, can degrade finished products, and give them a bad smell. Sulfur content of finished fuel is regulated and these regulations have become stricter (Jensen et al., 2016) in an effort to reduce SO_2 and SO_3, which are generated on combustion. Likewise, nitrogen content of the crude has ramifications on the refinery and end user side. Nitrogen compounds decompose under heat and can reduce catalyst effectivity and produce gums (Hoffmann et al., 2016). Additionally, NOx compounds are produced on combustion, a problem for global air quality that is carefully regulated. The amount of carboxylic acids in a crude is related to the oxygen content, O/C ratio, both of which are measured for crudes and fractions (Hoffmann et al., 2016). These acids can be very corrosive, especially at the high temps found in refineries and can attack carbon steel (Wauquier, 1995). Typical petroleum crudes have oxygen contents of 0.05-1.5% (Hoffmann et al., 2016).

Crude oil is also characterized by its combustion characteristics. The high heating value (HHV) is a measure of the amount of energy you can get out of a material by burning it. It is measured for fractions and the crude (Wauquier, 1995).

Water, salt, and sediment content are measured since these can cause damage to catalysts, plug piping, cause sediment deposits, and cause corrosion in the refinery. Water content of crude increases during storage and can be as high as 3% in petroleum crudes (Wauquier, 1995).

2.2.3. Biocrude characterization

Based on the techniques used by the petroleum industry, HTL biocrude characterization analyses are used to ascertain the quality of biocrudes produced using methods that are appropriate for small sample sizes. CHN values are typically used to estimate the HHV of the products, rather than direct measurement in a bomb calorimeter. Thermogravimetric analysis (TGA) is used to estimate fractional products instead of a distillation apparatus and can lend insight into the water content of the biocrude.

CHAPTER 3: MATERIALS AND METHODS

3.1. Feedstock

3.1.1. Feedstock collection and preparation

The feedstock for these experiments was wild-harvested from the Pine Point Boat Landing of Lake Tainter (44.955N, -91.88W), just north of Menomonie, WI. Five gallons was harvested in September 2016 (LT916) and September 2017 (LT917) from a wind-flocculated bloom by passing it through a series of screens. Window screen was used to strain out sticks and macroalgae before dewatering through two screens in series, 100 and 200 micron polypropylene mesh bags. The filtrate from both bags was combined for the feedstock. The retained bulk filtered algal bloom was stored in a bucket surrounded by a cool water bath, transported to UIUC, then transferred to the fridge before preparing it as an HTL feedstock. Under microscope, the microalgae appeared to be primarily Microcystis Aeruginosa, shown in Figure 4, a documented type of problem bloom in the lake (Kreitlow, 2001).

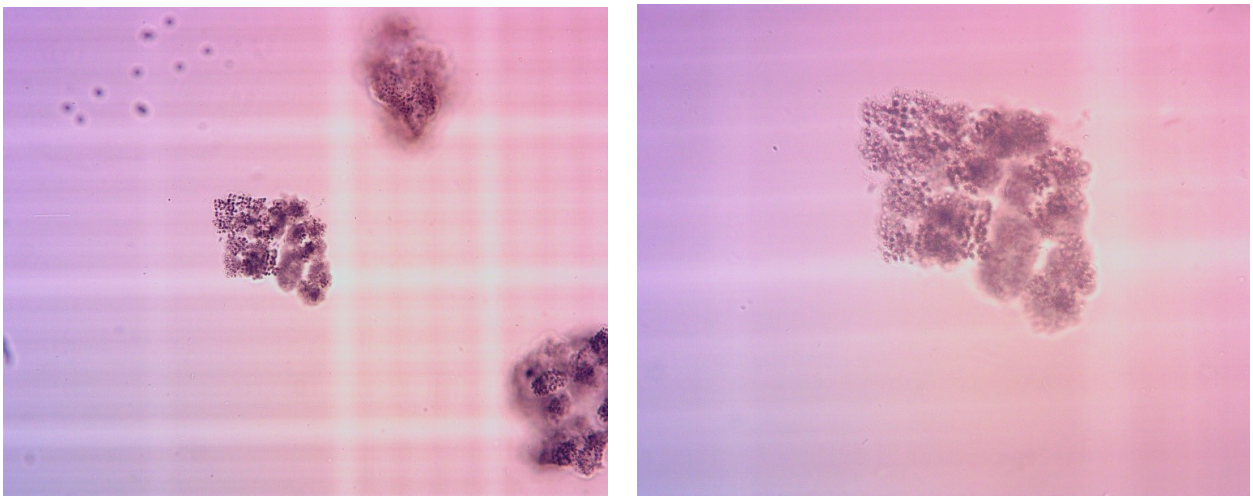

Figure 4: Microcystis Aeruginosa form globular colonies, pictured here one of the colonies from the wild-harvested biomass, at two different magnifications.

The bulk filtered algal bloom was used to produce four types of feedstocks for HTL (FW, AW, FD, and AD), as shown in Figure 5. Wild-harvested blooms were divided into fresh and aged feedstocks. The aged feedstock was stored in the fridge and allowed to decompose for 6 months before use. Both grades of algae were prepared in two ways, as a dry powder and a concentrated algal paste.

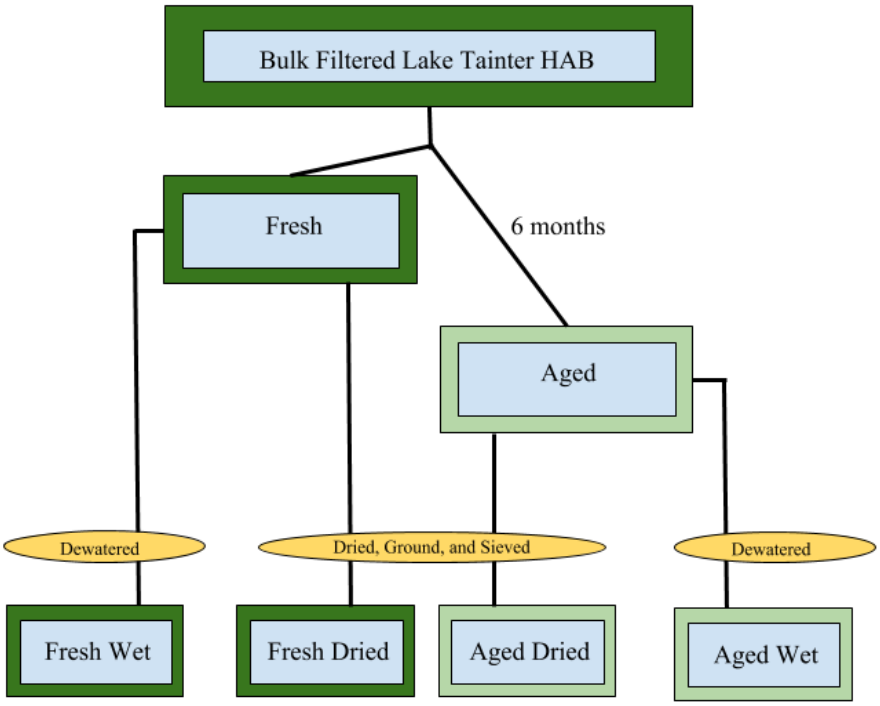

Figure 5: Four feedstocks were prepared from the wild-harvested Lake Tainter biomass, Fresh Wet (FW), Fresh Dried (FD), Aged Wet (AW), and Aged Dried (AD).

To keep the feedstock consistent, the HTL condition optimization work discussed herein was done using dried LT916 biomass, both fresh and aged (FD and AD). To produce the dry feedstock powder, the bulk filtered bloom was dried in a 105°C Yamato Mechanical Convection Oven according the biomass preparation protocol in ASTM method E1756. This dried feedstock

was ground in a blender and sieved with an ASTM wire screen, 300-micron mesh. The dry powder from fresh (FD) and aged (AD) LT916 was stored in a freezer and allowed to come up to room temperature before use in HTL.

To test the effect of drying on the results, both wet and dried feedstocks prepared from the same harvest were processed at the same conditions. The wet, never dried algal pastes (FW and AW) used were prepared from fresh LT917 and aged LT916 biomass. To produce a concentrated paste without drying the bloom, the bulk filtered slurry was further dewatered in the lab to produce the never dried feedstocks from fresh LT917 (FW) and aged LT916 (AW). Firstly, the bulk filtered slurry was filtered under vacuum, using milk filters. Small batches of the vacuum dried algae were sealed into milk filter tubes and any excess water was pressed out with towels. The wet feedstock was mechanically dewatered and measured to determine its total solid content; the dried feedstock was mixed to match.

3.1.2. Feedstock analyses

In the bulk filtered algal bloom and concentrated slurries, the total % solids of algae were defined as the residue from drying at 105°C, determined by ASTM method E1756. Ash content is defined as the residue from 550°C according to ASTM method E1755.

Proximate and ultimate analyses of the Lake Tainter algal bloom were performed on the dried feedstocks, fresh and aged from 2016. Methods are in the following subsections.

3.1.2.1. Proximate analysis of feedstocks

A complete forage analysis of the feedstocks was performed by Midwest Laboratories (MWL) of Omaha, NB details on their analysis techniques are shown in Table 3, next page.

Table 3: Forage analysis methods used by MWL for characterization of LT916, fresh dried and aged dried (Midwest Laboratories, 2017).

Feedstock Quality	MWL Method Description	Based on Method
Moisture Content	Mass lost on drying at 135°C	AOAC 930.15
Ash Content	Residue from 600°C muffle furnace	AOAC 942.05
Crude Protein	Combustion and detection of nitrogen	AOAC 990.03
Crude Fat	Ether soluble mass	AOAC 945.16
Acid Detergent Fiber (ADF)	Residue in filter bag after digestion	Ankom Technology
Neutral Detergent Fiber (NDF)	Residue in filter bag after digestion	Ankom Technology
Lignin	ADF sample residue is digested in sulfuric acid and ashed	AOAC 973.18

To satisfy the mass balance, the %mass of the carbohydrate fraction is found by calculation. The hemicellulose, cellulose, and lignin fractions are calculated as proportionally making up the carbohydrates using ratios determined from the NDF, ADF, and lignin analyses as shown in equations 1-4 (AAFCO, 2017). The loss of mass during the aging process is calculated by assuming the mass of the ash is constant over time.

$$\%\, carb = 100 - (\%protein + \%lipid + \%ash) \quad (1)$$

$$hemicellulose = (NDF - ADF) * \%carb/100 \quad (2)$$

$$cellulose = (ADF - lignin) * \%carb/100 \quad (3)$$

$$lignin = lignin * \%carb/100 \quad (4)$$

3.1.2.2. Elemental analysis of dried algae samples by ICP-MS and ICP-OES

Inductively coupled plasma (ICP) quantification of some metals (S. P, K, Mg, Ca, Na, Fe, Mn, Cu, Zn) in the dried feedstock was performed by Midwest Laboratories (MWL) using a wet ash procedure based on AOAC 985.01.

ICP analyses were conducted by University of Illinois-Urbana Champaign (UIUC) School of Chemical Sciences laboratory (SCS) for metals (Al, Ca, Cr, Cu, Fe, K, Mg, Mn, Na, P, Pb, Si, S, Ti) were performed by Kiran Subedi. ICP-MS (Perkin Elmer NexION 350D) was used to analyze trace elements. Major and minor elements and elements suffering from isobaric and polyatomic interferences in ICP-MS like P, S were analyzed using ICP-OES (Perkin Elmer Optima 8300). After the samples were brought to SCS, concentrated nitric acid (67-70%) was used to digest the dried algae samples, which were further subjected to an automated sequential microwave digestion in a CEM Discover SP-D microwave digester. The final product was a clear, transparent, aqueous digest. This was further diluted using double DI water to make the pH of the solution suitable for elemental analysis. The final solution was introduced to ICP-MS or ICP-OES for the elemental analysis. For most of the elements, two isotopes were analyzed by ICP-MS, and the one with lesser interference and higher abundance was used for the study. Similarly, at least two emission lines were monitored for each element when analyzed by ICP-OES.

3.1.2.3. CHN analysis and HHV

CHN analyses were conducted by Elizabeth Eves, UIUC SCS laboratory, on an Exeter Analytical-Model CE 440 CHN Analyzer (detection limit 0.1%, error 0.06% on a 2 mg sample). The samples were measured in duplicate and average values used for calculations. The biocrude is

cold welded in a consumable tin capsule and run as drop-in samples immediately. The solids and feedstock are crimped and sealed in the tin capsule and run with an auto-sampler.

The recovery (%R) [7] is calculated from the ratio of total mass of an element, R, in the product (R_p) [5] to the feedstock (R_f) [6] (Biller & Ross, 2011).

$$R_p = m_p * c_{Rp} \quad (5)$$

where m_p and c_{Rp} are mass of a product and concentration of R in that product (%R)

$$R_f = m_f * c_{Rf} \quad (6)$$

where m_f and c_{Rf} are mass of the feedstock and concentration of R in that product

$$\% R = \frac{R_p}{R_f} x100\% \quad (7)$$

The mass percentage of oxygen is found gravimetrically by difference using the CHN values of the biocrude [8]. The ash content is also considered when calculating oxygen for the feedstock [9] (Biller & Ross, 2011; Chen, 2013).

$$O_{biomass} = 100 - (C + H + N) \quad (8)$$

$$O_{biocrude} = 100 - (C + H + N + ash) \quad (9)$$

where C, H, O, and ash are the mass percentages of carbon, hydrogen, oxygen, and ash respectively on a dry weight basis

HHV of samples is computed using the Dulong equation [10] (Vargas-Moreno, Callejón-Ferre, Pérez-Alonso, & Velázquez-Martí, 2012):

$$HHV = 0.3383\,C + 1.422(H - \frac{O}{8}) \quad (10)$$

where HHV is in MJ/kg

3.2. HTL Experimental Methods and Analyses

3.2.1. HTL reactions

The HTL reactors used were 31.29 mL stainless steel batch reactors, built from seamless 316 tubing (0.75 in od, 0.065 in wall) and fitted with a needle valve. Passivation of the new reactors was conducted with acetic acid (10 g/L) at 300°C. Reactors were filled with 10g of feedstock, purged with nitrogen gas, and pressurized to 70 psi with nitrogen gas before the reaction.

Dried feedstocks were prepared for HTL by mixing the weighed, dried biomass powder with deionized water in the reactor vessel on shaking agitator, Barnstead Thermolyne Maxi Mix II model number M37615, on high for approximately 10s. Wet, never dried feedstocks were injected into the reactor using a syringe of the homogenized slurry.

Filled reactors were heated for the prescribed HT and an additional 5 minutes of warm up time in a preheated furnace set to the RT. Reactions were carried out in a Thermo Scientific Lindberg Blue M tubular furnace, model number TF55035A-1. Upon removing the reactor from the furnace, the reactor was immediately misted with water and allowed to hang freely to cool. After 2 minutes of hanging, the reactor was submerged in a room temperature water bath. The pressure in the reactor and temperature of the water bath are measured, the gas sampled, and the reactor dried with forced air before sampling the remaining products.

The dried feedstocks, fresh and aged, were subjected to a range of HTL conditions, shown below in Table 4, to determine an optimal operating window for maximum biocrude yield from this feed.

Table 4: Conditions for HTL reactions performed in this study with Lake Tainter HAB, fresh and aged.

Parameter of Interest	Values	RT (°C)	HT (min)	%TS (d.b)
Reaction Temperature (°C)	280, 300, 320, 340, 350	--	50	20%
Reaction Holding Time (min)	30, 40, 50, 60	340	--	20%
Total Solids (d.b.)	10%, 15%, 25%	300	60	--

The experiments comparing the HTL results from wet, never dried feedstocks to the feedstock prepared from dried powders were performed with 6-7%TS, at 340°C, for a 50 min HT.

All conditions were tested in triplicate.

3.2.2. HTL product yields

The following sections discuss the methods for analyses that were conducted on the different HTL product fractions as shown in Table 5. Samples were tested to determine the characteristics of the fuel, energy balance of the system, and relative distribution of key elements for each of the different operating conditions. All product fractions, gas, solids, HPW, and biocrude were measured for mass and %yield calculated on a dry, ash-free per mass basis as shown in equation 11 (Biller & Ross, 2011).

$$Y_n = yield\ of\ HTL\ product\ n$$
$$Y_n = \frac{mass\ of\ product\ n}{dry, ash\ free\ mass\ of\ biomass} * 100\% \quad (11)$$

Table 5: Analyses performed on HTL products

Solids	Biocrude	HPW
CHN	CHN	HACH TNT (TN, NH3)
ICP (S)	ICP (S, P) [a]	GC-MS[a]
	TGA[a]	
	GC-MS[a]	

[a]for runs with highest yield only (AD2050cw, FD2050d2w)

3.2.3. HTL product collection

A schematic of the stages of HTL product collection is shown in Figure 6, next page. The products are collected as described below.

The final reactor pressure is measured with the reactor still in the bath, using a gauge connected to the needle valve on the end of the cooled reactor. The temperature of the water bath after cooling the reactor is taken and used as the temperature of the gas in the chamber. The gas is sampled with a syringe and transferred to unlined sterile vacuum tubes then immediately resampled from the tube and measured by gas chromatography.

The remaining products are removed from the opened reactor chamber through repeated rinsing with dichloromethane (DCM). The DCM mixture is vacuum filtered using Whatman #1 papers to separate solids. The solids caught by the filter are dried in a 105°C furnace overnight to remove bound water, then weighed. The filtrate is gravity settled within minutes in 125 mL separatory funnels into aqueous and DCM-soluble layers. The aqueous portion, or Post-Hydrothermal Wastewater (HPW), is separated, weighed, and stored. The heavier DCM/biocrude product air dried at room temperature (20-22°C) for 24 hours, or until the aluminum pan

containing the product no longer changed weight. This solvent free, viscous liquid product is referred to as biocrude in this paper. After weighing the biocrude to determine yield, the biocrude was collected by dissolving it in DCM. Crucibles and aluminum pans, used for weighing solids and biocrude respectively, were prepared for product collection by kiln-drying at 105°C and cooled in a dessicator. All samples were stored in vapor-proof glass bottles for analysis.

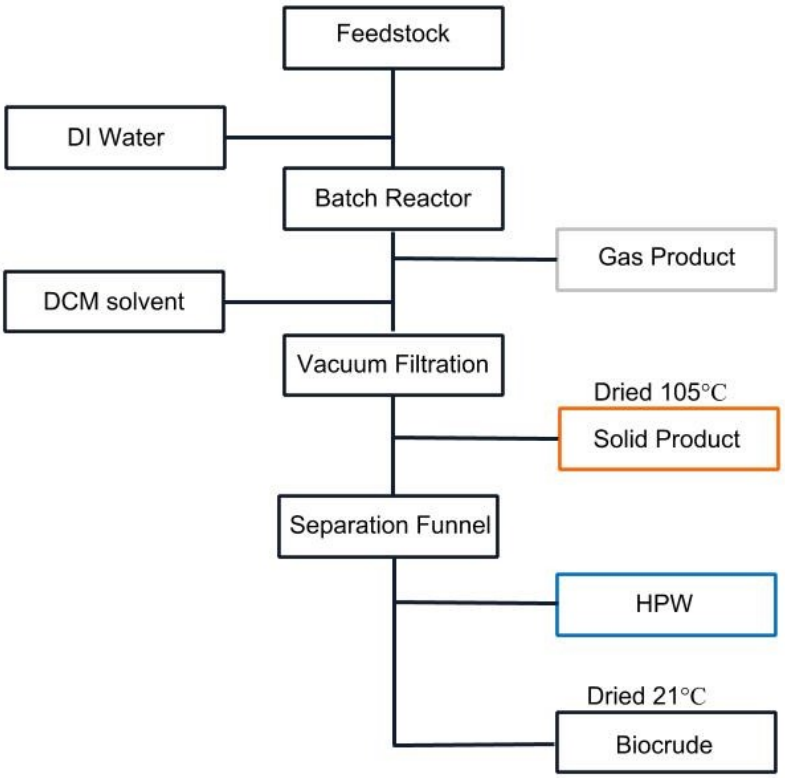

Figure 6: HTL product collection steps.

3.2.4. Gases

The ideal gas law is used to calculate the moles of gas generated by the reaction from the temperature and pressure of the cooled reactor. The approximate mass is calculated using an average concentration of 94% CO_2 and 6% CH_4 This same ratio is used calculating the carbon recovery of the gases. This average was calculated from the GC results as described below.

The composition of the gas product was measured by manual injection on a Shimadzu Gas Chromatograph, GC-17A, equipped with an 18'x1/8 Stainless Steel Silica Gel Column operated with N_2 carrier gas at 140°C. Concentrations were determined based on standard curves [12-14] determined on the machine.

$$H_2 = \frac{(A - 32530)}{1x10^6} \tag{12}$$

$$CH_4 = \frac{(A + 8040.2)}{348829} \tag{13}$$

$$CO_2 = \frac{(A + 6638.7)}{53814} \tag{14}$$

where A is the peak area of each detected gas and the result is in v/v.

3.2.5. Solids

The solid product fraction was measured to determine what proportion of carbon and nitrogen was retained at each HTL condition. The sulfur content of biocrude from the highest producing runs were tested by ICP, using the method in 3.1.2.2. The sulfur and CHN were analyzed in the UIUC SCS laboratory as described in sections 3.1.2.2 and 3.1.2.3.

3.2.6. Biocrude

Biocrude samples from the best producing run from each condition were measured to determine the proportion of carbon and nitrogen retained in the product, the fuel quality, and energy recovery of the process. CHN values for representative biocrude samples were analyzed in the UIUC SCS laboratory as described in section 3.1.2.3.

The calorific energy recovery (ER) of each condition was calculated using the biocrude yield and HHV of the biocrude [15] (Biller & Ross, 2011).

$$ER = Y_b * \frac{Biocrude\ HHV}{Biomass\ HHV} \quad (15)$$

The overall energy consumption ratio (ECR) was used to compare the energy cost of heating the water and biomass to different temperatures and the energy available from the biocrude produced at different conditions [16] (Minowa, Kondo, & Sudirjo, 1998; Vardon, 2012). An ECR less than one indicates a net energy profit. The ECR for each condition was calculated with heat recovery (R_h) at 0% and 50%. All other values were based on Minowa et al. (1995) derivation.

$$ECR = \frac{\left[W_i\, C_{pw} T + (1 - W_i) C_{pb} T\right](1 - R_h)}{Y * HHV * (1 - W_i) R_c}, where \quad (16)$$

W_i= initial water content of the HTL feedstock,

T= (T_r-T_o), the temperature increase to reaction temp from 20°C

C_{pw}=4.18 kJ/kg*K

C_{pb}=1.25 kJ/kg*K

R_h= efficiency of heat recovery

R_c=0.7, efficiency of combustion energy

Y=biocrude yield as a ratio [0,1]

HHV is in kJ/kg

The biocrudes from the highest producing runs (AD2050co, FD2050d2o) were tested more extensively than the other biocrude samples, for sulfur content, by TGA, and by GC-MS

The sulfur content was analyzed in the UIUC SCS laboratory by ICP as described in section 3.1.2.2.

TGA was performed at the Materials Research Laboratory of UIUC (FD2050D2o only). TGA was performed on a Q50-TGA instrument and conducted by ramping the temperature at 10°C/min to from room temp to 400°C, with an isothermal hold for 5 min at 40°C and 10 min at 100°C.

In preparation for GC-MS, the dried biocrude was sampled and rehydrated with DCM to a known concentration (AD2050Co=0.035g/mL, FD2050D2o=0.053g/mL). Reconstituted DCM/biocrude solution samples were filtered with a 0.45μm syringe filter before submitting the samples to the Microbiology Lab on UIUC campus for derivative (non-volatile) and direct injection (volatile) profiles. The GC-MS method and analysis of the results were conducted by Alex Ulanof and described in the following paragraphs.

For direct injection profiles, 1 μL of the sample was injected in a split mode (15:1) into the GC-MS system consisted of an Agilent 6890 (Agilent Inc, Palo Alto, CA, USA) gas chromatograph, an Agilent 5973 mass selective detector and Agilent 7683B autosampler. Gas chromatography was performed on a 30 m HP-5MS column with 0.25 mm inner diameter (I.D.) and 0.25 μm film thickness (Agilent Inc, Palo Alto, CA, USA) with an injection temperature of 2800°C, MSD transfer line of 250°C, and the ion source adjusted to 2300°C. The helium carrier gas was set at a constant flow rate of 1.1 mL/min. The temperature program was 2 min at 600°C, followed by an oven temperature ramp of 50°C/min to 3200°C for a final 5 min. The mass

spectrometer was operated in positive electron impact mode (EI) at 69.9 eV ionization energy in m/z 50-800 scan range. The spectra of all chromatogram peaks were evaluated with NIST Mass Spectral Database (NIST08) and W8N08 library (John Wiley & Sons, Inc., USA). To allow comparison between samples all data were normalized to the internal standard, pentadecanoic acid methyl ester (0.5μ).

For derivatized profiles, the dried extracts (200 μL) were derivatized with 100 μL methoxyamine hydrochloride (40 mg/ml in pyridine) for 90 min at 50 °C, then with 100 μL MSTFA (N-Methyl-N-(trimethylsilyl) trifluoroacetamide) at 50 °C for 120 min. Following a two hour incubation at room temperature, 5 μL of the internal standard (hentriacontanoic acid, 10 mg/mL) was added to each sample prior to derivatization. Metabolites were analyzed using a GC-MS system (Agilent Inc, CA, USA) consisting of an Agilent 7890 gas chromatograph, an Agilent 5975 mass selective detector and a HP 7683B autosampler. Gas chromatography was performed on a ZB-5MS (60m×0.32mm I.D. and 0.25μm film thickness) capillary column (Phenomenex, CA, USA). The inlet and MS interface temperatures were 250 °C, and the ion source temperature was adjusted to 230 °C. An aliquot of 1 μL was injected with the split ratio of 7:1. The helium carrier gas was kept at a constant flow rate of 2 mL/min. The temperature program was a 5 min isothermal heating at 70 °C, followed by an oven temperature increase of 5°C/min to 310°C and a final 10 min at 310 °C. The mass spectrometer was operated in positive electron impact mode (EI) at 69.9 eV ionization energy at m/z 50-800 scan range.

The spectra of all chromatogram peaks were compared with electron impact mass spectrum custom-built database (460 unique metabolites) using the AMDIS 2.71 (NIST, MD, USA) program. All known artificial peaks were identified and removed. Metabolite concentrations were reported as concentrations relative to the internal standard (i.e., target compound peak area divided

by peak area of internal standard: $N_i = X_i \times X^{-1}_{IS}$) per gram sample weight. The instrument variability was within the standard acceptance limit (5%).

The chemical species identified by A. Ulanof in the GC-MS spectra were classified according to chemical class based on functional groups. If a chemical could be considered part of two classes, priority was given in the following order: phenols (PHE), phosphorus containing compounds (PO), nitrogen, heterocyclic (NC), oxygen, heterocyclic (OC), cyclic hydrocarbons (CC), nitrogenous compounds (NX), oxygenates (OX), and linear or branching hydrocarbons (HC). The peak areas were normalized to each other by an additive of known concentration as described previously and the relative peak area computed from the normalized peak area as a ratio of the overall peak area. The relative peak areas of each compound detected in a class are summed to generate relative peak areas of a class.

3.2.7. HPW

The HPW fraction from runs selected for biocrude analysis for each operating condition was tested to monitor the nutrient recovery possibilities. Each sample was tested by colorimetry for total nitrogen and ammoniacal nitrogen (NH_3-N) concentrations using HACH test n'tube kits and methods 10072 and 10031 respectively, modified for use with a HACH spectrophotometer DR2010. Samples were diluted to be in the middle of the kit ranges. Total Nitrogen (TN) measurements of the sample were made in triplicate, but the ammoniacal nitrogen concentrations of the same sample was measured only once. Carbon recovery for HPW is calculated by difference using the carbon recovery values of the gas, solids, and biocrude products.

The HPW from the highest biocrude producing runs (AD2050cw, FD2050d2w) were tested with GC-MS. Samples were prepared filtered with a 0.45µm syringe filter before

submitting the samples to the Microbiology Lab on UIUC campus for derivative (non-volatile) and direct injection (volatile) profiles. The GC-MS method at the lab was developed by Alex Ulanof. For derivatized analysis, the digestion method is the same as was used for biocrude, described in section 3.2.6. Volatile spectra were measured as described in the following paragraph.

For direct injection samples, 1 μL was injected in a split mode (20:1) into the GC-MS system consisted of an Agilent 6890 (Agilent Inc, Palo Alto, CA, USA) gas chromatograph, an Agilent 5973 mass selective detector and Agilent 7683B autosampler. Gas chromatography was performed on a 30 m HP-InnoWax column with 0.25 mm inner diameter (I.D.) and 0.25 μm film thickness (Agilent Inc, Palo Alto, CA, USA) with an injection temperature of 250°C, MSD transfer line of 230°C, and the ion source adjusted to 230°C. The helium carrier gas was set at a constant flow rate of 1 mL/min. The temperature program started with 2 min at 70^0C, followed by an oven temperature ramp of 20°C/min to 130°C, to 230°C at 10°C/min for a final 10 min. The mass spectrometer was operated in positive electron impact mode (EI) at 69.9 eV ionization energy in m/z 30-800 scan range.

The spectra of all chromatogram peaks were evaluated with NIST Mass Spectral Database (NIST08) and W8N08 library (John Wiley & Sons, Inc., USA). To allow comparison between samples all data were normalized to an isopentanoic acid (0.1μM) internal standards.

As with the biocrude, the chemical species identified by A. Ulanof in the GC-MS spectra were classified according to chemical class based on functional groups. If a chemical could be considered part of two classes, priority was given in the following order: phenols (PHE), phosphorus containing compounds (PO), nitrogen, heterocyclic (NC), oxygen, heterocyclic (OC), cyclic hydrocarbons (CC), nitrogenous compounds (N_X), oxygenates (OX), and linear or branching

hydrocarbons (HC). The peak areas were normalized to each other by an additive of known concentration as described previously and the relative peak area computed from the normalized peak area as a ratio of the overall peak area. These are summed to generate relative peak areas of a class.

3.2.8. Statistical methods

SAS software was used to analyze data collected from fresh and aged Lake Tainter algae HTL runs. Operating conditions were used as explanatory variables for product yield response variables. The data were analyzed for simple descriptive statistics, such as means and standard deviations. One-way ANOVA analyses were used for each of the operating conditions per feedstock. The residuals were analyzed to confirm normality and homogeneity of variation using Shapiro-Wilk and Levene's tests respectively. In the case of aged dried feedstock gas yields as a function of reaction temperature, the variation in residuals was non-homogeneous, so Welch's ANOVA was used as the analysis method. Paired t-tests were used to compare the fresh and aged yields for individual products and conditions.

CHAPTER 4: RESULTS AND DISCUSSION

4.1. Feedstock Characterization

4.1.1. Proximate analysis

Tables 6 and 7 show the original results and calculated values for the proximate analysis of the feedstocks. As shown in Figure 7, the wild-harvested biomass is primarily protein and carbohydrates (fresh dried 53.7%d.b and 40.1%d.b. respectively). Crude lipids are a minor component (<1%). The high protein content and low lipid content is typical for fast growing cyanobacteria (Elliott et al., 2013; Sharma, Tiwari, Tripathi, & Rai, 2011; Vardon, 2012). The ash content is low (5.64%d.b.) (Elliott et al., 2015) compared to 25%-70%wt. for wastewater algae and marine strains (Biller & Ross, 2011; Hampel, 2013) and is close to reported values for cultivated, low ash freshwater strains (7-8%) (Biller & Ross, 2011).

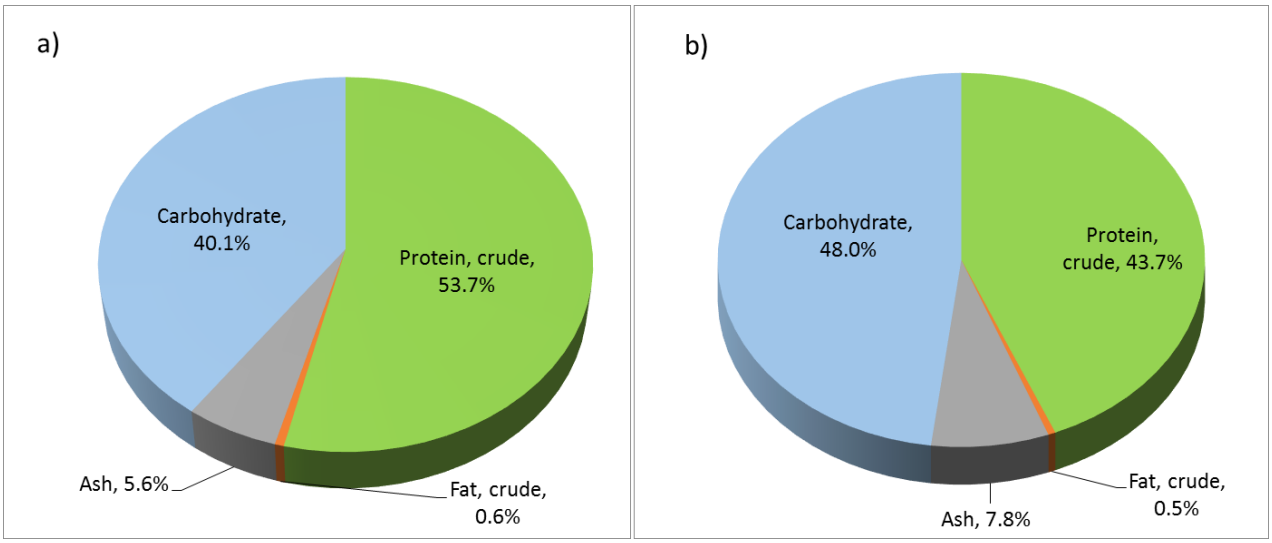

Figure 7: Fresh Dried LT916 (a) and Aged Dried LT916 (b) proximate analyses.

Table 6: LT916 feedstock analysis results (%d.b.), non-adjusted

Component	Feedstock	
	Fresh Dried	Aged Dried
Crude Protein	53.7	43.7
Crude Lipid	0.55	0.48
Ash	5.64	7.81
NDF	52.3	49.7
ADF	35.4	41.7
Lignin	9.8	3.0

Table 7: Calculated LT916 feedstock nutritional profiles (d.b.)

Component	Feedstock		
	Fresh Dried	Aged Dried	% Lost Due to Aging
Crude Protein	53.7	43.7	41.2
Crude Lipid	0.55	0.48	36.9
Ash	5.64	7.81	NA
Carbohydrates	40.1	48.0	13.6
Hemicellulose	12.9	15.5	--
Cellulose	19.7	29.7	--
Lignin	7.5	2.8	4.7

The foraging analysis shows the protein portion of the feedstock is most seriously affected during the aging process, losing nearly half its mass, as shown in Tables 6 and 7. A noticeable change in color of the feedstock over time indicates at least part of that loss is due to pigment proteins. The lipid portion also sees a proportionally large change, but because it is a small part of the feedstock makeup, this does not affect the overall composition significantly. Lignin in the fresh biomass is degraded as it aged, altering the carbohydrate proportions.

4.1.2. Ultimate analysis

Elemental analysis for carbon (C), hydrogen (H), nitrogen (N), and oxygen (O) values in the LT916 feedstock, in Figure 8 and Table 8, show comparable levels between aged and fresh feedstocks and are typical for low lipid, low ash *Nannochloropsis sp*. (Elliott et al., 2013). The high N content of the feed is slightly reduced in the aged samples, presumably because of the release of ammonia by the rotting biomass. The HHV of the feedstocks, calculated with Dulong's

formula (eq. 10), is just over 19 MJ/kg, similar to reported values for other protein and carbohydrate based biomass (Biller & Ross, 2011).

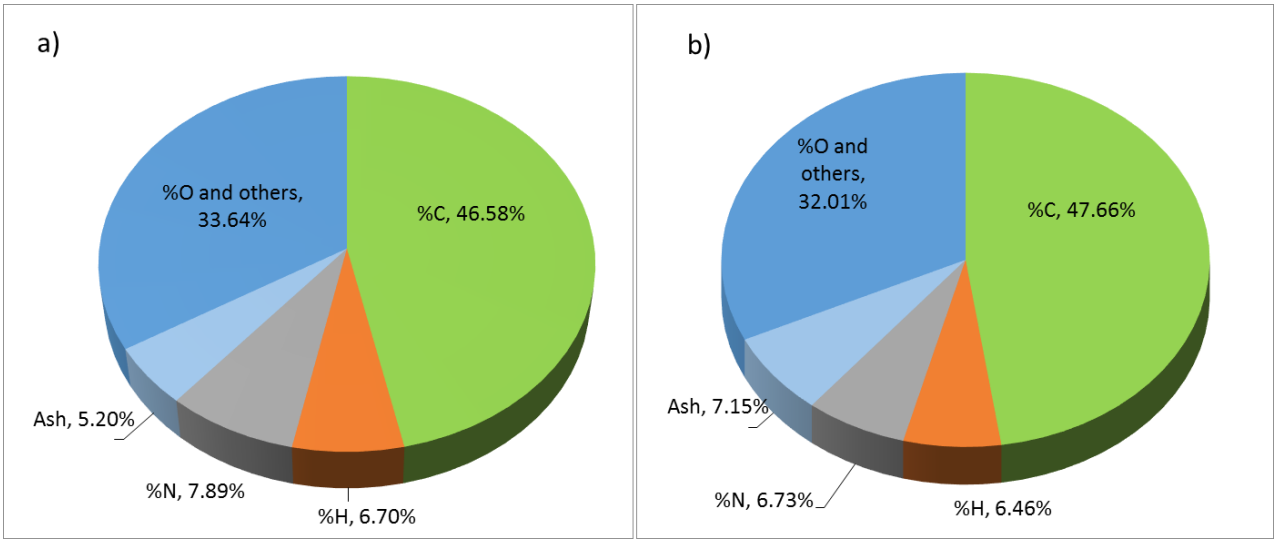

Figure 8: Fresh Dried LT916 (a) and Aged Dried LT916 (b) CHN, ash, and oxygen (by calc) mass percentages.

Table 8: LT916 feedstock elemental analysis and calculated HHV (%d.b.)

Feedstock	Fresh Dried	Aged Dried
C	46.58	47.66
H	6.70	6.46
N	7.89	6.72
Ash	5.64	7.81
O[a]	33.20	31.36
HHV (MJ/kg)	19.38	19.73

[a] Determined by difference.

These feedstocks have high N and O content which can be problematic when they are distributed to the biocrude downstream. Nitrogen compounds produce NOx compounds upon combustion. Without further hydrotreating, nitrogen and oxygen that end up in the biocrude can

poison refining catalysts and prevent full integration of this technology into current infrastructure (Hoffmann, Jensen, & Rosendahl, 2016; Jones et al., 2014; Wauquier, 1995).

ICP results for metals in the fresh and aged LT916 algae samples are shown in Tables 9, 10, and 11 determined by MWL and SCS. Both labs report slightly elevated magnesium, sodium, potassium, and phosphorus concentrations in the aged feedstock as compared to the fresh. For metals tested by MWL, the concentration in the aged feedstock is between 1.16 to 1.38 times the fresh feedstock level and can be attributed to the loss of mass while the algae decayed. The ICP results from SCS confirm the magnitude of the MWL results for calcium (Ca), iron (Fe), potassium (K), magnesium (Mg), manganese (Mn), Sodium (Na), phosphorus (P), and sulfur (S). The phosphorus levels in the fresh feedstock (0.76-0.78%wt) are similar those in algae harvested from water treatment ponds (0.2-1.3%wt.) (Hampel, 2013). Sulfur levels for LT916 are in the mid-range (.58-.74%d.b.) for microalgae, which have been reported with levels between 0.5-1%(d.b.) (Biller & Ross, 2011; Biller et al., 2012; Vardon et al., 2011). Silicon levels in the algae account for nearly 1/3 of the ash in the algae at 2%d.b.

Table 9: ICP results for fresh (FD) and aged (AD) LT916 as determined by Midwest Labs.

	Mineral Content (%d.b.)									
	Ca	Cu[a]	Fe[a]	K	Mg	Mn[a]	Na	P	S	Zn[a]
LT916FD	1.04	3.1	521	0.75	0.33	130	0.03	0.76	0.62	21.9
LT916AD	1.32	3.6	631	1.04	0.43	167	0.04	0.95	0.73	26.9

[a] indicates value in ppm instead of %d.b.

Table 10: ICP results for fresh (FD) and aged (AD) LT916 as determined by SCS.

	Mineral Content (%d.b.)												
	Al	Ca	Cr	Fe	K	Mg	Mn	Na	P	Pb	S	Si	Ti
LT916FD	0.02	1.18	0.02	0.08	0.69	0.53	0.03	0.04	0.78	0.01	0.74	1.9	0.001
LT916AD	0.04	1.06	0.01	0.07	0.94	0.62	0.01	0.15	0.87	n.d.	0.58	2.14	n.d.

n.d.= not detected

The C:N:P molar ratio of the fresh feedstock is 158:23:1 and the C:N ratio is 6.9:1. Balanced growth has a C:N:P ratio of 106:16:1 and a C:N ratio of 6.6:1. These are very high ratios for *Microcystis* (Tezuka, 1989), but within a realistic range for nutrient limiting conditions (Fagerbakke, Heldal, & Norland, 1996; Geider & La Roche, 2002). The N:P ratio is greater than 16 and the C:P ratio is greater than 106 indicating phosphorus was limiting. This is probable considering the density of the bloom. The C:N ratio indicates conditions for balanced growth, N was likely not limiting growth (Dodds & Whiles, 2010). The C:N:P ratio for the aged feedstock is 142:17:1 and the C:N ratio is 8.2:1. The phosphorus concentration increased in the aged feedstock and the nitrogen concentration decreased. These changes in composition are most likely due to dissolved inorganic nitrogen released on decomposition (Tezuka, 1989).

The wild-harvested bloom had low levels of heavy metal contaminants. The EPA regulation Part 503 (40 Code of Federal Regulations Part 503), a rule on biosolids applied to fields sets two types of limits: a ceiling concentration limit (CCL) that cannot be surpassed in any one biosolids application to a field and a more rigorous, pollutant concentration limit (PCL). If the bloom did not contain the high levels of cyanotoxins it does, the levels of heavy metals in the bloom are low enough to meet the pollutant concentration limit, meaning they could be applied to fields without tracking Cumulative Pollutant Loading Rates (US EPA, 2018). As shown in Table 11, in most cases, the heavy metal concentrations are low enough they could be concentrated many

times and remain below the pollutant concentration limits. For many of these elements, even if the heavy metals are concentrated in the solid HTL products many times, the solid product could still be applied to fields and meet the PCL. The levels of arsenic and selenium are high enough that concentrating 3 or 4 times would put it over the CCL and the lead level would be over the CCL at 8.4x its level in the feedstock.

Table 11: Biosolids heavy metal contaminants concentration limits (d.b.) regulated by the EPA and measured in LT916 fresh (FD) and aged (AD) biomass by ICP

Pollutant	CCL (mg/kg)	PCL (mg/kg)	FD (mg/kg)	AD (mg/kg)
Arsenic	75	41	26.8	31.58
Cadmium	85	39	0.07	0.08
Chromium	3000	1200	200	100
Copper	4300	1500	3.2	3.8
Lead	840	300	100	n.d.
Mercury	57	17	0.11	n.d.
Molybdenum	75	--	0.34	0.36
Nickel	420	420	15.11	16.3
Selenium	100	36	25.5	26.8
Zinc	7500	2800	22.8	28.2

4.2. Fresh Dried LT916 HTL

The following sections discuss the product distributions, energy returns, nutrient distributions, and fuel quality for fresh dried LT916 subjected to three ranges of reaction conditions (RT, HT, %TS). The biocrude and HPW products from the run with the best biocrude yield (FD2050D2) are characterized in more depth and these results are presented in the later sections.

4.2.1. Energy returns

This section discusses the mass product distributions, biocrude heating value, and associated energy returns for HTL conversion of fresh dried LT916.

4.2.1.1. Yields

Temperature

As shown in Figure 9, the biocrude yield initially increases with temperature and peaks at 340°C at 41.8±6.1% of the biomass dry, ash free weight (daf). Meanwhile, the gas fraction generally increases with temperature, reaching yields of 15-17%daf. There is a corresponding gas phase maximum at 350°C, just as the biocrude yield begins to drop. The amount of solid produced is reduced to less than 8%daf at higher temps. Biocrude yields for all conditions are listed in the section 4.2.1.2 in Table 16.

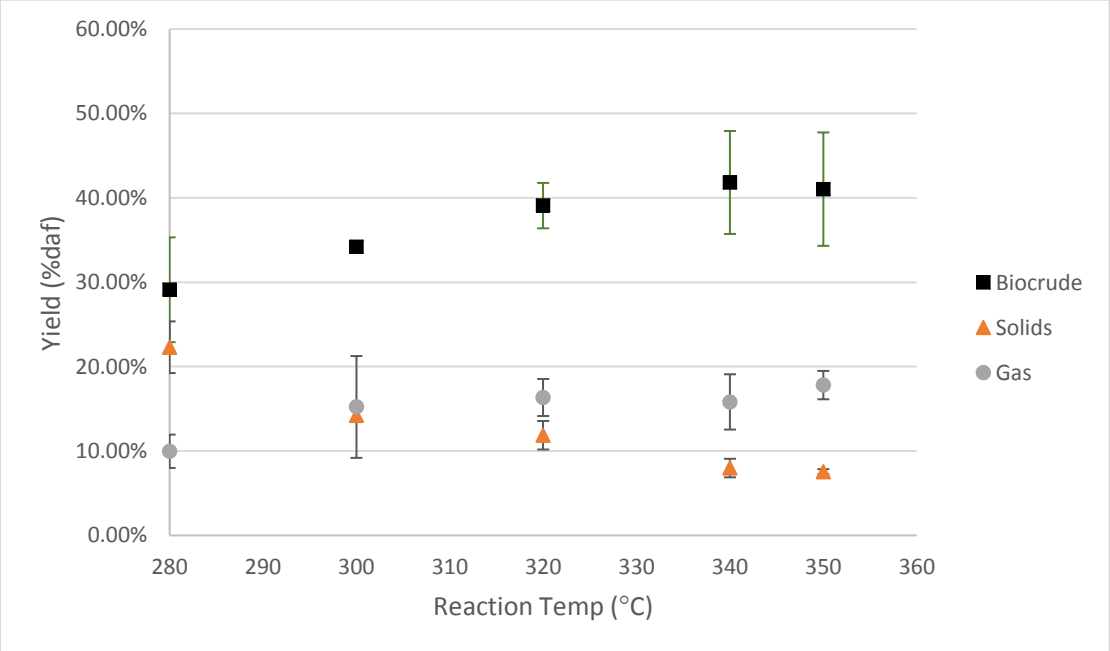

Figure 9: HTL product yields from Fresh Dried LT916 processed at different RT.

The solids and gas yield strongly respond to a change in reaction temperature, but the biocrude yields less so. A one-way ANOVA analysis of the biocrude yield as a function of temperature levels did not meet the significance level ($F(4,10) = 3.33$, $p = 0.056$) to reject the null. Paired two-sample analyses of the biocrude yields at different temperatures only show a statistical difference in average biocrude yield between 280°C and higher RT, as shown in Table 12. There was a statistically significant difference between temperature groups as determined by one-way ANOVA analyses of the solids ($F(4,10) = 38.20$, $p = 4.86 \times 10\text{-}6$) and gas product yields ($F(4,10) = 4.94$, $p = 0.0186$). Differences of Least Squares Means p-values, shown in Table 13, next page, show the degradation of biomass is statistically different as RT is increased, except for between 300°C and 320°C and between 340°C and 350°C. The p-values are smallest for comparing Least Squares Means for gas yield at RT=280°C to any other RT. The product differences between certain temperatures correspond to energy needed to hydrolyze different biochemical compounds as discussed in the following paragraphs.

Table 12: p-values from paired t-tests of biocrude yields from different RTs.

	p-values			
Temps (°C)	300	320	340	350
280	0.304	**0.043**	**0.003**	**0.016**
300	-	0.093	0.167	0.219
320	-	-	0.300	0.492
340	-	-	-	0.444

Table 13: Differences of Least Squares Means p-values from the ANOVA analyses of product yields at different RT for fresh dried LT916.

		p-values							
RT (°C)	Product	280		300		320		340	
300									
	solids	0.0002	[a]	NA					
	gas	0.0198	[a]	NA					
320									
	solids	<0.0001	[a]	0.1158	[b]	NA			
	gas	0.0074	[a]	0.5758	[b]	NA			
340									
	solids	<0.0001	[a]	0.0010	[a]	0.0176	[a]	NA	
	gas	0.0115	[a]	0.7589	[b]	0.7979	[b]	NA	
350									
	solids	<0.0001	[a]	0.0006	[a]	0.0103	[a]	0.7590	[b]
	gas	0.0021	[a]	0.2069	[b]	0.4584	[b]	0.3254	[b]

[a] significant difference in Least Squares Means product yield between the temperatures.
[b] no significant difference in product yield Least Squares Means detected
NA not applicable, same temp

Similar to the results of this study, a peak in biocrude yield near 350°C is observed in other studies (Shakya, Whelen, Adhikari, Mahadevan, & Neupane, 2015; Valdez et al., 2012; Yu et al., 2011). Feedstocks with high levels of lignin, like this HAB, tend to have higher RTs for maximum biocrude yield (Yin et al., 2010). Jena, Das, and Kastner (2011) observe a steep increase in biocrude yield 200-350°C and decreasing yields at higher temperatures. They also document increased gas yields across the entire temperature range and decreased solid yields. Guo et al. (2015), processing Lake Taihu cyanobacteria, observed the same peak at an RT of 350°C for biocrude yield.

The biocrude yields determined are consistent with RT-varied results from similar feedstocks under similar conditions, shown in Table 14 (Biller et al., 2012; Guo et al., 2015; Jena et al., 2011; Leow et al., 2015; Tian et al., 2015; Vardon et al., 2012). At 300°C, LT916 yields

(34.2±0.6%daf) are between the reported yields for two very low lipid, low ash feedstocks, despite the difference in HT. It is slightly higher than average yields reported in the NREL predictive modeling paper for HTL of low lipid, low ash *Nannochloropsis* at the same temp (33.2%daf) (Leow et al., 2015) and lower than Vardon (2012) defatted *Scenedesmus* (36%daf). The Biller et al. (2012) low lipid *Chlorogloeopsis fritschii* results show a slightly higher yield (38.6%) than LT916 at the same RT (300°C) and similar HT. The biocrude yield from LT916 is twice as high as the yield from the high carbohydrate Dianchi Lake bloom. Though, this is an anomaly with the Dianchi lake results, not LT916. The Dianchi Lake bloom has very high ash content compared to the other feedstocks shown here. Though the yield calculation is on a dry, ash free basis, the ash content does appear to affect the conversion as well. The Taihu Lake bloom results are slightly lower than the LT916 results at 340°C, though the solid loading rate is different. The lower %TS could account for this lower yield as results from this study and Guo et al. (2015) indicate. Not shown in the table, the maximum yield being achieved at a temperature of 340°C agrees with the optimal condition reported for *M. viridis* (33% yield at 340°C, 30 min with 5% sodium carbonate) (Yang et al., 2004).

Table 14: Fresh Dried LT916 biocrude product yields from 300°C, 340°C, and comparable studies.

Feedstock	Protein	Lipid	Carb	Ash	RT (°C)	HT (min)	%TS	Biocrude (%daf.)	Reference
LT916 (fresh dried)	53.7	0.55	40.1	5.64	300	50	20	34.2±0.6	this study
Nannochloropsis	74.7	n.d	19.4	5.9	300	30	20	33.2*	Leow et al. 2015
defatted *Scenedesmus*	72	<1	21	7	300	30	20	36	Vardon 2012
C. fritschii	50	7	44	7.6	300	60	9.8	38.6	Biller et al. 2012
LT916 (fresh dried)	53.7	0.55	40.1	5.64	340	50	20	42±6	this study
Taihu Lake HAB	53.69	7.83	20.01	8.11	350	60	10	38.46	Guo et al. 2015
Dianchi Lake HAB	24.8	1.9	73.2	41.6	340	60	10	16.8	Tian et al. 2015

These trends are explained in previous microalgae HTL works (Tian et al., 2015) and summarized in Shakya et al. (2017). At 280°C, protein begins hydrolyzing and is found in the HPW but at temperatures higher than 300°C, proteins and amino acids decompose further and are hydrophobic, distributing into the biocrude. At 260°C, large amounts of carbohydrates have been reported in the HPW, but around 300°C, they too decompose further, increasing the gas and solid yields (Li et al., 2014; Shakya et al., 2017). This is reiterated by Valdez, Tocco, and Savage (2014) whose model predicts that as the RT increases, so do the rates of conversion to biocrude. However, at high temperatures, greater than 300°C, the rate constant for conversion of biocrude to gas is increasingly higher and the rate of conversion between the liquid fractions becomes more significant. Although the rate of conversion from biocrude to HPW is consistently higher than in the other direction, at high temperatures the high rates of conversion make the difference more significant, 30%-40% of the concentration of biocrude is transferred to the HPW and approximately 25% of the concentration organic matter in HPW is transferred in the other direction, becoming hydrophobic.

Cumulatively, the data suggest an RT of 320°C or greater is beneficial for biocrude yield with a maximum conversion of biomass at 340°C. The highest biocrude yield was observed at an RT of 340°C and the co-product yields indicate this is a plateau for biomass conversion in the sub-critical temperature region.

Holding time

As the holding time is increased, the average biocrude yield slightly increases from 30-50 min with a small peak at 50 min at 41.8± 1.5%daf, as shown in Figure 10. The biocrude yield is around 40% for the entire range of HT, 30-60 min. The yield of gas increases and the solid product yield decreases as holding times are extended past 30 min.

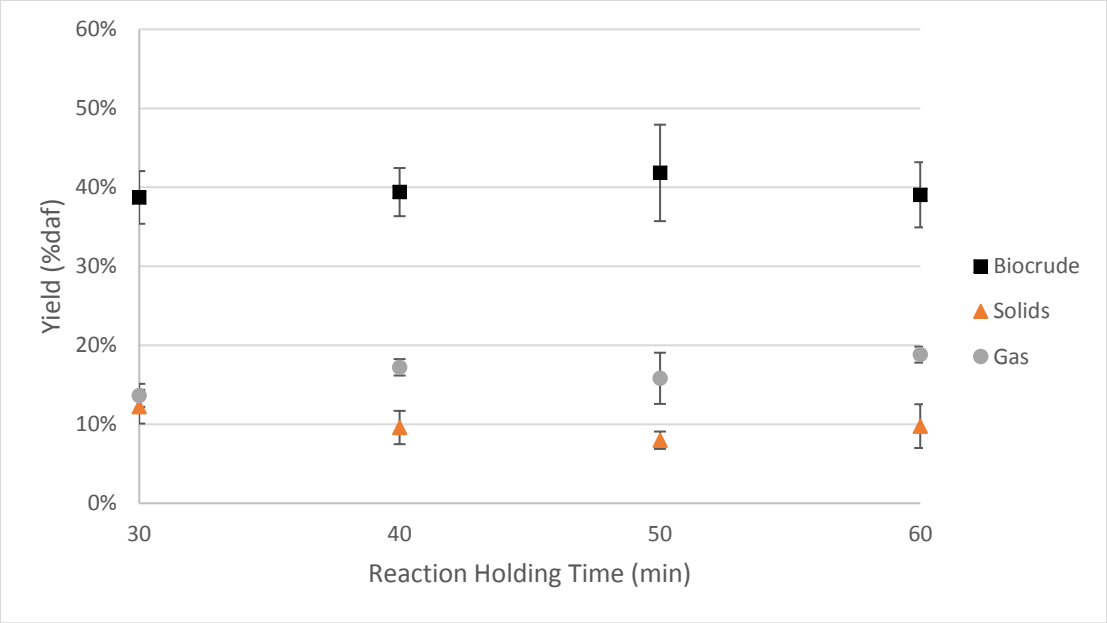

Figure 10: HTL product yields from Fresh Dried LT916 processed at different HT.

The trend fits with current HTL theory. Longer holding times allow more time for the biomass to decompose to biocrude or water-soluble organics. However, as the holding time is extended further, there is a negligible amount of mass being added to the liquid products and the mass being converted to gas phase dominates, reducing yield.

One-way ANOVA analyses of product yields as a function of holding times did not meet the significance level to reject the null for biocrude ($F(3,8)=0.04$, $p=0.9871$) or solids ($F(3,8)=0.70$, $p=0.5766$), but did indicate there is a probability gas yields are not constant over HT ($F(3,8)=5.41$, $p=0.0251$). Paired two sample t-tests showed that there is no significant difference in the means of the biocrude yields for any two individual holding times. Paired two sample t-tests showed statistically significant differences in the solid product average yields at the 30 min and 50 min conditions ($p=0.030$). The p-values of Differences in Least Square Means from the gas yields,

shown in Table 15, show the gas yield is probably higher at 60 min than at 30 or 50 min HT and probably higher at 40 min than 30 min.

Table 15: Differences of Least Squares Means p-values from the ANOVA analyses of product yields at different HT for fresh dried LT916.

		p-values					
HT (min)	Product	30		40		50	
40							
	gas	0.0388	[a]	NA			
50							
	gas	0.5653	[b]	0.0987	[b]	NA	
60							
	gas	0.0075	[a]	0.3099	[b]	0.0184	[a]

[a] significant difference in Least Squares Means product yield between the temperatures.
[b] no significant difference in product yield Least Squares Means detected
NA not applicable, same temp

These patterns agree with the results from others across this range (Valdez et al., 2012). Jena, Das, and Kastner (2011), also report no significant change to biocrude yield in this range of HT. The biocrude yield from low lipid, low ash *Scendesmus* sp across the same range of holding times (Valdez et al., 2014) is fairly level and drops at 60 min like the data here. The solid product yield drops over the range and gas yield increases measurably at the 60 min point. Guo et al. (2015) show a distinct increase in biocrude yield as holding time is increased from 10 to 50 min, but again there is evidence of a decrease in yield again at the long, 60 min holding times, for temperatures higher and lower than the one used here, 320°C and 370°C.

The best average biocrude yield was found at 50 min HT. The increase of gas production for HT increase from 50 min to 60 min HT and the decrease in solid yield for an HT increase from 30 min to 50 min support the choice of this HT for optimum biocrude yield.

Solid loading

The data in Figure 11, next page, shows the biocrude yields for HTL at 300°C and 60 min. The biocrude yield increases with the solid loading ratio, whereas the gas yield in proportion to the biomass in the feed slowly drops, and the solid product increases. The increase in biocrude yield is not proportional to the increase in solid loading in the product. From the data, we could expect further increase in bio crude yields, though slight, for increased concentration of the feed. However, physically obtaining an algal slurry with greater than 25%TS would require drying of the feedstock, which is energy intensive. Also, pumping that "slurry" would be more like pumping clumpy sand or dirt, though slurries of up to 35%wt. are possible (Elliott et al., 2013). Therefore, further increase in biomass may not have great utility due to the increased difficulty in pumping a slurry that thick.

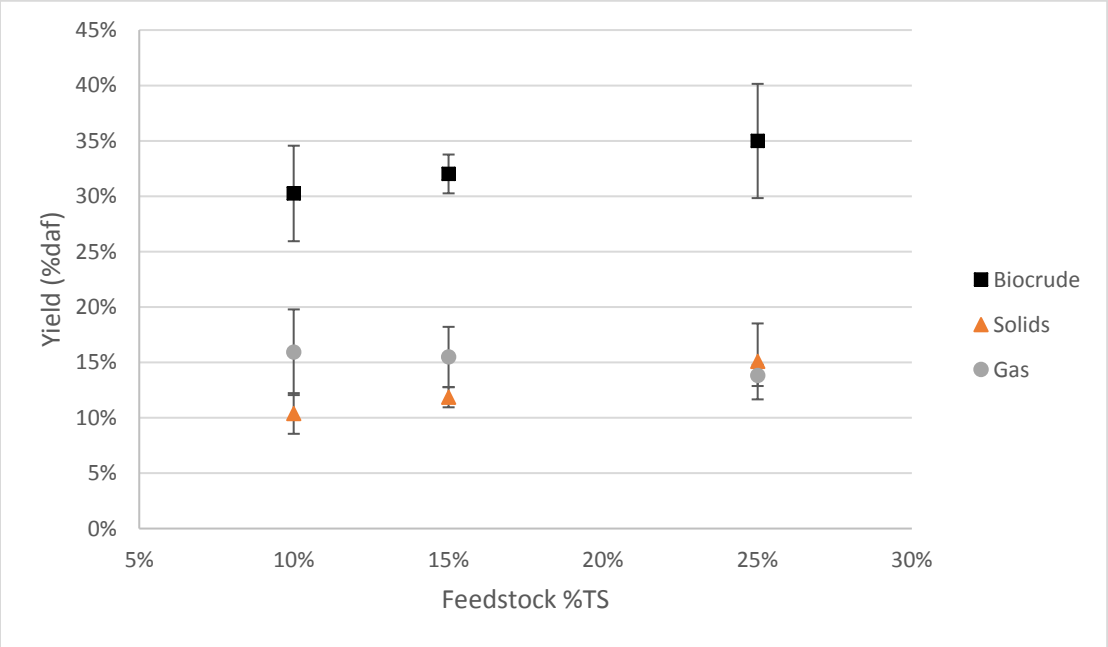

Figure 11: HTL product yields from Fresh Dried LT916 processed with different %TS.

One-way ANOVA analyses of product yields as a function of feedstock loading did not meet the significance level to reject the null for biocrude ($F(2,6)=1.07$, $p=0.3994$) or solids ($F(2,6)=3.25$, $p=0.1108$), but did indicate there is a probability gas yields are not constant over %TS changes ($F(2,6)=0.48$, $p=0.6392$). Paired two sample t-tests showed that there is not a significant difference in the means of the biocrude yields or gas yields for any two individual solid loading values. Paired two sample t-tests showed that there is a significant difference in the means of the solid product yields for 10% and 25%TS ($p=0.0381$), indicating the efficiency of decomposition of the biomass is lower at higher %TS. The feedstock is degraded more completely at lower %TS.

The effect of solids concentration in other whole algae HTL studies do not show a clear trend across this whole range of %TS. In Guo et al. (2015), processing at 370°C and 60 min holding time, the biocrude yield increases with increased %TS from 5-15%, but at the 20%TS level the average is lower, though this is a bit ambiguous due to a wide standard deviation. At higher %TS (25% and 30%), the biocrude yield decreases. Valdez et al. (2012), working at 350°C, 60 min, document an increase in biocrude, light and heavy fractions, between 10% and 15%TS and 15% and 35%TS, but a drop in yield in the middle of the range, at 20%TS. Jena, Das, and Kastner (2011) found an increase in biocrude yield from 10-20%TS, but no significant increase in yield for solid loadings 20-50%TS. They observed no significant change in the gas or solid yields across this range. They postulate the variation in results could be related to the availability of charged ions to organics at higher temps.

Although this study did not show a statistical difference in the the biocrude yield with a change with solid loading rate, the overall biocrude production will increase proportionally with

higher mass loading rates. There is no indication that the yield decreases as the %TS is increased between 10%TS-25%TS. Higher %TS is favorable for biocrude production.

4.2.1.2. Biocrude CHN and HHV

As shown in Table 16, the CHN values for biocrude have elevated carbon levels (67.7-73.5%wt.) and slightly elevated hydrogen levels (8.08-8.77%wt.) compared to the feedstock (46.6%C, 6.7%H). Nitrogen levels in the crude (5.9-9.02%wt.) can be slightly higher or lower than the original biomass (7.9%wt.). The range of values and the increased C and H levels are typical for HTL of high protein microalgae (Barlow et al., 2016; Biller & Ross, 2011; Biller et al., 2012; Leow et al., 2015; Ross et al., 2010; Tian et al., 2015) and nitrogen levels around 6% are typical (Brown et al., 2010). Even at the lowest value, the nitrogen in the crude is higher than petroleum refineries are prepared to accept. Crudes must be below 0.25%wt. or they need pretreatment to avoid deactivating catalysts in refineries (Dutton, 2018b). The initial decrease in nitrogen concentration in the biocrude with increased severity of the reaction could be a sign of deamination of amino acids. This supposition is supported by the observation that the nitrogen is redistributed into the HPW, as shown in section 4.2.2. At yet higher temperatures or longer holding times, there appears to be a repolymerization of nitrogen containing compounds (Chen, 2013).

H/C ratios of the biocrudes range from 0.115-0.127 with higher H/C ratios found at lower temperatures, 50 min holding time, and higher %TS. The highest O/C ratio is 0.243, corresponding to the condition with the highest yield, 20%TS, 340°C, and 50 min retention time. The H/C ratios of the crudes are similar to those reported for Utah Tar Sands crudes, but the O/C and N/C ratios are much higher (Bunger, Thomas, & Dorrence, 1979). These ratios are shown in

section 4.4.1, along with the data from the tar sands study. O/C ratios increase with severity of the reaction for RT 280-340°C, which is most likely linked to continued decomposition of cellulose (Chen, 2013).

The HHV of LT916 biocrudes produced by each condition are 32.2-35.7 MJ/kg, as shown in Table 16. This is almost double the HHV of the original feedstock (19.38 MJ/kg) and is near the average for petroleum crude tar. These values agree with HHVs measured (Jena et al., 2011; Shakya et al., 2017, 2015) and calculated (Biller & Ross, 2011; Biller et al., 2012; Jena et al., 2011; Leow et al., 2015; Ross et al., 2010; Tian et al., 2015) for low lipid microalgae at these temperatures; the increase in HHV as reaction temperature goes up is also confirmed (Biller et al., 2012).

Table 16: Fresh Dried LT916 biocrude product CHN results, yield, and HHV.

Condition	RT (°C)	HT (min)	%TS	C (%wt.)	H (%wt.)	N (%wt.)	Yield (%daf)	HHV (MJ/kg)
FD2050A	280	50	20%	67.7±0.3	8.61±0.08	7.2±0.1	29±6	32.2
FD2050B	300	50	20%	69.11±0.05	8.7±0.1	8.12±0.05	34.2±0.6	33.2
FD2050C	320	50	20%	69.16±0.04	8.68±0.09	8.05±0.04	39±3	33.2
FD2050D	340	50	20%	68.8±0.1	8.6±0.1	5.9±0.2	42±6	32.5
FD2050E	350	50	20%	73.5±0.2	8.77±0.04	8.2± NA	41±7	35.7
FD2030D	340	30	20%	70.7±0.2	8.4±0.1	8.00±0.02	39±3	32.9
FD2040D	340	40	20%	70.24±0.01	8.6±0.1	8.00±0.08	39±3	33.7
FD2050D	340	50	20%	68.8±0.1	8.6±0.1	5.9±0.2	42±6	32.5
FD2060D	340	60	20%	71.74±0.04	8.6±0.1	6.97±0.05	39±4	34.3
FD1060B	300	60	10%	70.1±0.5	8.08±0.01	8.2±0.1	30±4	32.8
FD1560B	300	60	15%	70.20±0.04	8.21±0.01	7.6±0.3	32±2	32.9
FD2560B	300	60	25%	70.27±0.01	8.48±0.06	9.02±0.02	35±5	33.7
feedstock	NA	NA	100%	46.6±0.3	6.70±0.1	7.9±0.3	NA	19.4

NA not applicable
±NA not applicable, same value for replicates

4.2.1.3. Energy recovery and energy consumption ratio

The energy recovery based on the biocrude from HTL of LT916 fresh dried algae ranges from 51.0%-79.6%, as shown in Table 17. The data shows better ER is possible at higher temperatures and with more concentrated biomass in the feedstock. The highest value for ER is at 50 min. The yield at 60 min is decreased compared to the 50 min holding time and the increased HHV of the biocrude from the longer HT does not compensate for the loss of product.

Table 17: Fresh Dried LT916 biocrude energy balances, ER and ECR for different heat recovery (HR).

Condition	RT (°C)	HT (min)	% TS	ER	ECR (50%HR)	ECR (0%HR)
FD2050A	280	50	20%	51.0%	0.356	0.712
FD2050B	300	50	20%	61.7%	0.317	0.633
FD2050C	320	50	20%	70.6%	0.297	0.593
FD2050D	340	50	20%	73.9%	0.302	0.605
FD2050E	350	50	20%	79.6%	0.290	0.579
FD2030D	340	30	20%	69.3%	0.322	0.644
FD2040D	340	40	20%	72.2%	0.310	0.619
FD2050D	340	50	20%	73.9%	0.302	0.605
FD2060D	340	60	20%	72.9%	0.307	0.613
FD1060B	300	60	10%	54.0%	0.784	1.568
FD1560B	300	60	15%	57.3%	0.473	0.946
FD2560B	300	60	25%	64.1%	0.234	0.468

Processing LT916 generates biocrude with a net energy profit (ECR<1) for most conditions tested. The ECR ranges from 0.234-0.784 for a system with 50% heat recovery (HR) and 0.468-1.568 for a system with 0% heat recovery. The ECR is largely impacted by the %TS and the heat recovery. For most temperatures and holding times, the ECR is around 0.3 for 20% biomass and 50% HR, twice as much for 0%HR. However, this could be an underestimate for some of the

higher holding times. The ECR calculation makes no attempt to estimate the heat leakage losses for a reactor maintaining the temperatures for longer holding times. It only considers the heat added to bring the feedstock up to temperature and the energy in the biocrude. The heat lost over time is equipment specific, determined by heat loss and insulation of the reactor.

Figure 12 shows the ECR for the experiments comparing %TS of the feedstock. The system with 50% HR breaks even energetically for feedstocks with 10% or greater biomass, but for 0% HR the breakeven point is not reached until the feedstock is at least 15% biomass. The best value, an ECR of 0.24, indicates that HTL of LT916 could be a competitive biofuel. This is comparable with the energy returns for the steam-assisted gravity drainage process used on petroleum tar sands (Nikiforuk, 2011; Veasey, 2015). However, it should also be noted that the ECR in this form does not account for the increased energy input for dewatering feedstock or for increased pumping power for a more concentrated feedstock slurry. The results and trends from these data agree with the values reported for similar algae (Biller & Ross, 2011; Leow et al., 2015; Li et al., 2014) showing HTL is only energetically favorable for solid loading over 10% (Biller & Ross, 2011).

Neither of these energy calculations, ER or ECR, considers the energy in the gases, solids, or HPW. In that way they may be conservative estimates.

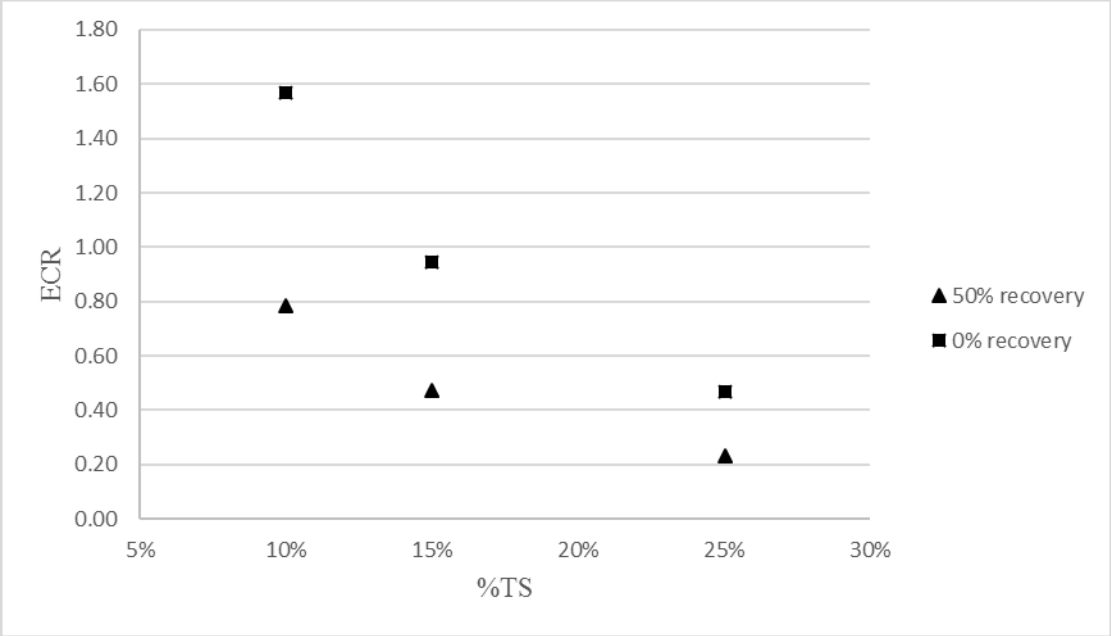

Figure 12: ECR of Fresh Dried LT916 biocrude production by HTL for feedstocks with different %TS and heat recovery (HR) of 0% and 50%.

4.2.2. Nutrient Recovery

4.2.2.1. Nitrogen recovery

Nitrogen concentrations in the biocrude range from 5.9-9.02%d.b., as shown in Table 18, next page. The lowest value, 5.9%d.b. (27.7%N recovered), was at 340°C, 50 min, 20%TS. The nitrogen concentration in the solids was between 4.11-6.19%d.b. Lower temperatures, shorter holding times, and lower %TS encourage nitrogen deposition in the solids. Total nitrogen (TN) in the HPW was found at concentrations of 4,000-12,200 mg/L. Higher TN concentrations in the HPW were associated with temperatures near 300°C, higher holding times, and higher %TS.

Table 18: Fresh Dried LT916 nitrogen concentrations and recoveries for biocrude, solids, and HPW.

	Biocrude		Solids		HPW	
Condition	%N (d.b.)	%N recovered	%N (d.b.)	%N recovered	TN (mg/L)	% N recovered
FD2050A	7.2±0.1	30.9%	6.19±0.06	14.1%	8300±700	46.2%
FD2050B	8.12±0.05	33.2%	5.5±0.2	9.3%	12200±400	68.1%
FD2050C	8.05±0.04	40.6%	5.1±0.1	8.1%	8400±300	46.7%
FD2050D	5.9±0.2	27.7%	4.70±0.01	4.2%	8400±100	47.0%
FD2050E	8.2± NA	48.0%	4.6±0.1	4.1%	7200±600	39.0%
FD2030D	8.00±0.02	39.0%	4.59±0.08	5.6%	7000±1000	37.0%
FD2040D	8.00±0.08	40.8%	5.3±0.2	6.9%	7400±500	40.7%
FD2050D	5.9±0.2	27.7%	4.70±0.01	4.2%	8400±600	47.0%
FD2060D	6.97±0.05	36.0%	4.11±NA	4.7%	9000±2000	48.9%
FD1060B	8.2±0.1	33.7%	4.63±0.03	5.2%	4000±1000	52.2%
FD1560B	7.6±0.3	30.7%	5.21±0.04	6.7%	6000±1000	49.4%
FD2560B	9.02±0.02	42.6%	5.8±0.3	8.9%	10000±2000	41.4%

±NA not applicable, same value for replicates

The nitrogen level in FD2050D biocrude is lower than the surrounding values would seem to predict. This sample was tested twice (both times in duplicate) and always tested low. The value here is the higher of the two analyses. The total mass of nitrogen accounted for in this data point was lower than its neighbors (79% compared to 90%). One reason for this could be ammonia that was volatilized before the liquid samples were tested. As shown later in Table 19, the percent of total N presenting as ammonium in these samples is low for this condition, supporting the theory. Organic acids have been shown to increase the ammoniacal compounds formed (Ross et al., 2010) and the biocrude from this condition has a substantial amount of palmitic acid. As the holding time is increased, the nitrogen partitions more into the HPW and less into the solids. As the %TS in the feedstock is increased, the nitrogen recovery in the biocrude and

solids rose while the nitrogen recovery in the HPW steadily dropped. The nitrogen concentration in the biocrude increased with increasing biomass, but not proportionally.

The nitrogen concentrations detected in the products are in agreement with reported values for similar conditions (Barlow et al., 2016; Biller & Ross, 2011; Biller et al., 2012; Jena et al., 2011; Ross et al., 2010; Shakya et al., 2017; Valdez et al., 2012). Valdez et al. (2012) show the majority of nitrogen is proportioned to each phase within 20 minutes, at a rate decided by the temperature of the reaction, and the variation in nitrogen with reaction time past that is less predictable. They report biocrude concentrations of 4-8%wt. for light and heavy crude. In their study, at the 50 min, 350°C condition they also show a low %N recovery compared to nearby data points. They point out a significant decline in biocrude nitrogen concentration across holding times of 30-60 min in the heavy crude at high temperatures (350°C) that is not redistributed into the light crude. As discussed later, in the LT916 biocrude recovered at 340°C, 50 min, only a small portion of the biocrude product is light crude (8%). This could also explain the low nitrogen recovery at this condition. Jena, Das, and Kastner (2011) report show increasing N concentrations in the HPW with increasing holding times up to 90 min and increasing solid loading up to 40%TS, as was seen with LT916. However, they show only show an increase in biocrude nitrogen containing compounds for RTs 200-250°C; then, the nitrogen in the biocrude decreases in with increasing temperature. Yu et al. (2011) observed increasing nitrogen recovery in the biocrude and lower nitrogen recovery in the solid products at temperatures leading up to 300°C with the yields of both products beginning to plateau at values near those observed in this study.

The amount of nitrogen found in the HPW as ammonium is shown in Table 19, as a concentration and as the percent of Total Nitrogen bound as ammoniacal nitrogen (%TN) in the HPW. Ammoniacal nitrogen concentrations in the HPW range from 2950-5575 mg/L. The

concentration increases with holding time (r^2=0.9976) and %TS (r^2=1) in the feedstock in a linear fashion. The ammonium concentration increases generally with reaction temperature. At 300°C, the ammonium concentration is high, compared to the surrounding temperatures. The ammoniacal nitrogen makes up 35.4-70.8% of the Total Nitrogen in samples. The %TN increases across increasing holding time and increasing %TS, though less linearly than the ammoniacal nitrogen concentrations (r^2=0.69 and r^2=0.80, respectively). The %TN also increases with temperature, but similarly to the concentration, the %TN at 300°C is higher than at 280°C or 320°C.

These trends are echoed in the work of Yu et al. (2011) . They also found %TN to be generally between 40%-70% at these conditions. The %TN in their study also increased with increasing temperatures (250-400°C) and holding times (0-90 min).

Table 19: Fresh Dried LT916 HPW ammonium concentrations and %TN.

Condition	NH_3-N (mg/L)	%TN
FD2050A	2950	35.4%
FD2050B	5575	45.8%
FD2050C	3775	44.9%
FD2050D	4700	55.8%
FD2050E	5075	70.8%
FD2030D	3675	55.1%
FD2040D	4200	56.6%
FD2050D	4700	55.8%
FD2060D	5325	59.7%
FD1060B	1775	40.7%
FD1560B	2575	40.4%
FD2560B	4150	42.8%

4.2.2.2. Carbon recovery

The percent carbon recovered in the biocrude and gas products increases with increasing temperature, as the percent carbon recovered in the solids decreases, as shown in Table 20. Increasing holding time has the same effect. As %TS is increased, the carbon recovery in the solids product increases and the carbon recovery in the gas decreases. The carbon recovery in the biocrude is considerably higher at 25%TS than at lower %TS. Overall, the biocrude is 67.7-73.5% carbon (d.b.), accounting for half to three-quarters of the initial feedstock carbon. The solids product is 35.4-53.9% carbon (d.b.) and accounts for 20% or less of the carbon balance. The gas products accounts for 7.3-11.5% of the carbon recovery and the HPW is 8.9-37.2%, by difference.

Table 20: Fresh Dried LT916 carbon concentrations and recoveries for all products: biocrude, solids, gas, and HPW.

	Biocrude		Solid		Gas	HPW
Condition	%C (d.b.)	%C recovered	%C (d.b.)	%C recovered	%C recovered	%C recovered
FD2050A	67.7±0.3	49.3%	53.9±0.5	20.8%	7.3%	22.7%
FD2050B	69.11±0.05	47.8%	50±2	14.4%	8.5%	29.3%
FD2050C	69.16±0.04	59.1%	47±1	12.8%	8.4%	19.7%
FD2050D	68.8±0.1	54.3%	45.9±0.1	6.9%	10.8%	28.0%
FD2050E	73.5±0.2	72.6%	47±2	7.0%	11.5%	8.9%
FD2030D	70.7±0.2	57.3%	35.4±0.5	7.3%	9.1%	26.2%
FD2040D	70.24±0.01	60.6%	44±1	9.6%	10.9%	18.9%
FD2050D	68.8±0.1	54.3%	45.9±0.1	6.9%	10.8%	28.0%
FD2060D	71.74±0.04	62.8%	37.9±0.3	7.4%	11.5%	18.3%
FD1060B	70.1±0.5	49.0%	41.8±0.1	4.0%	9.8%	37.2%
FD1560B	70.20±0.04	48.3%	41.0±0.2	6.7%	8.9%	36.1%
FD2560B	70.27±0.01	56.2%	43±2	14.0%	8.7%	21.1%

These results agree with trends in the literature for carbon recovery in high protein and carbohydrate feedstocks. The results are highly temperature dependent. At low temperatures, carbon recovery in the HPW and solids dominates. At higher temperatures, the carbon is more likely in the biocrude (Elliott et al., 2015, 2013; Jena et al., 2011). The biocrude carbon recovery values at 340-350°C are in agreement with the range reported by PNNL for similar temperatures (50.3%-81.8%) (Elliott et al., 2013), though on the low end, close to those reported for other low lipid algae. (Leow et al., 2015; Ross et al., 2010). In a previous work, Biller and Ross (2011), showed very low carbon recovery in the crude for purely protein or carbohydrate model feedstocks of 10%-30% in the biocrude and 20%-45% for algal feedstocks, pointing to a synergistic effect of mixed protein and carbohydrate feedstocks that is demonstrated in the LT916 study as well. Yu et al. (2011) report a higher range for carbon in the HPW (35%-40%) at temperatures 220-300°C, but their recoveries at 300°C agree with the values here. Biller et al. (2012) confirm that up to 40% of carbon can be recovered in the HPW at these temps from low lipid algae.

4.2.3. Best yield condition characterization

In addition to the previously discussed tests, the products from the trial that produced the best biocrude yield (FD2050d2) were tested further to determine fuel quality characteristics and chemical makeup of the HPW. Further fuel quality tests included determining the sulfur content, distillation fractions, and chemical species, by GC-MS. HPW was also analyzed by GC-MS.

For the fresh dried LT916, the best biocrude yield was for HTL conditions of 20% biomass, 50 min holding time, 340°C reaction temperature.

4.2.3.1. Sulfur content

As shown in Table 21, the sulfur content of the biocrude is low, 0.07% by mass, less than 0.5% classifying it as a "sweet" oil (Dutton, 2018b). The recovery of sulfur in the biocrude and the solids combined is only 10%, suggesting the majority of the sulfur ends up in the HPW or volatilized. High temperatures can result in high levels of sulfur in the biocrude, but levels less than 0.5% are typical (López Barreiro et al., 2013; Vardon et al., 2011).

Table 21: FD2050D2 solid and biocrude product sulfur concentrations and recoveries

Sample name	Sample type	%S (d.b.)	%S recovery
FDLT916	feedstock	0.65%	NA
FD2050D2s	best run-solids	0.54%	6%
FD2050D2o	best run-biocrude	0.07%	4%

NA not applicable

4.2.3.2. GC-MS

The major peaks on the GC-MS spectra of FD2050D2 biocrude and HPW products, derivative (non-volatile) and volatile, were identified and classified into chemical groups as discussed in section 3.2.6. Table 22, next page, shows the relative peak area as a percent of the total peak area for each group.

Table 22: Fresh Dried LT916 product GC-MS results. Relative peak area for each chemical class as a percent of the total peak area of detected compounds.

Product	Sample	PHE	PO	NC	OC	CC	NX	OX	HC
HPW	volatile	0.2%		37.6%	0.9%	7.8%	12.0%	41.4%	
HPW	non-vol	3.7%	0.3%	57.4%		0.9%	1.4%	36.4%	
crude	volatile					1.5%		78.9%	19.6%
crude	non-vol	6.1%	2.4%	5.2%		5.8%	1.2%	79.3%	

The class of compounds with the largest peak areas detected in the crude are oxygenates, followed by hydrocarbons in the volatiles and phenols in the non-volatiles. The single largest peak in the crude volatile spectrum is for hexanedioic acid, bis(2-ethylhexyl) ester, shown in Figure 13, which represents 59.47% of the total peak area. The single largest peak in the crude non-volatile spectrum is for palmitic (hexadecenoic) acid, shown in Figure 14, which represents 63.63% of the total peak area. One phosphorus containing compound, phosphoric acid is detected. It must be in small quantity because phosphorus in the biocrude doesn't register by ICP, its relative peak area in the GC-MS spectrum is 2.40% of the total non-volatile biocrude spectrum.

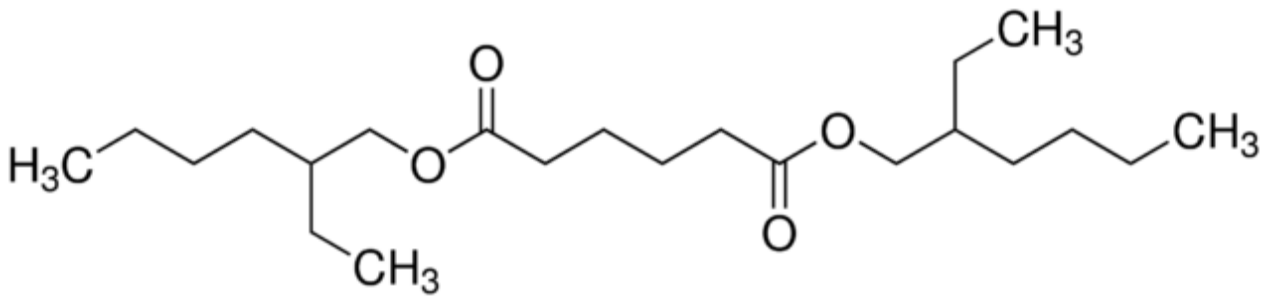

Figure 13: Hexanedioic Acid, Bis(2-Ethylhexyl) Ester, the compound with the largest peak in volatile crude of FD2050D2, as shown on Sigma Aldrich website (Sigma Aldrich, n.d.-c).

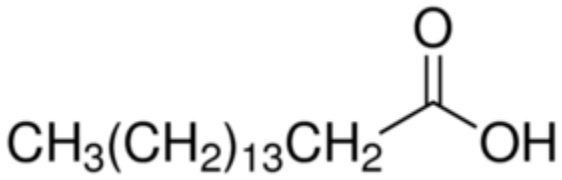

Figure 14: Palmitic acid (hexadecenoic), as shown on Sigma Aldrich website (Sigma Aldrich, n.d.-f)

Most compounds detected in the non-volatile compounds in the HPW are oxygenates, followed by nitrogen heterocycles. The reverse is true of the volatiles, nitrogen heterocycles are the largest class followed by oxygenates. The single largest peak in the HPW volatile spectrum is for 3-Pyridinol which represents 15.78% of the total peak area. However, in this sample the three next nearest peaks are close in relative area and deserve mention: acetic acid (13.85%), butanoic acid (13.44%), and Benzene acetic acid (12.59%), shown in Figure 15, next page. Also pictured, the single largest peak in the crude non-volatile spectrum is for pyroglutamic acid (pidolic acid) which represents 53.09% of the total peak area. The phosphorus compounds identified are monomethyl phosphate and phosphoric acid in the HPW.

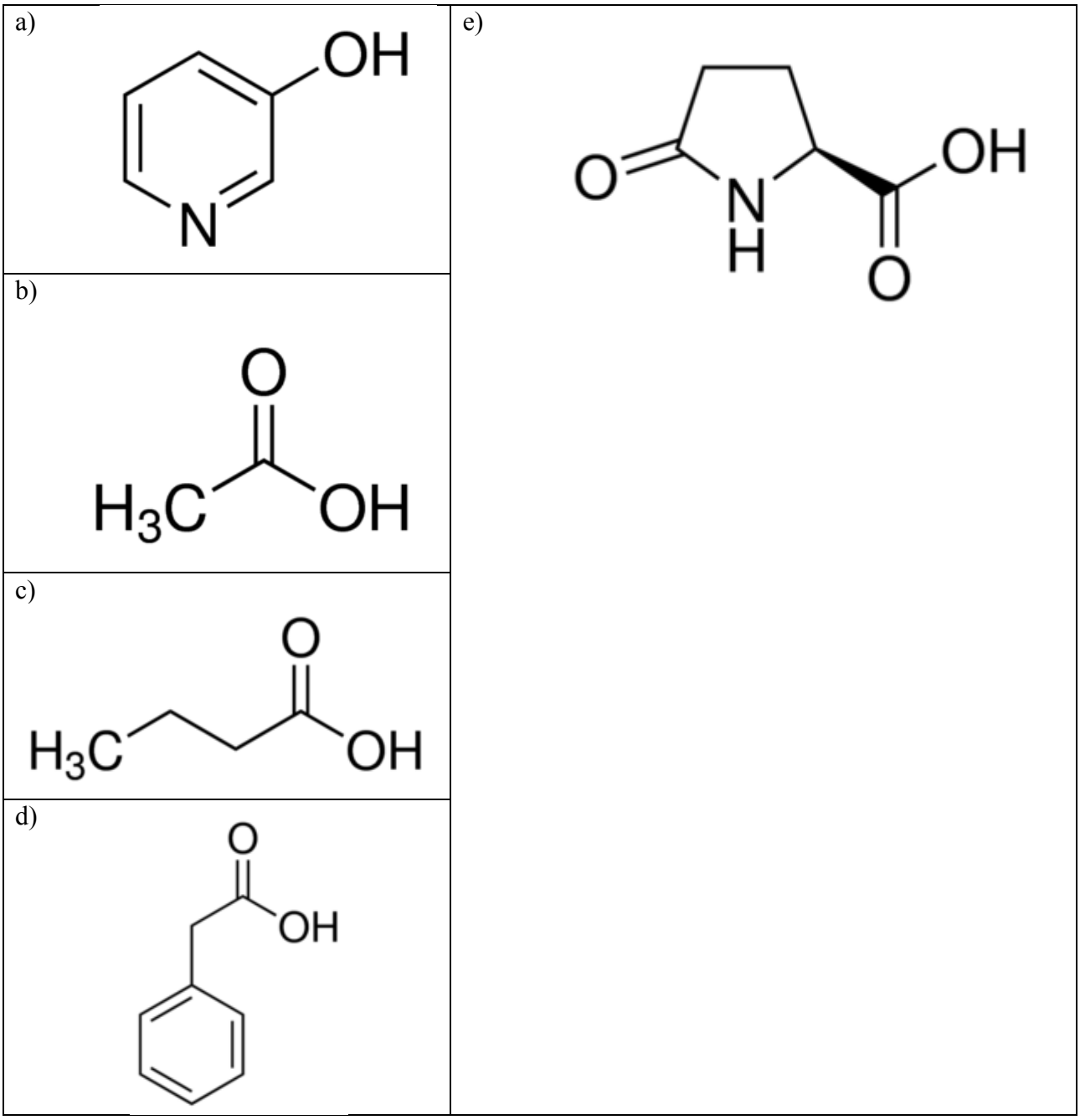

Figure 15: HPW compounds with largest peak areas, as shown on Sigma Aldrich website. Left, volatile GC-MS top four compounds by relative peak area, (a) 3-pyridinol, (b) acetic acid (c) butanoic acid, and (d) Benzene acetic acid. Right, derivative GC-MS top compound by relative peak area, (e) pyroglutamic acid (Sigma Aldrich, n.d.).

Relative peaks areas and types of compounds identified by GC-MS in the biocrude and HPW are supported in the literature. Large amounts of palmitic acid have been observed in bio-

oils from *Nannochloropsis* (Brown et al., 2010; Li et al., 2014) and the Taihu Lake HAB (Guo et al., 2015). The relative peak area covered by HC for FD2050D2 agrees with the average for the low-lipid algae biocrude produced by Li et al. (2014) at temperatures up to 300°C and holding times 30-90 min, though the Dianchi Lake HAB biocrude had HC peak areas half this size (Tian et al., 2015). Often, high hydrocarbon content at high temperature is explained by decarboxylation of fatty acids (Shakya et al., 2015), but this is not possible because of the very low level of lipids in the LT916 starting feedstock (<1%). However, the same phenomena has been observed with woody biomass and agricultural residues of very low lipid content, suggesting another route of hydrocarbon formation (Brown et al., 2010) from carbohydrates (Tian et al., 2015) or decarboxylation of protein polymerization intermediates like organic acids (Li et al., 2014). The OX relative peak areas in the crude are high but in the range of the 75% maximum reported by Li et al. (260°C, 90 min) and less than the 80% maximum reported by Tian et al. (2015). Compared to Li et al., LT916 biocrude (340°C) has low relative peak areas for NC. This difference has been documented for high and low temperature crudes (Guo et al., 2015). The OX level in the HPW is similar to those reported by Tian et al. for Dianchi Lake HAB HPW from HTL processing at 340°C using higher holding times (60, 90 min). The Tian et al. study also found extremely high levels of nitrogen-containing compounds in the HPW from higher temperatures (340°C).

4.2.3.3. TGA

The thermogravimetric results of the biocrude from FD2050D2o are shown in Figure 16, next page. The calculated percent mass of the light (70-200°C), medium(200-350°C), and heavy (350°C+) fractions are shown later in Figure 17. The medium crude is the largest fraction at 52%, indicating the fuel may be good for kerosene or diesel supply line supplementation. The gasoline fraction, the light portion, is only 8%wt.

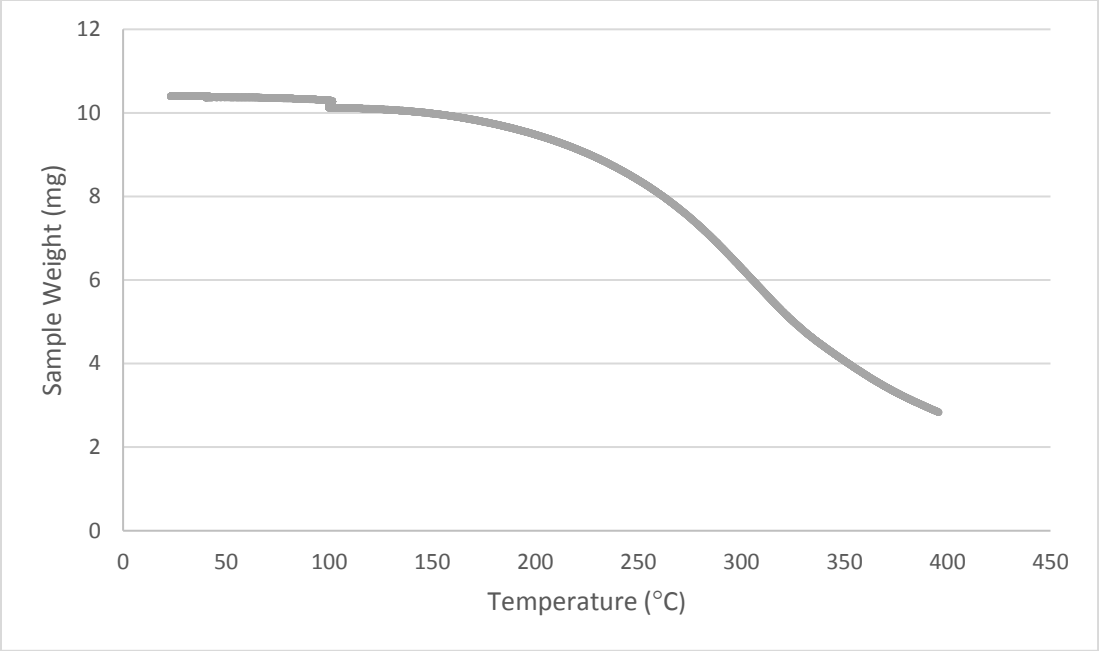

Figure 16: Weight of FD2050D2 biocrude sample vs. temperature from TGA testing.

The small jog in the weight of the sample at 40°C and 100°C in Figure 16 is due to two isotherms, at the boiling points of DCM and water respectively. The percentage of mass lost during the 40°C isotherm was 0.02% and during the 100°C isotherm it was 0.09%. This indicates a small level of DCM and water contaminants in the recovered crude. A small percentage of the biocrude (0.4%) is shown to be volatile at temperatures lower than 70°C. This is probably an underestimation. The collection of biocrude involves a solvent drying step at room temperature; it is possible that some light weight compounds are lost with the DCM.

The large medium weight fraction of FD2050D2o is unusual. As shown Table 23, next page, compared to hardwood biocrude, Spirulina biocrude, and even tar-sands crudes, FD2050D2o has a much larger medium fraction and the smallest heavy fraction. Around 60% of the mass is in

the fuel range (<350C) compared to 30-55% from other sources. This should prove good for the energy quality and economics of the HAB biocrude production.

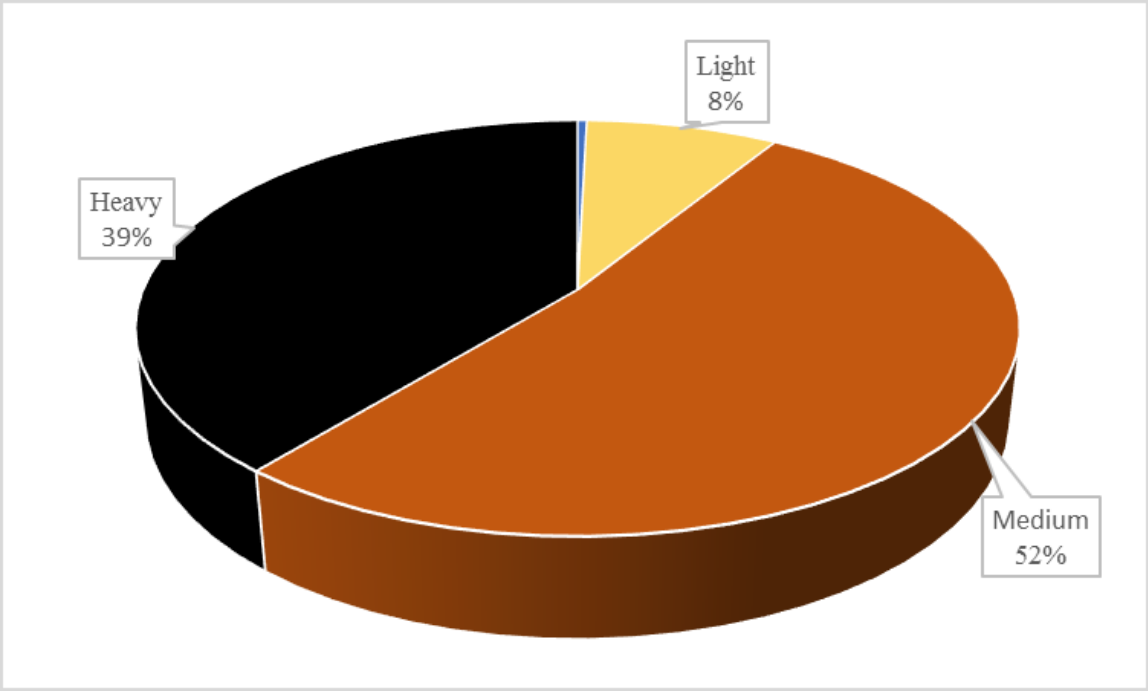

Figure 17: Mass percentages of light, medium, and heavy crude fractions in the FD2050D2 biocrude.

Table 23: Mass of light, medium, and heavy fractions from Fresh Dried LT916 biocrude (RT=340°C, HT=50 min, %TS=20%) and comparable studies.

Feedstock	%C	%H	%N	%O	Light	Med	Heavy	Reference
LT916 (fresh dried)	68.75	8.58	5.93	16.74	8	52	39	this study
Hardwood	83.88	10.41	0.4	5.31	14.61[a]	33.23	48.66	(Hoffmann et al., 2016)
Spirulina	68.9	8.9	6.5	14.9	<5	≈25	70	(Vardon et al., 2011)
Athabasca tar-sand bitumen	82.5	10.2	0.47	1.7	3	17.3[b]	79.7	(Bunger et al., 1979)

[a] cold trap catches 1.11% (15-100°C)
[b] 200-365°C

4.2.4. Fresh dried LT916 conclusion

The previously discussed results indicate the feedstock from Lake Tainter should be processed at temperatures of 320-340°C for 50 min, with a preference for the higher temperature. The H/C ratio in this range is high, the yield is high, and the N/C ratio is low. Slightly better HHV, ER, and ECR for this feedstock is possible at 350°C at the sacrifice of yield and increased nitrogen in the biocrude. Higher %TS also improves ER and ECR in this setting, but in practical use, pumping and dewatering energy costs need to be considered.

This study has shown that up to 41.8±6.1%daf biocrude yield can be produced from HTL of the fresh dried LT916 feedstock. Peak biocrude yield was produced at an RT of 340°C and HT of 50 min with 20%TS feedstock. The biocrude produced has an HHV of 32.5 MJ/kg, giving the process an ER of 73.9% and ECR of 0.605 with 0%HR and 0.302 with 50%HR. This biocrude has a low sulfur content (0.07%wt.), but a high nitrogen content (5.93%wt) and oxygen content (16.74%wt. by calc.), nearly 10x what a petroleum crude would contain. The light and medium fractions (bp<350°C) are 60%wt. of the crude. At this temperature, 47% of the nitrogen in the feedstock is recoverable in the HPW, 55.8% of it as ammoniacal nitrogen. Phosphorus may be recoverable in the HPW as monomethyl phosphate and phosphoric acid.

High nitrogen content, oxygen content, and probable acid nature of the biocrude indicate upgrading is needed for transportation grade fuel.

4.3. Aged Dried LT916 HTL

The following sections discuss the product distributions, energy returns, nutrient distributions, and fuel quality for aged dried LT916 subjected to three ranges of reaction conditions (RT, HT, %TS). The biocrude and HPW products from the run with the best biocrude yield (AD2050C) are characterized in more depth and these results are discussed.

Since the aged dried LT916 values are close to those determined in the fresh dried LT916 results, to avoid repetition, no attempt is made to validate the results by comparison with other literature in this section. The differences between the two feedstocks are discussed in section 4.4.

4.3.1. Energy returns

This section discusses the product distributions and associated energy returns for HTL conversion of aged dried LT916 for reactions conducted at RT of 280-350°C, HT of 30-60 min, and 10-25%TS.

4.3.1.1. Yields

Temperature

As shown in Figure 18, the biocrude yield initially increases with temperature and peaks at 320°C and 340°C at 37±2% of the biomass dry ash free weight (daf). Meanwhile, the gas fraction initially increases with an increase in temperature and peaks at 340°C at 17.7±0.6%daf. The solid product fraction decreases in yield as the reaction temperature rises, reduced to around 14.5%daf at higher temps.

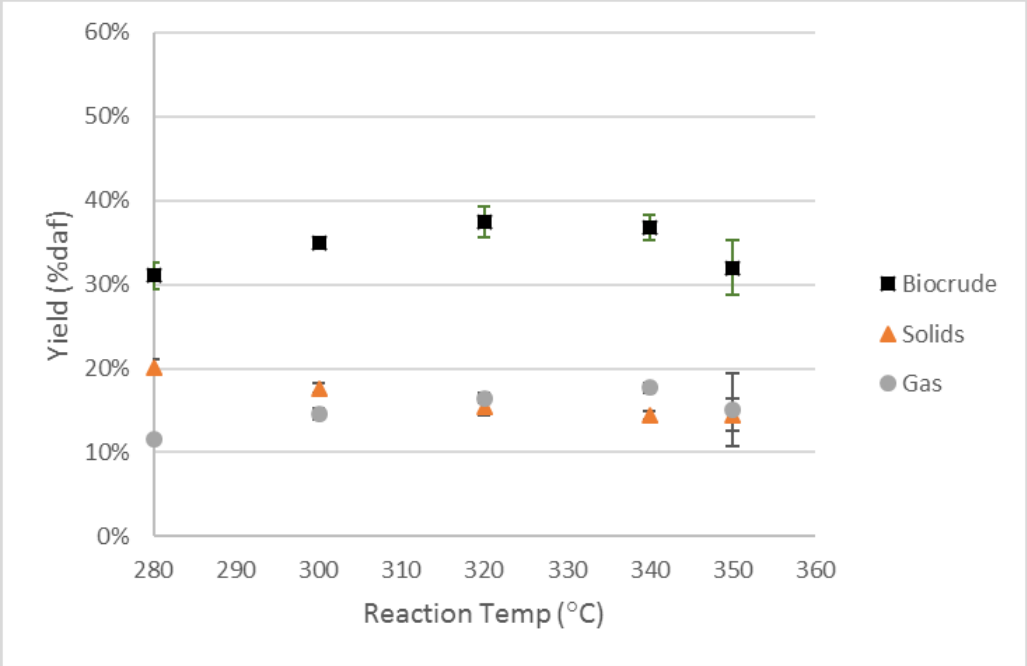

Figure 18: HTL product yields from Aged Dried LT916 processed at different RT.

The yields of biocrude, solids, and gas strongly respond to a change in reaction temperature in the aged feedstock. There was a statistically significant difference between temperature groups as determined by analyses of the biocrude yield (one-way ANOVA: $F(4,10)=6.42$, $p=0.0079$), the solids (one-way ANOVA: $F(4,10)=15.36$, $p=0.0003$), and gas product yields (Welch's ANOVA: $F(4,10)=46.99$, $p=0.0186$) as a function of RT. Differences of Least Squares Means p-values, shown in Table 24, next page, comparing biocrude yields show there is a statistical probability that the yield is lower at 350°C than at 320°C or 340°C and that biocrude yield at 300-340°C is higher than 280°C. The p-values also show the solids yield decreases with increasing RT, though the difference at higher temperatures is not significant. The gas yield increases when the RT is increased from 280°C to higher temperatures up to 340°C. These temperatures correspond to energy needed to hydrolyze different biochemical compounds as discussed in fresh temperature section 4.2.1.1.

Cumulatively, the data suggest an RT of 320°C or 340°C is beneficial for biocrude yield with a maximum conversion of biomass at 320°C. The highest biocrude yield was observed at an at an RT of 320°C and the co-product yields indicate that 320-340°C is a plateau for biomass conversion in the sub-critical temperature region.

Table 24: Differences of Least Squares Means p-values from the ANOVA analyses of product yields at different RT for aged dried LT916.

		p-values							
RT (°C)	Product	280		300		320		340	
300									
	biocrude	0.0322	[a]	NA					
	solids	0.0180	[a]	NA					
	gas	0.0039	[a]	NA					
320									
	biocrude	0.0024	[a]	0.1551	[b]	NA			
	solids	0.0003	[a]	0.0320	[a]	NA			
	gas	0.0006	[a]	0.0224	[a]	NA			
340									
	biocrude	0.0042	[a]	0.2575	[b]	0.7430	[b]	NA	
	solids	<0.0001	[a]	0.0045	[a]	0.2761	[b]	NA	
	gas	0.0002	[a]	0.0037	[a]	0.0722	[b]	NA	
350									
	biocrude	0.5284	[b]	0.0967	[b]	0.0071	[a]	0.0126	[a]
	solids	<0.0001	[a]	0.0051	[a]	0.3064	[b]	0.9422	[b]
	gas	0.3035	[b]	0.8714	[b]	0.6295	[b]	0.3978	[b]

[a] significant difference in Least Squares Means product yield between the temperatures.
[b] no significant difference in product yield Least Squares Means detected
NA not applicable, same temp

Holding time

The biocrude yield peaks at the 50 min HT, producing 37±2%daf for an RT of 350°C, 20%TS. The gas yield also peaks at 50 min at 17.7±0.7%. At 30 and 60 min, the average biocrude yield is lower, 33-34%daf, as shown in Figure 19, next page. Over this range, the solid product yield decreases slowly.

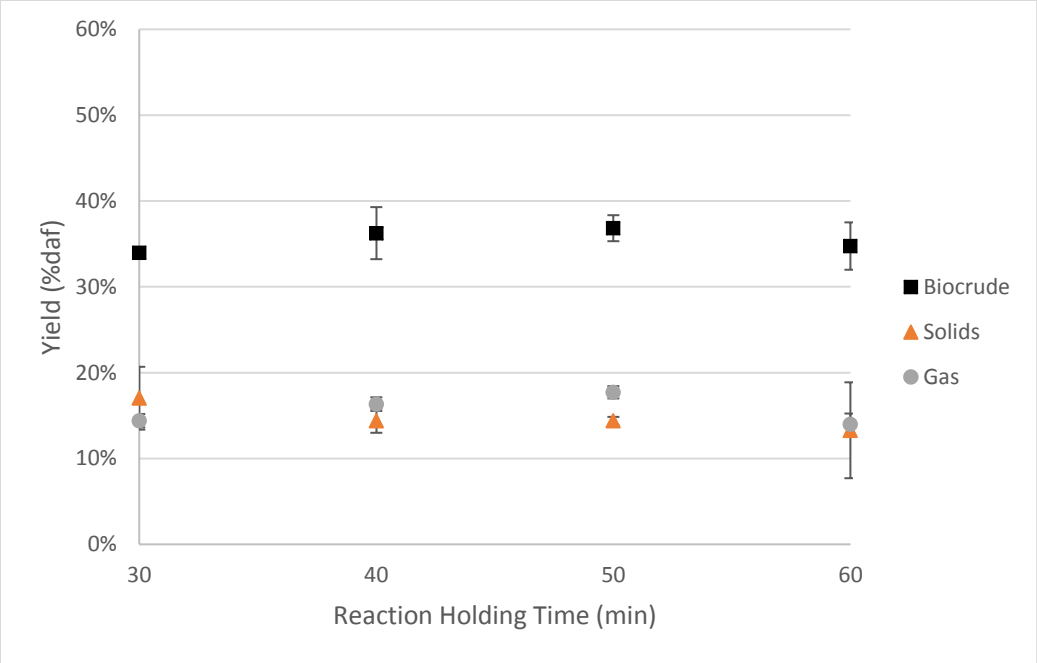

Figure 19: HTL product yields from Aged Dried LT916 processed at different HT.

One-way ANOVA analyses of product yields as a function of holding times did not meet the significance level to reject the null for biocrude ($F(3,8)=0.44$, $p=0.7333$), solids ($F(3,8)=0.58$, $p=0.6424$), or gas yields ($F(3,8)=1.79$, $p=0.2269$) as HT is increased. However, because of the limited availability of the feedstock, more trials could not be run. Paired two sample t-tests showed that there is no significant difference in the means of the product yields for any two individual holding times.

Solid loading

The data in Figure 20, next page, shows the biocrude yields for HTL at 300°C and 60 min for different %TS. The biocrude average yield increases with the solid loading ratio and the average gas yield does too, slightly. There is no clear trend for the solid product and it is nearly constant over the changes in %TS in the feedstock.

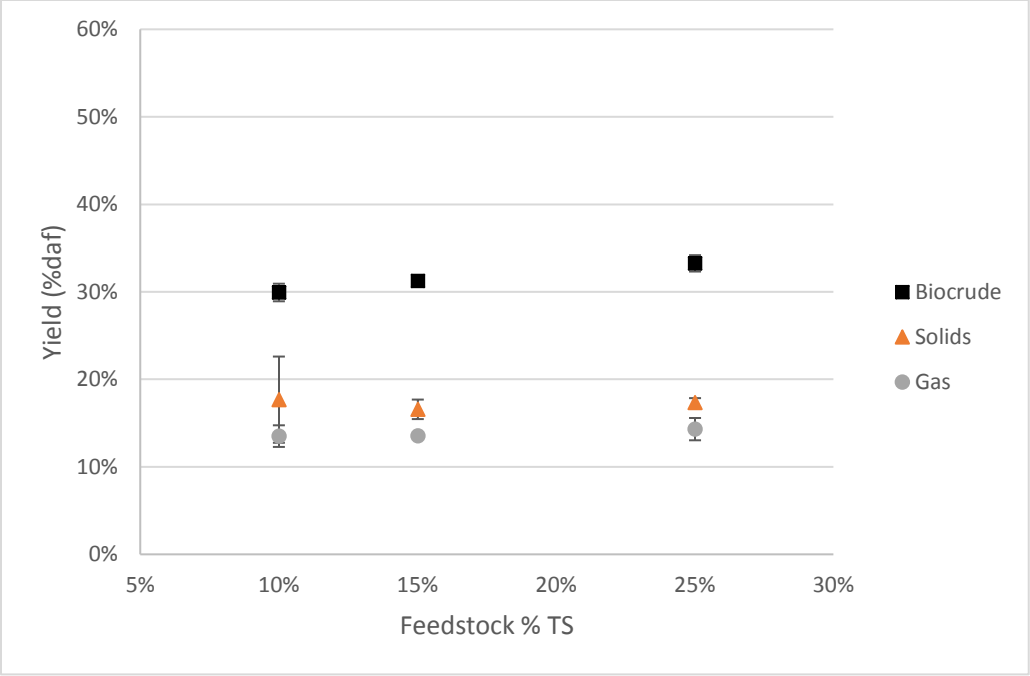

Figure 20: HTL product yields from Aged Dried LT916 processed with different %TS.

One-way ANOVA analyses of product yields as a function of feedstock loading did indicate there is a probability the biocrude yield increases with higher %TS ($F(2,6) = 10.86$, $p = 0.0101$). However, there was not significant statistical evidence to reject the null for solids yield ($F(2,6) = 0.12$, $p = 0.08925$) or gas yields ($F(2,6) = 0.58$, $p = 0.5907$). Least Squares Difference post-hoc analysis indicates the 25%TS mean biocrude yield is statistically different than the 10%TS and 15%TS means, as shown in Table 25, next page.

Table 25: Differences of Least Squares Means p-values from the ANOVA analyses of product yields at different %TS for Aged Dried LT916.

		p-values			
%TS (d.b.)	Product	10		15	
15					
	biocrude	0.1215	[b]	NA	
25					
	biocrude	0.0360	[a]	0.0304	[a]

[a] significant difference in Least Squares Means product yield between the temperatures.
[b] no significant difference in product yield Least Squares Means detected
NA not applicable, same temp

4.3.1.2. Biocrude CHN and HHV

As shown in Table 26, next page, the CHN values for biocrude have elevated carbon levels (67.5-73.15%wt.) and slightly elevated hydrogen levels (8.2-9.1%wt.) compared to the feedstock (47.7%C, 6.5%H). Nitrogen levels in the crude (4.23-7.61%wt.) can be slightly higher or lower than the original biomass (6.7%wt.). The nitrogen concentrations decrease with severity pointing to deamination of proteins as with the fresh dried feedstock (section 4.2).

H/C ratios range from 0.114-0.134 with higher H/C ratios found at lower temperatures, 30 min holding time, and higher %TS. The highest O/C ratio is 0.277, corresponding to, 25%TS, 300°C, and 60 min retention time. The H/C ratios of the crudes are similar to those reported for Utah Tar Sands crudes, but the O/C and N/C ratios are much higher as shown in section 4.4.1 (Bunger et al., 1979).

The HHV of LT916 biocrudes produced by each condition are 31.6-34.7 MJ/kg, as shown in Table 26. This is almost double the HHV of the original feedstock (19.73 MJ/kg). The HHV of biocrudes increases with temperature, holding times, and %TS.

Table 26: Aged Dried LT916 biocrude product CHN results

Condition	RT (°C)	HT (min)	%TS	C (%wt.)	H (%wt.)	N (%wt.)	Yield (%daf)	HHV (MJ/kg)
AD2050A	280	50	20%	69.0±0.2	8.44±0.01	6.5±0.2	31±2	32.5
AD2050B	300	50	20%	69.66±0.04	8.30±0.01	7.61±NA	34.9±0.1	32.8
AD2050C	320	50	20%	71.08±0.08	8.47±0.01	7.3±0.1	37±2	33.7
AD2050D	340	50	20%	72.05±0.08	8.48±0.04	7.20±0.05	37±2	34.3
AD2050E	350	50	20%	72.92±0.04	8.4±0.1	7.47±0.01	32±3	34.7
AD2030D	340	30	20%	67.5±0.2	8.51±0.08	5.4±0.1	34.0±0.6	31.6
AD2040D	340	40	20%	70.3±0.1	8.2±0.1	7.4±0.1	36±3	32.9
AD2050D	340	50	20%	72.05±0.08	8.48±0.04	7.20±0.05	37±2	34.3
AD2060D	340	60	20%	73.15±0.07	8.3±0.1	7.22±0.06	35±3	34.6
AD1060B	300	60	10%	70.5±0.2	8.30±0.06	7.11±NA	30±1	33.2
AD1560B	300	60	15%	70.89±0.08	8.43±0.01	7.26±0.01	31.2±0.6	33.6
AD2560B	300	60	25%	67.91±0.06	9.1±0.1	4.2±0.1	33.3±0.9	32.5
feedstock	NA	NA	100%	47.66±0.04	6.46±0.08	6.73±0.04	NA	19.73

NA not applicable
±NA not applicable, same value for replicates

4.3.1.3. Energy recovery and energy consumption ratio

The energy recovery based on the biocrude from HTL of LT916 aged dried algae ranges from 54.1-68.8%, as shown in Table 27. The data shows the maximum ER, 68.8%, is possible at 320°C and 340°C for a 50 min holding time. No clear trend is noticeable for ER across holding times. Better ER is possible with more concentrated biomass in the feedstock.

The ECR for processing LT916 indicates a net energy profit (ECR<1) for most conditions tested. The ECR ranges from 0.255-0.784 for a system with 50% heat recovery (HR) and 0.510-1.567 for a system with 0% heat recovery. The ECR is largely impacted by the %TS and the heat recovery. For most temperatures and holding times, the ECR is around 0.3 for 20% biomass and 50% HR, twice as much for 0%HR. However, this could be an underestimate for some of the higher holding times as discussed in the Fresh Dried LT916 HTL section 4.2.1.3.

Table 27: Aged Dried LT916 biocrude energy balances, ER and ECR for different heat recovery (HR), holding time (HT), and reaction temp (RT), and %TS.

Condition	RT (°C)	HT (min)	% TS	ER	ECR (50%HR)	ECR (0%HR)
AD2050A	280	50	20%	54.5%	0.331	0.662
AD2050B	300	50	20%	62.5%	0.314	0.627
AD2050C	320	50	20%	68.8%	0.305	0.610
AD2050D	340	50	20%	68.8%	0.326	0.651
AD2050E	350	50	20%	60.5%	0.382	0.763
AD2030D	340	30	20%	58.6%	0.382	0.764
AD2040D	340	40	20%	65.1%	0.344	0.688
AD2050D	340	50	20%	68.8%	0.326	0.651
AD2060D	340	60	20%	65.5%	0.342	0.683
AD1060B	300	60	10%	54.1%	0.784	1.567
AD1560B	300	60	15%	57.2%	0.475	0.951
AD2560B	300	60	25%	59.0%	0.255	0.510

Figure 21, next page, shows the ECR for the experiments comparing %TS of the feedstock. The system with 50% HR breaks even energetically for feedstocks with less than 10% biomass, but for 0%HR the breakeven point is at 15% biomass. The best value, an ECR of 0.24, is at the highest concentration of biomass in the feedstock, 25%TS, and 50% HR.

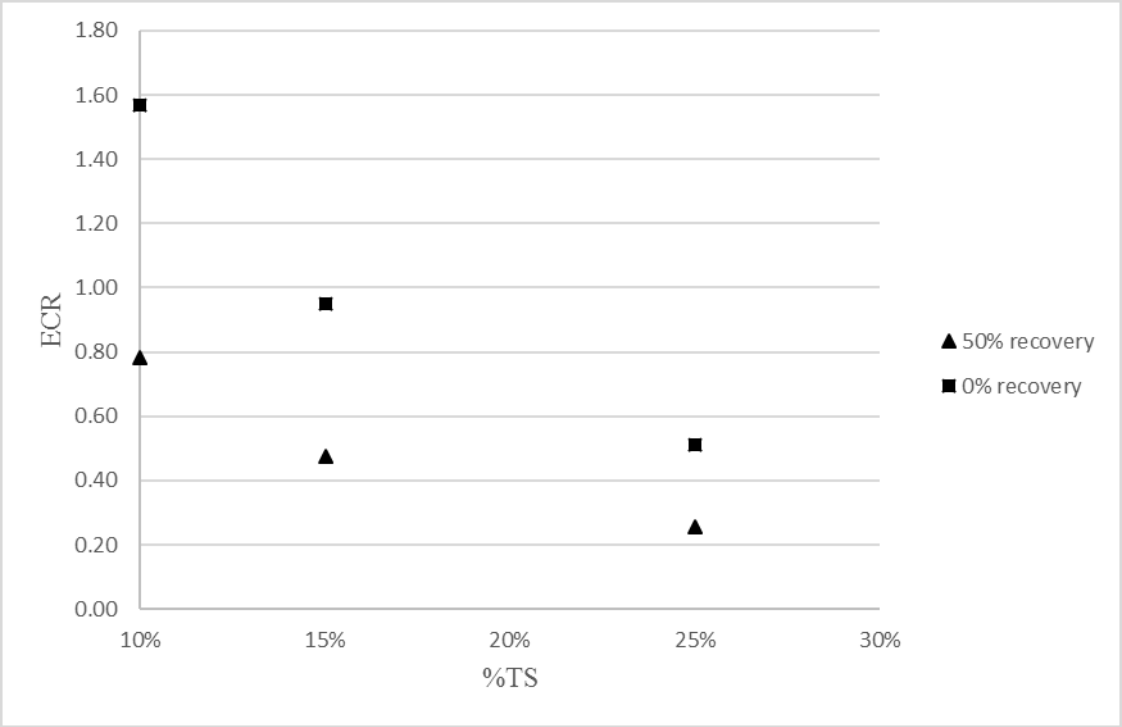

Figure 21: ECR of Aged Dried LT916 biocrude produced with different %TS feedstocks, heat recovery (HR) of 0% and 50%.

4.3.2. Nutrient recovery

4.3.2.1. Nitrogen recovery

The average nitrogen concentration in the solids was between 3.49-7.3% (d.b.). As shown in Table 28, lower temperatures, shorter holding times, and lower %TS encourage nitrogen deposition in the solids. Total nitrogen (TN) in the HPW was found at average concentrations of 1800-8800 mg/L. Higher TN concentrations in the HPW were associated with higher %TS. The 340°C, 50 min condition had peak TN concentration in HPW measured for both the temp and holding time ranges. However, this point is also one where the overall amount of N recovered is

high (95% for biocrude+solids+HPW). The total N recovered in the biocrude and solids is lowest at the highest temp, 350°C, and the shortest holding time, 30 min.

Table 28: Aged Dried LT916 nitrogen concentrations and recoveries for biocrude, solids, and HPW

	Biocrude		Solids		HPW	
Condition	%N (d.b.)	%N recovered	%N (d.b.)	%N recovered	TN (mg/L)	%N recovered
AD2050A	6.5±0.2	29.5%	7.3±0.2	21.4%	6300±400	40.9%
AD2050B	7.61±NA	36.9%	7.07±0.08	17.8%	4500±100	29.3%
AD2050C	7.3±0.1	38.8%	6.12±0.04	12.5%	4500±600	29.2%
AD2050D	7.20±0.05	38.3%	4.85±0.06	9.6%	7300±800	47.0%
AD2050E	7.47±0.01	35.7%	3.0±0.2	7.0%	6000±400	39.0%
AD2030D	5.4±0.1	25.7%	5.41±0.03	10.3%	4500±300	29.7%
AD2040D	7.4±0.1	40.7%	3.49±0.02	6.3%	7000±500	45.56%
AD2050D	7.20±0.05	38.3%	4.85±0.06	9.6%	7300±800	47.0%
AD2060D	7.22±0.06	34.2%	4.7±0.2	12.1%	6500±500	42.3%
AD1060B	7.11±NA	30.6%	4.89±0.04	15.8%	1800±100	24.4%
AD1560B	7.26±0.01	32.1%	5.23±0.01	11.4%	3800±400	34.3%
AD2560B	4.2±0.1	19.9%	5.66±0.08	14.0%	8800±900	44.4%

±NA not applicable, same value for replicates

As temperature increases, the biocrude initially increases in %N and the solids decrease in %N. At its peak, RT= 320°C, 38.8% of the feedstock nitrogen is recovered in the crude and 29.2%, is recovered in the HPW. As the holding time is increased, the nitrogen appears to partition more into the HPW and less into the solids or biocrude. As the %TS is increased past 15%, the nitrogen recovery and nitrogen concentration in the HPW and solids increased while the %N measured in the biocrude tapered down. The nitrogen concentration in the biocrude produced with 25%TS is nearly half the concentration of the crude at 15%, though the overall recovery in all products is the same.

The amount of nitrogen found in the HPW as ammoniacal nitrogen is shown in Table 29 in a concentration and as percentage of Total Nitrogen bound as ammoniacal nitrogen (%TN) in the HPW. Ammoniacal nitrogen concentrations in the HPW from ADLT916 ranges from 1425-4075 mg/L and the concentration increases with reaction temperature (r2=0.964), holding time (r^2=0.927), and %TS (r^2=.989) in the feedstock in a linear fashion. The ammoniacal nitrogen makes up 32.6-81.4% of the total nitrogen in samples. The %TN increases across increasing temperature and holding time, though less linearly (r^2=0.647 and r^2=0.701, respectively) than the ammoniacal nitrogen concentrations. The %TN as NH_3-N decreases with %TS although the NH_3-N concentration is increasing.

Table 29: Aged Dried LT916 HPW ammoniacal nitrogen concentrations and %TN as NH_3-N present in the aqueous phase.

Condition	NH_3-N (mg/L)	%TN
AD2050A	2038	32.6%
AD2050B	2400	53.3%
AD2050C	2900	64.4%
AD2050D	3900	53.8%
AD2050E	3975	66.3%
AD2030D	2225	49.4%
AD2040D	3175	45.4%
AD2050D	3900	53.8%
AD2060D	4075	62.7%
AD1060B	1425	81.4%
AD1560B	2075	55.3%
AD2560B	2950	33.7%

4.3.2.2. Carbon recovery

The percentage of carbon recovered in the biocrude, shown in Table 30, increases with increasing temperature as carbon recovery in the solids decreases. The biocrude is 67.5-73.15% carbon (d.b.), accounting for about half of the feedstock carbon. The solids product is 27%-50.9% carbon (d.b.), approximately 10%-20% of the carbon balance. The gas product accounts for approximately 10% of the feedstock carbon and the HPW about one quarter.

Table 30: Aged Dried LT916 product carbon concentrations and recoveries.

	Biocrude		Solid		Gas	HPW
Condition	%C (d.b.)	%C recovered	%C (d.b.)	%C recovered	%C recovered	%C recovered
FD2050A	69.0±0.2	44.0%	50.7±0.8	20.9%	7.2%	27.9%
FD2050B	69.66±0.04	47.5%	50.8±0.4	18.0%	8.9%	25.6%
FD2050C	71.08±0.08	53.2%	47.1±0.3	13.5%	10.1%	23.2%
FD2050D	72.05±0.08	53.8%	41.4±0.3	11.6%	10.6%	24.0%
FD2050E	72.92±0.04	49.0%	27±2	8.6%	10.6%	31.9%
FD2030D	67.5±0.2	44.9%	47±2	12.5%	8.2%	34.4%
FD2040D	70.3±0.1	54.2%	33.7±0.2	8.5%	9.4%	27.8%
FD2050D	72.05±0.08	53.8%	41.4±0.3	11.6%	10.6%	24.0%
FD2060D	73.15±0.07	48.8%	48±2	17.2%	9.4%	24.6%
FD1060B	70.5±0.2	42.6%	49.3±0.2	22.4%	8.2%	26.8%
FD1560B	70.89±0.08	44.0%	50.5±0.1	15.5%	7.9%	32.6%
FD2560B	67.91±0.06	44.9%	50.9±0.3	17.7%	7.6%	29.8%

4.3.3. Best Yield Condition Characterization

In addition to the previously discussed tests, the products from the trial that produced the best yield (AD2050C) were tested further to determine fuel quality characteristics and chemical

makeup of the HPW. Further fuel quality tests included determining the sulfur content, and chemical species, by GC-MS. HPW was also analyzed by GC-MS. The results of these analyses are discussed in the following subsections

For the aged dried LT916, the best biocrude yield was produced at HTL conditions of 20% TS feedstock, 50 min holding time, 320°C reaction temperature. This is 20°C lower than the fresh dried condition with the best yield.

4.3.3.1. Sulfur content

As shown in Table 31, the sulfur content of the biocrude is 0.76%wt., ten times that of the fresh dried crude tested and no longer considered a "sweet" crude oil (Dutton, 2018b). It is at the low end of the range for petroleum crudes though, which can be as high as 5% (C. U. Jensen et al., 2016). The recovery of sulfur in the AD2050C biocrude is large, 37.2%. Overall recovery between biocrude and solids is small. Like the fresh dried results, most of the sulfur is distributed to the HPW.

Table 31: AD2050C solid product and biocrude sulfur concentrations and recoveries

Sample name	Sample type	%S (d.b.)	%S recovery
ADLT916	feedstock	0.73%	NA
AD2050Cs	best run solids	0.52%	9.8%
AD2050Co	best run biocrude	0.76%	37.2%

NA not applicable

4.3.3.2. GC-MS

The major peaks on the GC-MS spectra of AD2050c biocrude and HPW products, derivative (non-volatile) and volatile, were identified and classified into chemical groups as discussed in section 3.2.6. Table 32 shows the relative peak area as a percent of the total peak area for each group.

Table 32: Aged Dried LT916 product GC-MS results. Relative peak area for each chemical class as a percent of the total peak area of detected compounds.

Product	Sample	PHE	PO	NC	OC	CC	NX	OX	HC
HPW	volatile	0.2%		28.7%	0.5%	13.2%	7.2%	50.1%	
HPW	non-vol	4.3%	0.6%	56.0%	0.3%	6.7%	1.5%	30.7%	
crude	volatile			10.2%				50.2%	39.5%
crude	non-vol	4.5%	1.4%	7.5%		1.8%	5.9%	78.9%	

Like the fresh dried results, the largest peak areas for compounds detected in the crude are oxygenates, followed by hydrocarbons in the volatiles and phenols in the non-volatiles. One phosphorus containing compound, phosphoric acid is detected. Most compounds detected in the non-volatile compounds in the HPW are oxygenates, followed by nitrogen heterocycles. The reverse is true of the volatiles, nitrogen heterocycles are the largest class followed by oxygenates. The phosphorus compounds are monomethyl phosphate and phosphoric acid in the HPW.

4.3.4. Aged dried LT916 conclusion

Comparing the results from the fresh dried and aged dried products shows that the aging the feedstock would not significantly affect the yields of a hypothetical HTL processing plant. Over the prescribed temperature range, the aged biocrude has a higher HHV and lower O/C ratio. Unfortunately, it also has a lower H/C ratio and more %N than the fresh biocrude.

This study has shown that up to 37±2%daf biocrude yield can be produced from HTL of the aged dried LT916 feedstock at 320°C and 50 min retention time with 20%TS feedstock. The crude produced has an HHV of 33.7 MJ/kg, giving the process an ER of 68.8% and ECR of 0.610 with 0% HR and 0.305 with 50%HR. This biocrude has a sulfur content higher than average (0.76%wt.), a high nitrogen content (7.28%wt), and oxygen content (13.18%wt. by calc.). At 320°C, 29.2% of the nitrogen in the feedstock is recoverable in the HPW, 64.4% of it as ammoniacal nitrogen. Phosphorus is found in the HPW as monomethyl phosphate and phosphoric acid.

High sulfur content, nitrogen content, oxygen content, and probable acid nature of the biocrude indicate upgrading is needed for transportation grade fuel.

4.4. Aged vs. Fresh Comparison

4.4.1. Yields and energy returns

The product yields from the two feedstocks, fresh and aged LT916, were similar across the RT range, 280-350°C. As shown in Figure 22, the aged dried LT916 (ADLT916) biocrude yield peaks at a lower temperature (320°C) than the fresh dried feedstock (FDLT916) (340°C). At temperatures higher than 320°C, the fresh dried biocrude yield continues to climb, but the aged

biocrude yield begins to drop. Unlike the fresh feedstock, the aged feedstock biocrude yields at 350°C are significantly lower than the yield at 340°C. Both feedstocks demonstrated a decrease in solid product yield and increased gas yields as the temperature increased. Paired t-tests comparing product yields at 340°C and 350°C between the feedstocks only met the significance level for the solids products (p=0.018 and p=0.017, respectively). The implication is that the yield of an HTL plant operating at the optimum temperature for biocrude yield from the fresh feedstock would not see a large difference in biocrude yield if aged feedstock were also used.

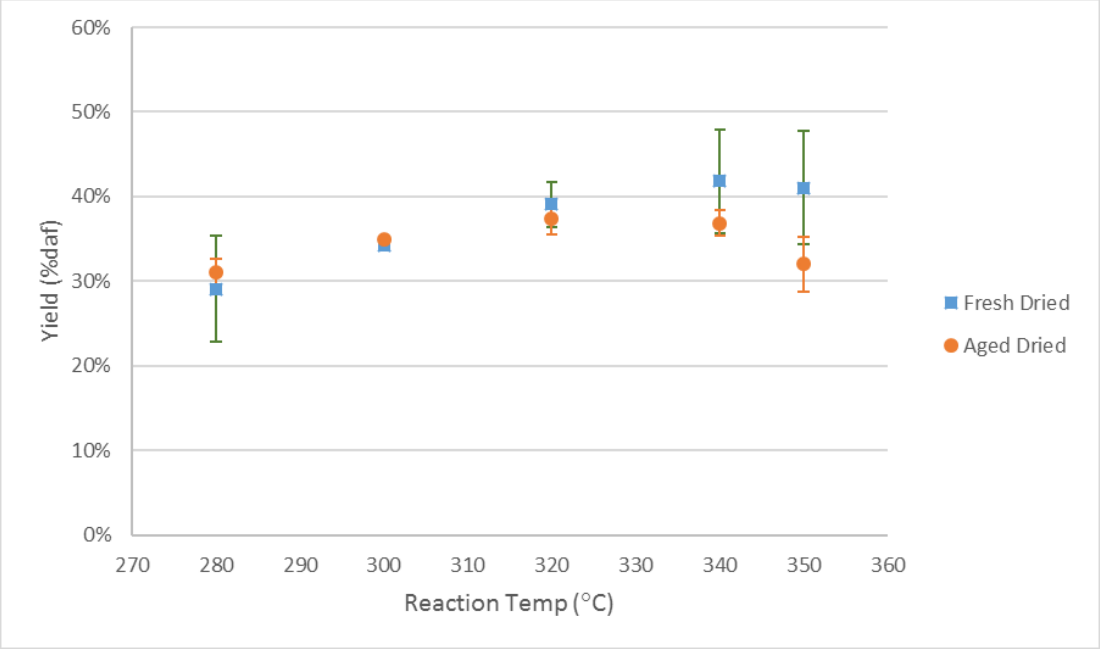

Figure 22: Fresh Dried and Aged Dried biocrude yields for RTs 280-350°C.

The yield response of the feedstocks to changing holding times are similar, as shown in Figure 23. The biocrude yield is trending upward slightly for HTs of 30-50 min, peaking at 50 min, and lower for an HT of 60 min. The solid product yield decreases with holding time for both feedstocks. The gas product yield increases with holding time for FDLT916 as shown in Figure 24. This is also true for ADLT916 for most of the range, though the gas yield peaks at 50 min and

drops at 60 min. The fresh dried biomass has consistently higher average biocrude yields than the aged dried feedstock. However, in paired t-tests of biocrude yields at each HT, only the 40 min HT showed a statistical difference in the biocrude yield (p=0.038).

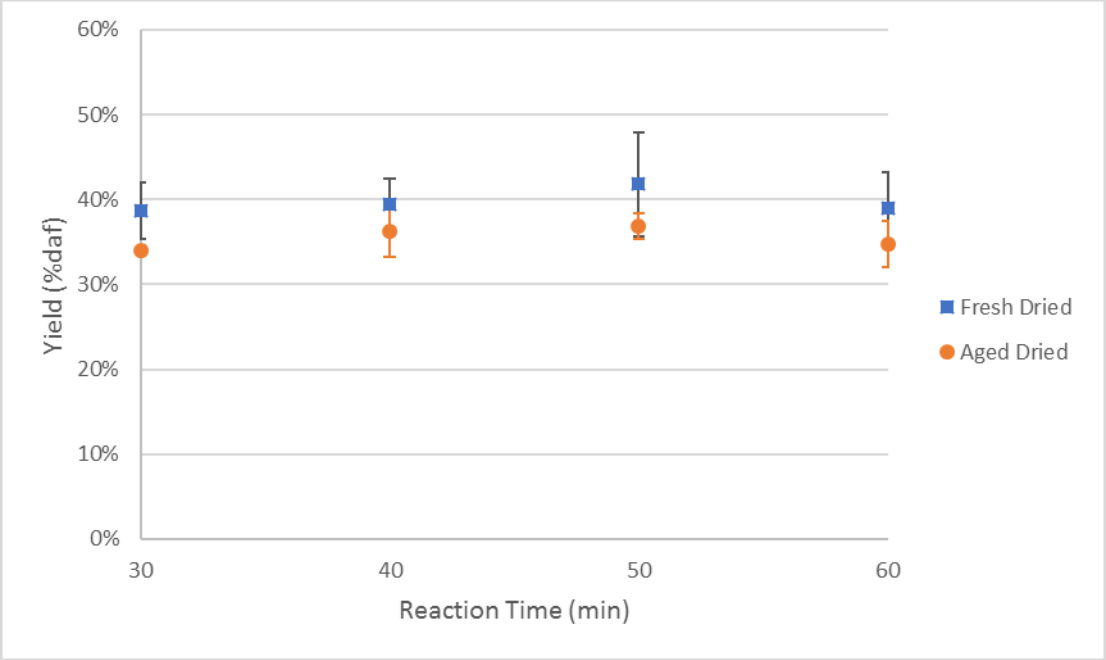

Figure 23: Fresh Dried and Aged Dried biocrude yields over the range of HTs, 30-60 min.

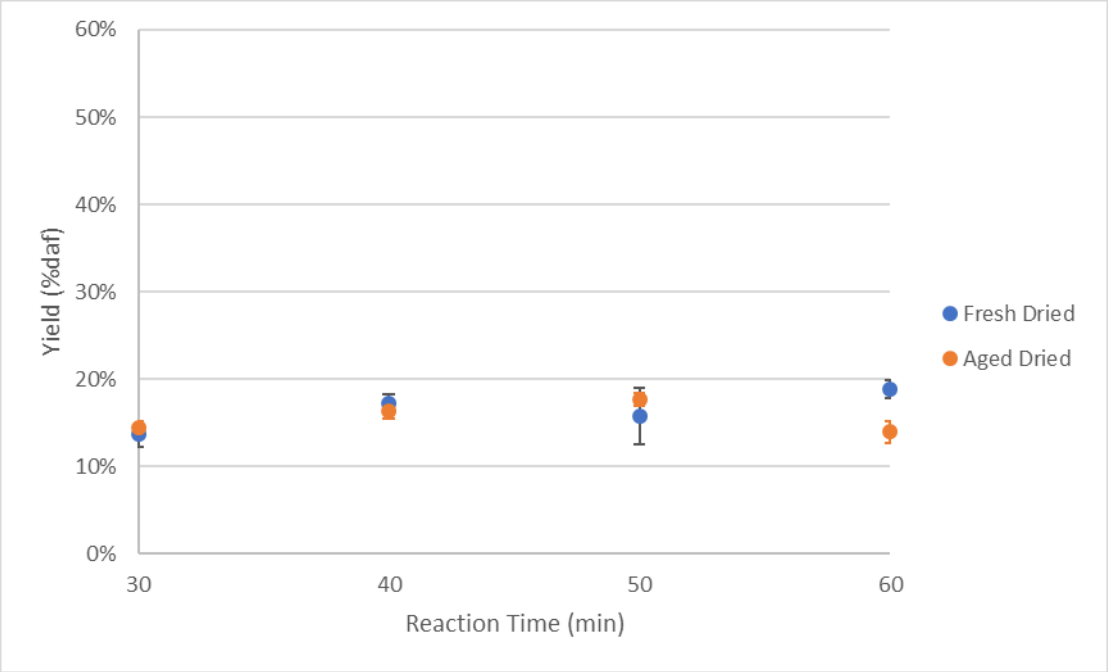

Figure 24: Gas product yield from FD and AD LT916 for different HTs.

For both feedstocks, the biocrude yield increases as the %TS is increased, as shown in Figure 25, next page. The increase in biocrude yield is not proportional to the increase in solid loading in the product. A paired t-test comparing biocrude average yields for the temperature ranges did not meet the significance level ($p=0.152$) which is to be expected for the RT of 300°C, based on the temperature range results. The biocrude yield of both ADLT916 and FDLT916 at 25% biomass in the feedstock was 33%-34%daf. As %TS is increased, the gas yield of the aged feedstock increases and the solid yield decreases. The reverse was true of the fresh feedstock, solid yields increased, and gas yields decreased as %TS was increased. This could be due to the decomposition of the aged feedstock. The decomposed feedstock may be more readily converted to bio-oil, leaving less solid residue. Furthermore, the biocrude may be more readily converted from bio-oil to gas. More detailed study would be needed to confirm and explain this.

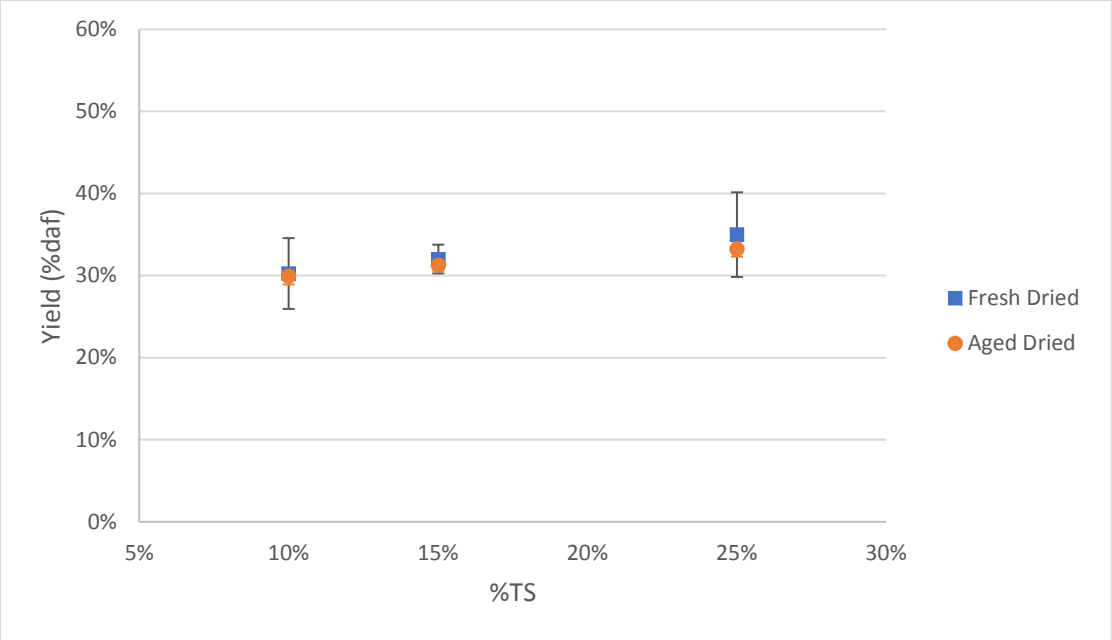

Figure 25: Fresh Dried and Aged Dried biocrude yields for different %TS feedstocks.

Overall, the aged dried LT916 feedstock yields are more consistent, with smaller standard deviations and smaller variances than the fresh dried feedstock, sometimes by orders of magnitude. The difference could be due to decomposed cell wall structures in the aged feedstock, enhancing the extractability of the inner compounds (López Barreiro et al., 2013).

The Van Krevelen plots of the biocrudes produced by the two feedstocks, shown in Figure 26, next page, show the ranges overlap. Both feedstocks have H/C ratios close to those reported for the Utah Tar Sands, but higher O/C and N/C ratios (Bunger et al., 1979). However, the H/C ratio of other petroleum crudes are much higher, in the range of 1.4-2.0 (He et al., 2016). As shown in Table 33, next page, both feedstocks produce crudes with higher H/C ratios at the lower end of the temperature range and the upper end of the %TS range. The H/C ratio of the aged feedstock biocrudes peaks (0.126) for the lowest holding time, 30 min, but the fresh feedstock was

highest at 50 min (0.125). The O/C ratio is high in crudes with high H/C ratios whereas the N/C ratio is lower in those crudes.

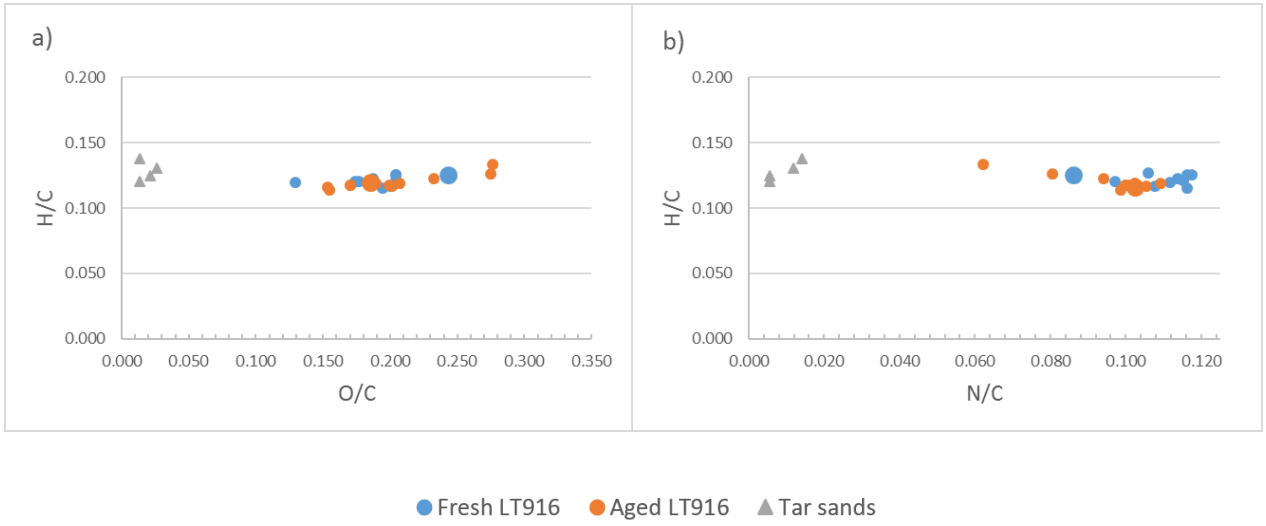

Figure 26: Van Krevelen plots of Fresh and Aged LT916 biocrudes produced at all conditions alongside crudes from the Utah Tar Sands, legend is for both charts.

Table 33: Fresh Dried and Aged Dried LT916 biocrudes H/C, O/C, and N/C values.

			Fresh Dried			Aged Dried		
RT (°C)	HT (min)	%TS	H/C	O/C	N/C	H/C	O/C	N/C
280	50	20%	0.127	0.244	0.106	0.122	0.232	0.094
300	50	20%	0.125	0.204	0.117	0.119	0.207	0.109
320	50	20%	0.125	0.204	0.116	0.119	0.185	0.102
340	50	20%	0.125	0.243	0.086	0.118	0.170	0.100
350	50	20%	0.119	0.129	0.112	0.116	0.153	0.102
340	30	20%	0.121	0.204	0.115	0.126	0.275	0.081
340	40	20%	0.123	0.187	0.114	0.117	0.201	0.105
340	50	20%	0.125	0.243	0.086	0.118	0.170	0.100
340	60	20%	0.120	0.177	0.097	0.114	0.154	0.099
300	60	10%	0.115	0.194	0.116	0.118	0.199	0.101
300	60	15%	0.117	0.200	0.108	0.119	0.189	0.102
300	60	25%	0.121	0.174	0.128	0.134	0.277	0.062

The CHN values for biocrude from HTL of fresh and aged feedstocks are similar. The hydrogen levels in ADLT916 biocrudes are slightly higher and the nitrogen levels slightly lower, presumably due to a larger carbohydrate and lower protein content in the aged feedstock. The range for HHV of the crudes is slightly lower for the aged samples, but the individual results are intertwined as shown in Figure 27. For some conditions, the ADLT916 biocrude has a higher HHV. For others, the FDLT916 biocrude tests higher. At 340°C, the RT for maximum biocrude yield using FDLT916, the aged biocrude has a higher HHV again showing it would not be detrimental to an HTL plant to use the aged feedstock. A detailed comparison of nitrogen values in the products from each feedstock is found in the next section (4.4.2).

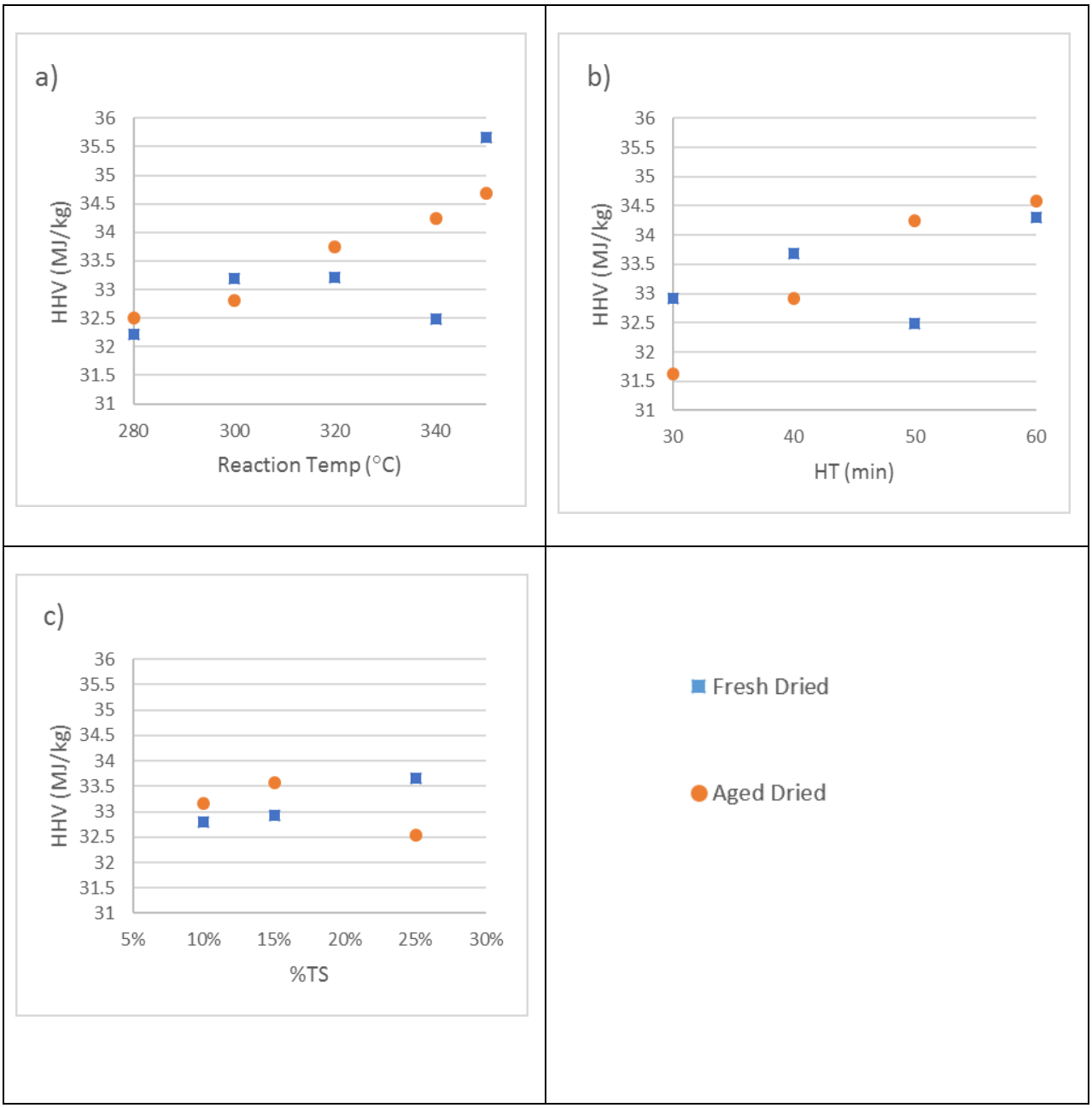

Figure 27: HHV of biocrudes produced from fresh dried (blue boxes) and aged dried (orange circles) LT916 as reaction conditions are varied: RT (a), HT (b), and %TS (c). Legend is for all charts.

The aged feedstock had slightly better ER at lower temperatures and the fresh feedstock had higher ER at temperatures of 320°C and above. The ECR of the biocrude from fresh feedstock was generally 0.02-0.05 lower than the aged biocrudes, indicating better energy return with fresh biomass. At 300°C, the %TS varied runs showed little difference between the two with 50% HR, as shown in Figure 28.

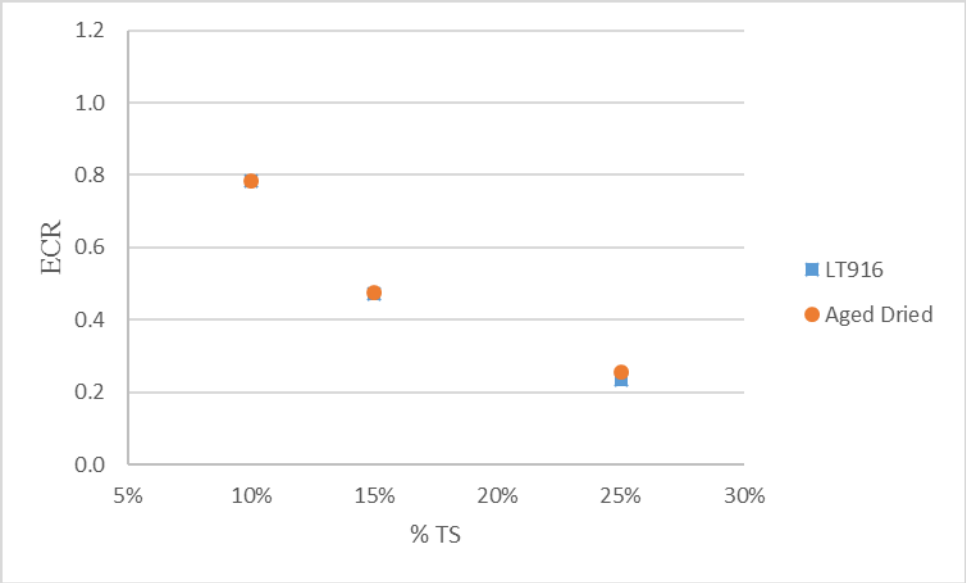

Figure 28: ECR of Fresh Dried and Aged Dried LT916 with 50% heat recovery.

4.4.2. Nutrient recovery

Figure 29 shows the concentrations of nitrogen in the biocrude and solids over a range of reaction temperatures, as determined by ICP. For both feedstocks, as the temperature increases, the concentration of nitrogen in the solids decreases and so does nitrogen recovery in the solids, as shown in Figure 30, next page. The biocrude from the aged dried feedstock is usually lower in nitrogen content than biocrude from the fresh dried feedstock at the same temperature. This is primarily because the aged feedstock starts with less nitrogen.

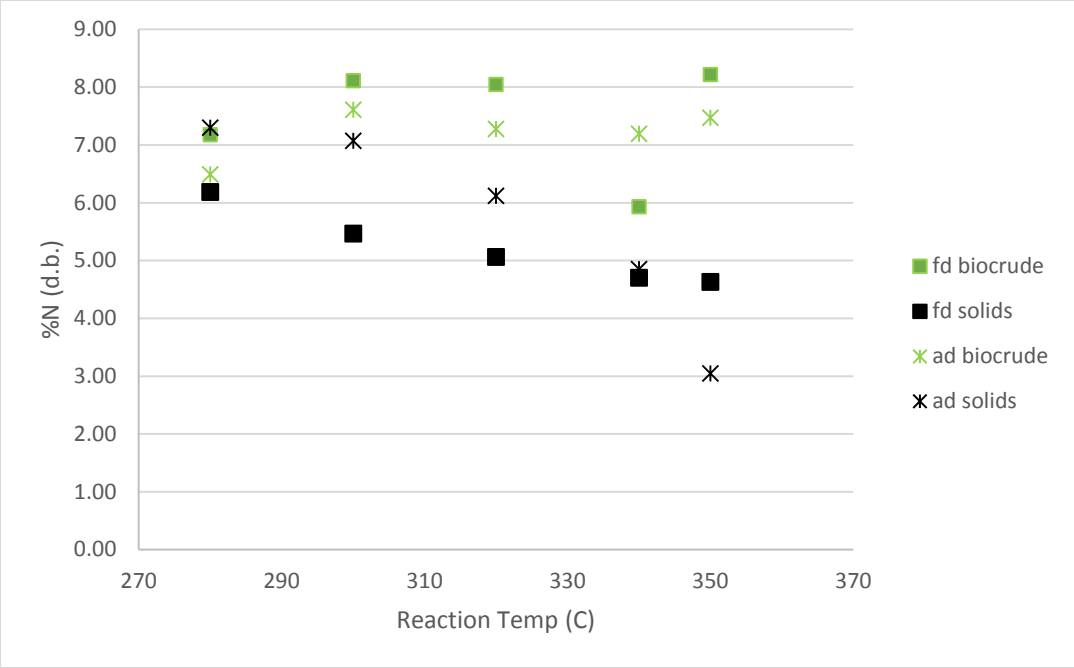

Figure 29: Percent mass of nitrogen (d.b.) in the Fresh Dried and Aged Dried LT916 biocrude and solid products.

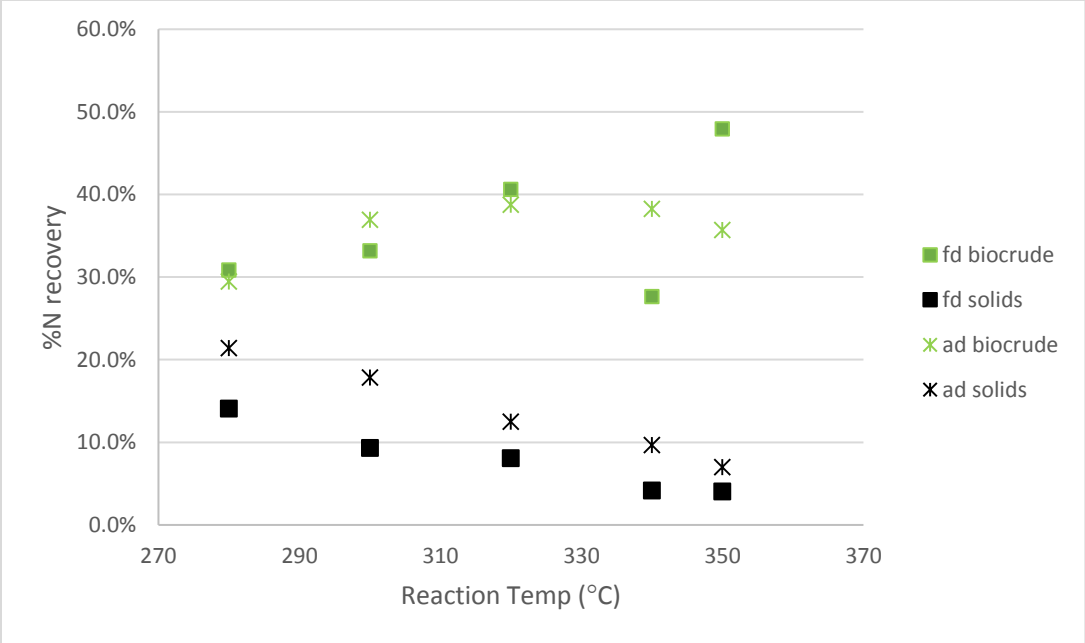

Figure 30: Nitrogen recovered in the biocrude and solid products from Fresh Dried and Aged Dried LT916

The total nitrogen and ammonium levels of the two feedstocks were distinctly different across the range of %TS tested. Both feedstocks saw increased nitrogen as ammoniacal nitrogen concentrations over the range. The fresh dried feedstock maintained the same ratio of NH3-N to TN in the HPW despite the solid loading changes. The aged dried feedstock has 80% of the TN in HPW as NH3-N for low %TS, but that drops steadily to 33.7% as biomass dry wt. is increased to 25% of the slurry (g/g).

At 350°C, the carbon recovery in the fresh dried biocrude is higher than in the aged dried biocrude, due to decreased biocrude yield from the aged feedstock at this condition. Solid and gas carbon recoveries are generally close for the two feedstocks and follow similar trends: reduced carbon in the solids, with increased reaction severity and lower %TS, and increased carbon in the gas product, under the same conditions.

Phosphoric acid is present in the HPW and the biocrude GC-MS analyses of products from both feedstocks, though the relative concentrations are not the same. The normalized peak areas show a higher concentration of phosphoric acid in the aged dried products. The fresh dried biocrude (FD2050D2o) has a peak area for phosphoric acid half the size of the aged dried sample (AD2050Co). In the HPW, AD2050Cw has a phosphoric acid peak area three times that of FD2050D2w. However, the monomethyl phosphate normalized peak is larger in the biocrude FD2050D2o (peak area=10.4) is almost twice that of AD2050Co (peak area=6.1).

The fresh dried crude (FD2050D2o) has a much lower sulfur content (0.07%) than the aged dried crude (AD2050Co) (0.76%). The sulfur content of the solid product produced from the aged feedstock (0.52%) is approximately the same as the fresh solids (0.54%).

4.4.3. GC-MS

The GC-MS results from each of the best yield conditions are similar, but not identical. As shown in Table 34, below, the major differences in peak area in the biocrude are the aged biocrude has more hydrocarbons and less oxygenates in the crude than the fresh biocrude. In the HPW, the aged sample has more oxygenates, more carbon heterocycle, and less nitrogen heterocycle compounds. The volatile crude analysis for the fresh dried feedstock shows the largest peak area (59.47%) was for Hexanedioic acid, bis(2-ethylhexyl) ester. The aged sample had a smaller peak for this compound (19.06%) but has other large peaks for Heptadecane (26.81%) and n-Hexadecanoic acid (24.85%).

Table 34: Aged Dried LT916 liquid products, differences in relative peak area compared to Fresh Dried LT916 liquid products (fresh-aged results).

Product	Sample	PHE	PO	NC	OC	CC	NX	OX	HC
HPW	volatile			8.9%	0.4%	-5.5%	4.8%	-8.7%	
HPW	non-vol	-0.6%	-0.4%	1.4%	-0.3%	-5.8%	-0.1%	5.7%	
crude	volatile			-10.2%		1.5%		28.6%	-19.9%
crude	non-vol	1.6%	1.0%	-2.4%		4.0%	-4.7%	0.4%	

4.4.4. FD vs. AD conclusion

The fresh dried biocrude has better energy returns than the aged dried LT916 biocrude, due in part to slightly better yield and to slightly better HHV. Yet, aging the feedstock would not have a crippling effect on the biocrude yields of a hypothetical HTL plant. At the optimal conditions for biocrude yield determined for the fresh dried feedstock, 340°C, 50min, 20%TS, the aged dried LT916 biocrude yield is not statistically significantly different. The length of aging time for the feedstock in this study is also longer than what might be expected for a seasonal crop, so the

effects observed here are more extreme. The aged feedstock may have an advantage in that it has less variation in the biocrude yields and can be processed at less severe conditions. The biocrudes produced from the aged feedstock have slightly lower nitrogen levels and comparable H/C ratios compared to the fresh dried LT916 biocrudes.

4.5. Wet vs dried

The following sections discuss the product distributions and energy returns for HTL of dried and wet (never dried) Lake Tainter algae, both fresh (LT917) and aged (LT916). The feedstocks were processed at 340°C for 50 min of holding time. The wet feedstocks were tested to determine the %TS and the dried feedstocks mixed to match. Solid loading and biomass ash content for each feedstock are shown in Table 35.

Table 35: Fresh (wet and dry) and aged (wet and dry) feedstock solid loading and ash content.

Feedstock	%TS (g/g)	Ash content (d.b.)
Fresh LT917	7.06±0.03	6.0±0.1
Aged LT916	5.8±0.1	7.25±0.02

4.5.1. Yields

Complete yield data for all products from the wet/dry study, as shown in Figure 31, the average biocrude yield from feedstocks that were never dried (wet) is slightly higher than the dried feedstock and the solid product yields are lower. The fresh LT917 wet and dry yields standard deviations do not overlap for biocrude or solids. The fresh, wet LT917 generates more biocrude and less solids than the fresh, dried LT917. However, paired t-tests show a significant difference in the biocrude yield between feedstocks, but not between wet and dry preparation as shown in Table 36.

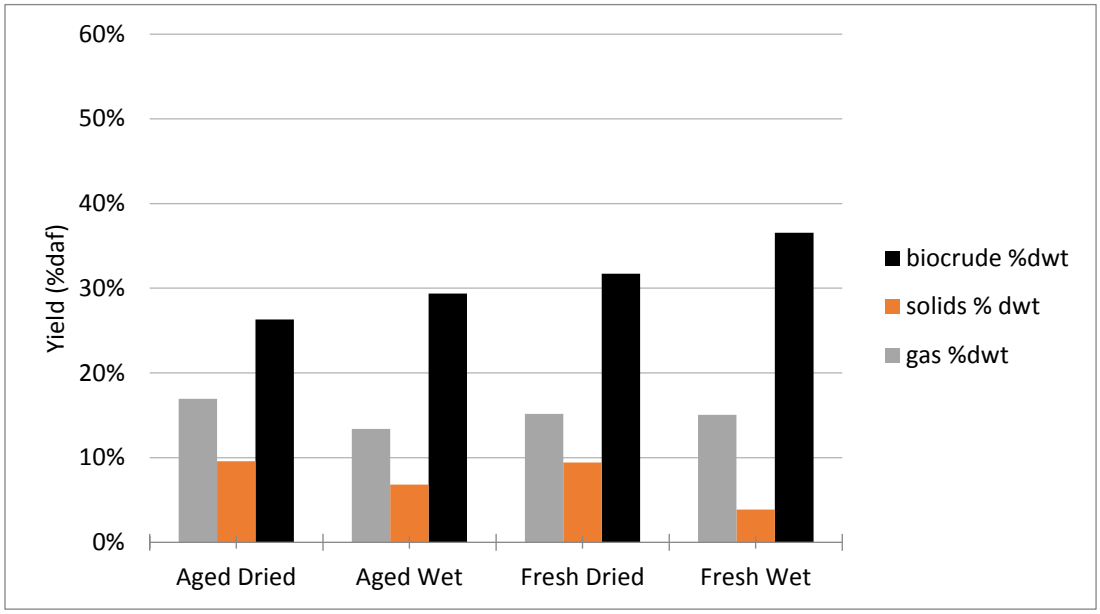

Figure 31: Product yields from wet vs. dry trials of Lake Tainter HAB.

Table 36: P-values for product yields of wet vs dry Lake Tainter HAB feedstocks.

p-value	Fresh Dried	Aged Dried	Aged Wet
Fresh Wet	0.115	NA	0.030
Fresh Dried	NA	0.002	NA
Aged Wet	NA	0.121	NA

NA not applicable

4.5.2. CHN and HHV

As shown in Table 37, the CHN values for biocrudes from both aged and fresh biomass, wet and dry preparations are similar. The HHV of biocrudes produced from any of these feedstocks are 32-34 MJ/kg, like those measured in the fresh and aged dried LT916 studies.

Table 37: Wet vs. dry biocrude product CHN results

Condition	C (%wt.)	H (%wt.)	N (%wt.)	HHV (MJ/kg)
fw 0750D	70.75±0.08	8.34±0.02	6.5±0.1	33.22
fd 0750D	69.41±NA	8.18±0.08	7.2±0.1	32.39
aw 0750D	71.54±0.06	7.76±0.02	6.61±0.06	32.72
ad 0750D	71.9±0.1	8.1±0.1	5.77±0.01	33.38

4.5.3. Nutrient recovery

Nitrogen and ammoniacal nitrogen levels in the HPW from wet and dried biomass were alike. As shown in Table 38, a larger difference was evident between the aged and fresh groupings than between wet and dry. The fresh dried HPW total nitrogen and ammoniacal nitrogen concentrations are higher than would be expected based on the %TS experiments. The value is between the concentrations found for 10%TS and 15%TS. Aged dried HPW total nitrogen concentrations are also higher than would be expected from the %TS findings for that feedstock, but the ammoniacal nitrogen concentrations are lower than the 10%TS findings, as would be expected.

Table 38: Wet vs. dry HPW nutrient concentrations

Condition	TN (mg/L)	NH_3-N (mg/L)
fw 0750D	5900±400	2140
fd 0750D	5600±300	2100
aw 0750D	3100±250	940
ad 0750D	2850±150	720

4.6. Impact on MFSP

The viability of the LT916 HAB as an HTL feedstock can be considered by comparing its performance to the base case used in the PNNL document distributed by the DOE, *Process Design and Economics for the Conversion of Algal Biomass to Hydrocarbons: Whole Algae Hydrothermal Liquefaction and Upgrading* (Jones et al., 2014). The model parameters used for a hypothetical plant in the document are shown in Table 39, next page, alongside the values determined for processing the fresh and dried Lake Tainter Bloom. For the purposes of this comparison, the variables that could be most influential in reducing the Minimum Fuel Selling Price (MFSP) are: the feedstock cost, cost of the dried algae substitute for mixed feed, fuel yield, and scale of plant. The sensitivities of these variables are shown in Figure 32, below. These sensitivities were used to determine a probable MFSP for the Lake Tainter HAB biocrudes

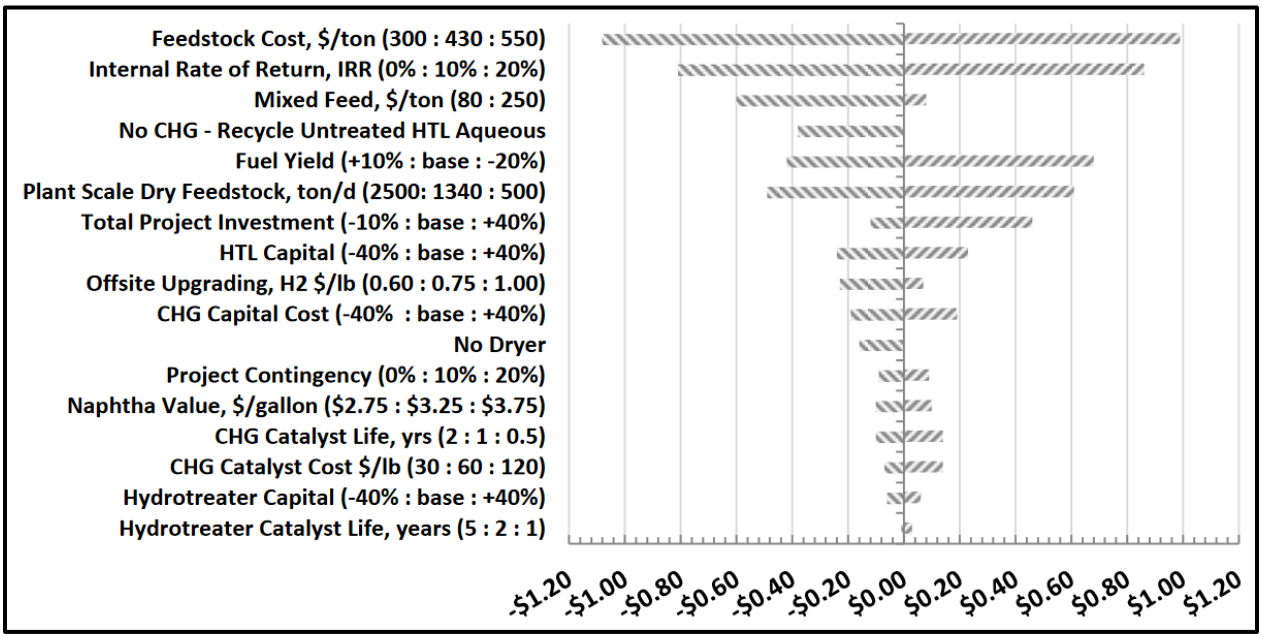

Figure 32: MFSP sensitivities in $/gallon of diesel Jones et al. (2014).

Table 39: Sensitivity analysis model parameters not affecting MFSP

Model Parameter	Jones et al.	FDLT916	ADLT916
RT (°C)	349	340	320
HT (min)	[a]	50	50
%TS (d.b.)	20	20	20
Biocrude Quality			
C (%daf)	77	69	71.00
H (%daf)	10.4	9	8
O (%daf)	8	17	16
N (%daf)	4.2	6	7
S (%daf)	0.3	0.07	0.5
P (%daf)	[b]	0	[c]
Ash (%d.b.)	0.14	[c]	[c]
Moisture (%wt.)	2.3		
Nutrient Recovery			
% N recovery (HPW)	63%	47%	51%
%P recovery (solids)	90%	89%	[a]

[a] Not applicable to steady state simulation
[b] Phosphorus partioning is not directly modeled in Aspen because of the small quantity, most of which reports to the solid phase.
[c] not measured

The Jones et al. analysis uses a hypothetical HTL plant, cultivating and processing whole algae, upgrading the biocrude, and treating the HPW on-site. The plant processes a 20%TS feedstock is raised on 10,000 acres of ponds and prepared for $430/ton. This amounts to a total of 884 million lbs. of algae per year (daf) (4550 million lbs./year total flow). The plant operates for 330 days a year (7920 operating hours), using 1340 tons of algae a day (daf). Year-round processing is accomplished in the model either by storing the algal feedstock, or by substituting forestry wastes as the winter feedstock, a scenario called mixed feed. Stored algae would be prepared by drying 30% of the dewatered algae to a 10% moisture level. The mixed feed scenario assumes a savings for the plant due to the less expensive woody biomass and for not using the

algae dryer, but increased costs for equipment for handling wood compared to the base case. The biocrude produced is treated onsite to less than 1%daf oxygen and less than 0.05%daf nitrogen. The HPW produced is treated with CHG. The economic assumptions are a 10% internal rate of return (IRR), financed with 60% debt at 8.0%apr.

Adjustments in MFSP for Lake Tainter HAB biocrudes were calculated for three different scenarios, as shown later in Table 40. In the first, the fresh dried feedstock is used to model yields in the growing season and like the Jones et al. basecase dried for winter processing (FDLT916). In the second, the fresh feedstock is used when available and the aged for winter processing. The biocrude yield for this scenario is an average of the fresh dried and aged dried results (FD/AD). In the third, the aged dried feedstock is used to model yields in the growing season and assumed to be dried for winter processing (ADLT916). Although this would not make sense in practice, it is shown here as a comparative estimate of the value of the processing the aged dried feedstock.

The estimated cost of feedstock for the Lake Tainter HAB includes the cost of harvesting and dewatering but not the cost of feeding or tending the algae. As mentioned, the feedstock cost for the Jones et al. analysis is $430/ton, $90 of which is attributed to dewatering. The cost of raising algae, the remaining $340/ton, is based on the findings in the 2013 DOE *Biomass Multi-Year Program Plan*, where the harvesting costs are stated to be 19% of the overall feedstock price (DOE, 2013). The feedstock cost of the Lake Tainter HAB used to estimate the MFSP is $155/ton in all three scenarios. In the second scenario (FD/AD), there is not a need for a dryer to prepare the algae for the winter like that used the mixed feed scenario in the Jones et al. (2014) paper. The aged feedstock would need some storage facilities and there would be capital costs associated with their construction. This trade off was assumed to be comparable to equipment costs related to the mixed feed scenario.

The feedstock availability governs the size of the plant. The harvesting possibilities for Lake Tainter were calculated in two ways and the more conservative estimate used the MFSP calculations, by the size of the lake compared to the model algae farm and by observations made at Lake Tainter. In the Jones et al. model the algae rearing footprint is 10,000 acres and the algae farm generates 1340 tons per day. Lake Tainter covers 1751.68 acres. A proportional estimate of feedstock based on these sizes would suggest a possible harvest of 235 tons per day from the lake. A similar value was estimated in the second, observation-based method. When collecting algae, the bulk filtered slurry was 3.28%TS, after concentrating the flocculated bloom 25-30 times. Using a 10:1 ratio for high: low density blooms (WHO, 2003), this suggests the low density HAB is 0.011%-0.013%TS (0.12 kg algae/m^3), an estimate in agreement with other bloom monitoring data (LaLiberte & Kampa, 1999; WHO, 2003). With an average flow rate of 42.28m^3/s (5.07 kg algae/s), if the lake was top-drained to maximize the algae collection, a biomass yield of 484 tons/day could be expected. However, the wild bloom can only be expected to be in full bloom for 5 months of the year (Kreitlow, 2001). If the entire 5-month yield is spread over a 9-month growing cycle as in the Jones et al. model, the adjusted daily yield is 269 tons/day. The scale of the plant and its effect on MFSP was estimated using the more conservative value, 235 tons/day.

As shown in Table 40, next page, using the plant to process the Lake Tainter algae bloom instead of cultivated strains would have some cost benefits and some liabilities. The biocrude yield from LT916 is lower than the yield for the Jones et al. base case. Additionally, the available feedstock only warrants the building of a small plant and economy of scale is diminished. These adjustments increase the price of the fuel produced. However, the impact of not feeding or raising the feedstock is so large, it overwhelms these handicaps. Using the inexpensive, wild-harvested HAB could reduce the price of diesel produced at the hypothetical plant by $0.71-1.37/gallon of

diesel. The combination of these influences reduces the MFSP to $3.40-4.06/gallon of diesel ($3.20-3.83/gge), depending on the age of the feedstock. The HTL plant using the stored, aged HAB has the lowest MFSP, nearest the BETO target of $3.00/gge. A further $0.16/gge could be saved by elimination of the dryer and substituting another low cost feed in the winter (Jones et al., 2014). This is a significant improvement on process economics for a whole algae HTL processing plant.

Table 40: Adjustments to MFSP of diesel based on LT916 parameters and Jones et al. sensitivities.

	Jones et al.			FDLT916		FD/ AD		ADLT916	
Model Parameter	Case	P.I ($)	Per Unit	Case	P.I ($)	Case	P.I ($)	Case	P.I ($)
feedstock cost ($/ton)	430	+3.51	cost ratio	155	-2.24	155	-2.24	155	-2.24
cost of mixed feed ($/ton)	NA	-0.60	$350/ton saved	NA		155	-0.58	NA	
size of plant (ton/day d.b.)	1340	+0.60	500 ton less /day	235	0.79	235	0.79	235	0.79
biocrude yield (%daf)	59	+0.68	20% less yield	42	0.58	39.5	0.67	37	0.75
Sum of Price Adj. ($)					-0.88		-1.37		-0.71
Adjusted MFSP ($)	4.77				3.89		3.40		4.06
Adjusted MFSP ($/gge)	4.49				3.67		3.20		3.83

P.I.= Price Impact ($/ gallon of diesel)

CHAPTER 5: CONCLUSIONS

5.1. LT916 HTL Products

The cyanobacterial bloom from Lake Tainter, WI is a promising HTL feedstock for biocrude production. The operating conditions for maximum biocrude yield from the fresh feedstock are RT of 340°C and an HT of 50 min. HTL of the fresh Lake Tainter produces a sweet crude, with a H/C ratio like the Utah Tar Sands. The biocrude yield from HTL of the fresh dried LT916 feedstock at this condition is 42±6%daf. The oxygen content and nitrogen content of the crude are higher than typical petroleum crudes and would require further upgrading, hydrotreating, to be integrated into the petroleum fuel infrastructure. The aged HAB produced similar biocrude yields to the fresh HAB at lower temperatures, achieving maximum biocrude yield at a lower RT than fresh LT916, at 320°C and at the same HT of 50 min, with 37±2%daf.

In the biocrude from fresh LT916, produced at the maximum yield condition (FD2050D), the medium weight crude fraction is the largest at 52%, indicating the fuel may be good for kerosene or diesel supply line supplementation. The gasoline fraction, the light portion, is only 8%wt. The biocrude produced has an HHV of 32.5 MJ/kg, giving the process an ER of 73.9% and ECR of 0.605 with 0%HR and 0.302 with 50%HR. This biocrude has a low sulfur content (0.07%wt.), but a high nitrogen content (5.93%wt) and oxygen content (16.74%wt. by calc.), nearly 10x what a petroleum crude would contain. The solid yield for FD2050D is 8±1%daf and contains 7% of the carbon and 4% of the nitrogen in the feedstock. In the HPW, 47% of the nitrogen in the feedstock is recoverable, 55.8% of it as bioavailable, ammoniacal nitrogen.

As reaction temperatures and holding times are increased up to the optimal conditions for biocrude yield, it improves the process. The HHV, the carbon recovered in the crude, and the yield

increased with increasing RT. Longer holding times reduce the nitrogen in the crude and slightly increase the biocrude yield. Unfortunately, the nitrogen content of the biocrude also increases with increased RT, except for the optimal condition. At 50 min HT, the biocrude had the lowest nitrogen concentration, 5.9±0.2% (d.b.). However, the nitrogen is increasingly distributed from the biocrude to the HPW over time and is also more likely to be in the ammonium form.

The aged feedstock retains value as a fuel feedstock. The average yield and HHV of the biocrudes from aged LT916 are slightly reduced at higher temperatures, compared to the fresh results, but not in a statistically significant way. The nitrogen content is lower in the aged feedstock's biocrudes, but so is the amount of hydrocarbon compounds and the proportion of oxygenates is higher. Since the biocrude needs further treatment for either feedstock, this is not a hinderance to using the aged feedstock.

A 18-29% decrease in MFSP is possible using the wild-harvested cyanobacterial bloom. Factors that increase the MFSP of fuel produced from Lake Tainter algae, compared to the base case in Jones et al. (2014), are the lower biocrude yield of this feedstock and the small scale of a plant that would be needed to process the bloom. Still, the low feedstock cost of the wild-harvested feedstock is a such a strong influence on the MFSP of whole algae HTL, it appears to be a more cost-competitive option for fuel production. Using the Lake Tainter algae in the winter or some other low-cost feedstock, an MFSP of $3.20/gge could be possible, more than a dollar lower than the Jones et al. (2014) base case and further cost savings are possible using alternate low-cost winter feedstocks.

5.2. Future Work

The Jones et al. document notes that the biocrude can be hydrotreated and cracked to reduce the sulfur, oxygen, and nitrogen content of the fuel, but suggests pretreatment could offer cost savings. Lower nitrogen content in the Lake Tainter biocrude is probably possible using a method developed by Jazrawi et al. (2015). In it, the feedstock is processed twice. The first time, it is processed at a low temperature, where nitrogen is released into the HPW. The HPW from the first stage is removed and the feedstock for the second stage is the remaining products from the first stage in fresh water. With this method, Jazrawi et al. achieved 55% less nitrogen in the biocrude. Coupled with longer HTs, multi-stage processing can result in higher yields, as high as 55% for low-lipid algae (Jones et al., 2014; Li et al., 2014). However, the lower temperature processing step may not be severe enough to destroy MCs in the HAB. Future work in this direction should determine if the HPW effluent from the first stage requires further processing to treat it for cyanotoxins and if this is an effective way to reduce nitrogen in the biocrude and increase yield.

Higher yields from this feedstock may be possible. With faster heating rates and shorter residence times, yields of up to 58% were reported for some strains (Jones et al., 2014; López Barreiro et al., 2013). The possibility for increased product yields under these superheated conditions should be investigated for the Lake Tainter HAB. No catalysts were used in this study, but they should be investigated.

Future work on this feedstock should include further characterization of the biocrude product fractions. This is best accomplished by running the feedstock at larger scale, so the sample size is not restrictive for distillation. Each of the distilled fractions can be characterized

with GC-MS and FTIR to reveal their unique character. This would provide further insight on the best uses for the biocrude from this feedstock and upgrading possibilities.

On a related note, large scale collection and dewatering of the HAB has yet to be investigated for this project. It should be ascertained whether the harvesting can be done in a profitable way, economically and energetically. Potential regulatory hurdles with environmental protection groups should also be identified.

The toxicity of HPW is a persistent problem and of great concern to the author of this work. An effective method of treating the HPW is crucial since HPW is produced in large quantities. Using the nutrients in the HPW would improve process economics through the sale of another by product and complete the nutrient cycle from the lake back to the land. As discussed in the introduction, currently the treatment for this product is gasification (Jones et al., 2014). Additionally, some biological treatment methods have been demonstrated, using it to grow food (Mazur, 2016), algae (Zhang et al., 2016; Zhou et al., 2013), and microbes, in anaerobic digesters (Posmanik et al., 2017). However, there is some inhibitory effect of HPW on growth, unless it is diluted 20:1 or more. Mycoremediation used in the bioremediation of diesel contaminated soils and oil spills, could prove to be a more effective treatment (Salami & Elum, 2010). Supporting this hypothesis is the observation of white mold on surfaces of improperly stored HTL equipment, full of full-strength HPW, in our lab. Ligninolytic fungi have specialized enzymes that allow them to consume lignocellulosic intermediates like those found in the HPW (Jang et al., 2009). The ability of microbes to degrade hydrocarbons can be ranked in the following order: linear alkanes > branched alkanes > small aromatics > cyclic alkanes. Complex aromatics like polycyclic aromatic hydrocarbons (PAHs) may not be removed or degraded at all whereas fungi are capable of degrading and digesting them (Das & Chandran, 2011). Mycoremediation of the HPW may

enhance the recycling of nutrients into agricultural use by decontamination and sequestration, providing another valuable biproduct from the processing of the HAB.

REFERENCES

AAFCO. (2017). Critical Factors in Determining Fiber in Feeds and Forages. In *AAFCO's Laboratory Methods and Services Committee* (p. 14). AAFCO. Retrieved from https://www.aafco.org/Portals/0/SiteContent/Laboratory/Fiber_Best_Practices_Working_Group/Fiber-Critical-Conditions-Final.pdf

Alba, L. G., Torri, C., Samori, C., Spek, J. J. van der, Fabbri, D., Kersten, S. R. A., & Brilman, D. W. F. (2012). Hydrothermal Treatment (HTT) of Microalgae: Evaluation of the Process As Conversion Method in an Algae Biorefinery Concept. *Energy & Fuels*, *26*(1), 642–657. https://doi.org/10.1021/ef201415s

Barlow, J., Sims, R. C., & Quinn, J. C. (2016). Techno-economic and life-cycle assessment of an attached growth algal biorefinery. *Bioresource Technology*, *220*, 360–368. https://doi.org/10.1016/j.biortech.2016.08.091

Biller, P., & Ross, A. B. (2011). Potential yields and properties of oil from the hydrothermal liquefaction of microalgae with different biochemical content. *Bioresource Technology*, *102*(1), 215–225. https://doi.org/10.1016/j.biortech.2010.06.028

Biller, P., Ross, A. B., Skill, S. C., Lea-Langton, A., Balasundaram, B., Hall, C., … Llewellyn, C. A. (2012). Nutrient recycling of aqueous phase for microalgae cultivation from the hydrothermal liquefaction process. *Algal Research*, *1*(1), 70–76. https://doi.org/10.1016/j.algal.2012.02.002

Brennan, L., & Owende, P. (2010). Biofuels from microalgae—A review of technologies for production, processing, and extractions of biofuels and co-products. *Renewable and Sustainable Energy Reviews*, *14*(2), 557–577. https://doi.org/10.1016/j.rser.2009.10.009

Brown, T. M., Duan, P., & Savage, P. E. (2010). Hydrothermal Liquefaction and Gasification of Nannochloropsis sp. *Energy & Fuels*, *24*(6), 3639–3646. https://doi.org/10.1021/ef100203u

Bunger, J. W., Thomas, K. P., & Dorrence, S. M. (1979). Compound Types and Properties of Utah and Athabasca Tar Sand Bitumens. *Fuel*, *58*(3), 183–195. https://doi.org/10.1016/0016-2361(79)90116-9

Cao, Q., Steinman, A. D., Yao, L., & Xie, L. (2017). Increment of root membrane permeability caused by microcystins result in more elements uptake in rice (Oryza sativa). *Ecotoxicology and Environmental Safety*, *145*, 431–435. https://doi.org/10.1016/j.ecoenv.2017.07.066

Changi, S. M., Faeth, J. L., Mo, N., & Savage, P. E. (2015). Hydrothermal Reactions of Biomolecules Relevant for Microalgae Liquefaction. *Industrial & Engineering Chemistry Research*, *54*(47), 11733–11758. https://doi.org/10.1021/acs.iecr.5b02771

Chen, W.-T. (2013). *Hydrothermal liquefaction of wastewater algae mixtures into bio-crude oil* (Master's). University of Illinois Urbana-Champaign. Retrieved from http://hdl.handle.net/2142/45591

Chen, W.-T., Zhang, Y., Zhang, J., Yu, G., Schideman, L. C., Zhang, P., & Minarick, M. (2014). Hydrothermal liquefaction of mixed-culture algal biomass from wastewater treatment system into bio-crude oil. *Bioresource Technology*, *152*, 130–139. https://doi.org/10.1016/j.biortech.2013.10.111

Chorus, I., & Bartram, J. (Eds.). (1999). *Toxic cyanobacteria in water: a guide to their public health consequences, monitoring, and management*. London ; New York: E & FN Spon.

Corbel, S., Mougin, C., & Bouaïcha, N. (2014). Cyanobacterial toxins: Modes of actions, fate in aquatic and soil ecosystems, phytotoxicity and bioaccumulation in agricultural crops. *Chemosphere*, *96*, 1–15. https://doi.org/10.1016/j.chemosphere.2013.07.056

Dãrãban, I. M., Rosendahl, L. A., Pedersen, T. H., & Iversen, S. B. (2015). Pretreatment methods to obtain pumpable high solid loading wood–water slurries for continuous hydrothermal liquefaction systems. *Biomass and Bioenergy*, *81*, 437–443. https://doi.org/10.1016/j.biombioe.2015.07.004

Das, N., & Chandran, P. (2011). Microbial Degradation of Petroleum Hydrocarbon Contaminants: An Overview [Research article]. https://doi.org/10.4061/2011/941810

Dodds, W. K., & Whiles, M. R. (2010). Chapter 17 - Nutrient Use and Remineralization. In W. K. Dodds & M. R. Whiles (Eds.), *Freshwater Ecology (Second Edition)* (pp. 437–467). London: Academic Press. https://doi.org/10.1016/B978-0-12-374724-2.00017-9

DOE. (2013). Biomass Multi-year Program Plan -May 2013. Bioenergy Technologies Office. Retrieved from https://www1.eere.energy.gov/bioenergy/pdfs/mypp_may_2013.pdf

Dote, Y., Sawayama, S., Inoue, S., Minowa, T., & Yokoyama, S. (1994). Recovery of liquid fuel from hydrocarbon-rich microalgae by thermochemical liquefaction. *Fuel*, *73*(12), 1855–1857. https://doi.org/10.1016/0016-2361(94)90211-9

Dutton, J. (2018a). Distillation and Boiling Points | FSC 432: Petroleum Refining. Retrieved August 6, 2018, from https://www.e-education.psu.edu/fsc432/content/distillation-and-boiling-points

Dutton, J. (2018b). Sulfur and Nitrogen Content | FSC 432: Petroleum Refining. Retrieved August 4, 2018, from https://www.e-education.psu.edu/fsc432/content/sulfur-and-nitrogen-content

Eboibi, B. E., Lewis, D. M., Ashman, P. J., & Chinnasamy, S. (2014). Effect of operating conditions on yield and quality of biocrude during hydrothermal liquefaction of halophytic microalga Tetraselmis sp. *Bioresource Technology*, *170*, 20–29. https://doi.org/10.1016/j.biortech.2014.07.083

EIA. (2016). Use of Oil - Energy Explained, Your Guide To Understanding Energy - Energy Information Administration. Retrieved July 27, 2018, from https://www.eia.gov/energyexplained/index.php?page=oil_use

Elliott, D. C., Biller, P., Ross, A. B., Schmidt, A. J., & Jones, S. B. (2015). Hydrothermal liquefaction of biomass: Developments from batch to continuous process. *Bioresource Technology*, *178*, 147–156. https://doi.org/10.1016/j.biortech.2014.09.132

Elliott, D. C., Hart, T. R., Schmidt, A. J., Neuenschwander, G. G., Rotness, L. J., Olarte, M. V., … Holladay, J. E. (2013). Process development for hydrothermal liquefaction of algae feedstocks in a continuous-flow reactor. *Algal Research*, *2*(4), 445–454. https://doi.org/10.1016/j.algal.2013.08.005

EPA. (2014). Cyanobacteria and Cyanotoxins: Information for Drinking Water Systems. Office of Water. Retrieved from https://www.epa.gov/sites/production/files/2014-08/documents/cyanobacteria_factsheet.pdf

Fagerbakke, K., Heldal, M., & Norland, S. (1996). Content of carbon, nitrogen, oxygen, sulfur and phosphorus in native aquatic and cultured bacteria. *Aquatic Microbial Ecology*, *10*, 15–27. https://doi.org/10.3354/ame010015

Gągała, I., & Mankiewicz-Boczek, J. (2012). The Natural Degradation of Microcystins (Cyanobacterial Hepatotoxins) in Fresh Water - the Future of Modern Treatment Systems and Water Quality Improvement. *Pol J Environ Stud*, *21*, 1125–1139.

Gaumnitz, L. (2010, August). Less P is Key. *Wisconsin Natural Resources Magazine*. Retrieved from https://dnr.wi.gov/wnrmag/2010/08/phos.htm

Geider, R., & La Roche, J. (2002). Redfield revisited: variability of C:N:P in marine microalgae and its biochemical basis. *European Journal of Phycology*, *37*(1), 1–17. https://doi.org/10.1017/S0967026201003456

Guo, Y., Song, W., Lu, J., Ma, Q., Xu, D., & Wang, S. (2015). Hydrothermal liquefaction of Cyanophyta: Evaluation of potential bio-crude oil production and component analysis. *Algal Research*, *11*, 242–247. https://doi.org/10.1016/j.algal.2015.06.025

Hampel, K. (2013). *The Characterization of Algae Grown on Nutrient Removal Systems and Evaluation of Potential Uses for the Resulting Biomass*. Western Michigan University.

Hannon, M., Gimpel, J., Tran, M., Rasala, B., & Mayfield, S. (2010). Biofuels from algae: challenges and potential. *Biofuels*, *1*(5), 763–784.

He, Y., Liang, X., Jazrawi, C., Montoya, A., Yuen, A., Cole, A. J., … Haynes, B. S. (2016). Continuous hydrothermal liquefaction of macroalgae in the presence of organic co-solvents. *Algal Research*, *17*, 185–195. https://doi.org/10.1016/j.algal.2016.05.010

Hoffmann, J., Jensen, C. U., & Rosendahl, L. A. (2016). Co-processing potential of HTL bio-crude at petroleum refineries – Part 1: Fractional distillation and characterization. *Fuel*, *165*, 526–535. https://doi.org/10.1016/j.fuel.2015.10.094

Jang, K.-Y., Cho, S.-M., Seok, S.-J., Kong, W.-S., Kim, G.-H., & Sung, J.-M. (2009). Screening of Biodegradable Function of Indigenous Ligno-degrading Mushroom Using Dyes. *Mycobiology*, *37*(1), 53. https://doi.org/10.4489/MYCO.2009.37.1.053

Jazrawi, C., Biller, P., He, Y., Montoya, A., Ross, A. B., Maschmeyer, T., & Haynes, B. S. (2015). Two-stage hydrothermal liquefaction of a high-protein microalga. *Algal Research*, *8*, 15–22. https://doi.org/10.1016/j.algal.2014.12.010

Jena, U., Das, K. C., & Kastner, J. R. (2011). Effect of operating conditions of thermochemical liquefaction on biocrude production from Spirulina platensis. *Bioresource Technology*, *102*(10), 6221–6229. https://doi.org/10.1016/j.biortech.2011.02.057

Jensen, C. U., Hoffmann, J., & Rosendahl, L. A. (2016). Co-processing potential of HTL bio-crude at petroleum refineries. Part 2: A parametric hydrotreating study. *Fuel*, *165*, 536–543. https://doi.org/10.1016/j.fuel.2015.08.047

Jones, S. B., Zhu, Y., Anderson, D. B., Hallen, R. T., Elliott, D. C., Schmidt, A. J., … Kinchin, C. (2014). *Process Design and Economics for the Conversion of Algal Biomass to Hydrocarbons: Whole Algae Hydrothermal Liquefaction and Upgrading* (No. PNNL--23227, 1126336). https://doi.org/10.2172/1126336

Kreitlow, J. (2001). *What's This Green Goop in My Water? (Algae/Blue-green Algae)*. Retrieved from https://www.uwsp.edu/cnr-ap/UWEXLakes/Documents/programs/convention/2012/JimKreitlow-What%27sThisGreenGoopInMyWater.pdf

LaLiberte, P., & Kampa, E. (1999). Phosphorus Content of Water and Suspended Sediment in the Red Cedar Basin. Wisconsin DNR, West Central Region. Retrieved from https://fyi.uwex.edu/redcedar/files/2017/08/P-content-of-water-and-sediment-1999.pdf

Landais, P. (1997). Petroleum Geochemistry and Geology, Second Edition Edited by John M. Hunt, W. H. Freeman, et al. 1996. ISBN 0-7167-2441-3. 743 pp. *Energy & Fuels*, *11*(6), 1314–1314. https://doi.org/10.1021/ef960184w

Leow, S., Witter, J. R., Vardon, D. R., Sharma, B. K., Guest, J. S., & Strathmann, T. J. (2015). Prediction of microalgae hydrothermal liquefaction products from feedstock biochemical composition. *Green Chemistry*, *17*(6), 3584–3599. https://doi.org/10.1039/C5GC00574D

Li, H., Liu, Z., Zhang, Y., Li, B., Lu, H., Duan, N., … Si, B. (2014). Conversion efficiency and oil quality of low-lipid high-protein and high-lipid low-protein microalgae via hydrothermal liquefaction. *Bioresource Technology*, *154*, 322–329. https://doi.org/10.1016/j.biortech.2013.12.074

Lone, Y., Koiri, R. K., & Bhide, M. (2015). An overview of the toxic effect of potential human carcinogen Microcystin-LR on testis. *Toxicology Reports*, *2*, 289–296. https://doi.org/10.1016/j.toxrep.2015.01.008

Lópa-Rodas, V., & Costa, E. (1997). Characterization of Morphospecies and Strains of Microcystis (cyanobacteria) from Natural Populations and Laboratory Clones Using Cell Probes (lectins and Antibodies)1. *Journal of Phycology*, *33*(3), 446–454. https://doi.org/10.1111/j.0022-3646.1997.00446.x

López Barreiro, D., Zamalloa, C., Boon, N., Vyverman, W., Ronsse, F., Brilman, W., & Prins, W. (2013). Influence of strain-specific parameters on hydrothermal liquefaction of microalgae. *Bioresource Technology*, *146*, 463–471. https://doi.org/10.1016/j.biortech.2013.07.123

Lyon, B. (2004). Dangerous when wet? DNR discovers toxins, issues advisory about blue-green algae risks. Retrieved August 16, 2018, from https://chippewa.com/dunnconnect/news/local/dangerous-when-wet-dnr-discovers-toxins-issues-advisory-about-blue/article_aa93e6a0-b124-54a7-a6ac-e11085d44184.html

Lyon, B. (2018, August 27). County gets first report of blue-green algae illness | Local | chippewa.com. Retrieved September 12, 2018, from

https://chippewa.com/dunnconnect/news/local/county-gets-first-report-of-blue-green-algae-illness/article_34781610-3865-5680-86a8-9dcdbd8809cb.html

Machado, J., Campos, A., Vasconcelos, V., & Freitas, M. (2017). Effects of microcystin-LR and cylindrospermopsin on plant-soil systems: A review of their relevance for agricultural plant quality and public health. *Environmental Research*, *153*, 191–204. https://doi.org/10.1016/j.envres.2016.09.015

Mazur, Z. (2016). *THE CO-CULTIVATION OF RICE AND ALGAE TO IMPROVE PROCESS ECONOMICS FOR ALGAL BIOFUEL PRODUCTION*. Retrieved from http://hdl.handle.net/2142/95401

Midwest Laboratories. (2017). *Detailed Method Descriptions* (Personal Communication).

Minowa, T., Kondo, T., & Sudirjo, S. T. (1998). Thermochemical liquefaction of indonesian biomass residues. *Biomass and Bioenergy*, *14*(5–6), 517–524. https://doi.org/10.1016/S0961-9534(98)00006-3

Minowa, T., Yokoyama, S., Kishimoto, M., & Okakura, T. (1995). Oil production from algal cells of Dunaliella tertiolecta by direct thermochemical liquefaction. *Fuel*, *74*(12), 1735–1738. https://doi.org/10.1016/0016-2361(95)80001-X

Nikiforuk, A. (2011, October 26). Two More Ethical Challenges to Canada's Oil Sands. http://thetyee.ca/Opinion/2011/10/26/Oil-Sands-Challenges/

Patel, B., Tamburic, B., Zemichael, F. W., Dechatiwongse, P., & Hellgardt, K. (2012). Algal Biofuels: A Credible Prospective? [Research article]. https://doi.org/10.5402/2012/631574

Posmanik, R., Labatut, R. A., Kim, A. H., Usack, J. G., Tester, J. W., & Angenent, L. T. (2017). Coupling hydrothermal liquefaction and anaerobic digestion for energy valorization from

model biomass feedstocks. *Bioresource Technology*, *233*, 134–143. https://doi.org/10.1016/j.biortech.2017.02.095

Raikova, S., Smith-Baedorf, H., Bransgrove, R., Barlow, O., Santomauro, F., Wagner, J. L., … Chuck, C. J. (2016). Assessing hydrothermal liquefaction for the production of bio-oil and enhanced metal recovery from microalgae cultivated on acid mine drainage. *Fuel Processing Technology*, *142*, 219–227. https://doi.org/10.1016/j.fuproc.2015.10.017

Ramirez, J., Brown, R., & Rainey, T. (2015). A Review of Hydrothermal Liquefaction Bio-Crude Properties and Prospects for Upgrading to Transportation Fuels. *Energies*, *8*(7), 6765–6794. https://doi.org/10.3390/en8076765

Ross, A. B., Biller, P., Kubacki, M. L., Li, H., Lea-Langton, A., & Jones, J. M. (2010). Hydrothermal processing of microalgae using alkali and organic acids. *Fuel*, *89*(9), 2234–2243. https://doi.org/10.1016/j.fuel.2010.01.025

Salami, A., & Elum, E. A. (2010). Bioremediation of a Crude Oil Polluted Soil with Pleurotus Pulmonarius and Glomus Mosseae Using Amaranthus Hybridus as a Test Plant. *Journal of Bioremediation & Biodegradation*, *01*(03). https://doi.org/10.4172/2155-6199.1000113

Shakya, R., Adhikari, S., Mahadevan, R., Shanmugam, S. R., Nam, H., Hassan, E. B., & Dempster, T. A. (2017). Influence of biochemical composition during hydrothermal liquefaction of algae on product yields and fuel properties. *Bioresource Technology*, *243*, 1112–1120. https://doi.org/10.1016/j.biortech.2017.07.046

Shakya, R., Whelen, J., Adhikari, S., Mahadevan, R., & Neupane, S. (2015). Effect of temperature and Na2CO3 catalyst on hydrothermal liquefaction of algae. *Algal Research*, *12*, 80–90. https://doi.org/10.1016/j.algal.2015.08.006

Shanmugam, S., Adhikari, S., & Shakya, R. (2017). Nutrient Removal and Energy Production from Aqueous Phase of Bio-Oil Generated via Hydrothermal Liquefaction of Algae. *Bioresource Technology*, *230*. https://doi.org/10.1016/j.biortech.2017.01.031

Sharma, N. K., Tiwari, S. P., Tripathi, K., & Rai, A. K. (2011). Sustainability and cyanobacteria (blue-green algae): facts and challenges. *Journal of Applied Phycology*, *23*(6), 1059–1081. https://doi.org/10.1007/s10811-010-9626-3

Sigma Aldrich. (n.d.-a). 3-Hydroxypyridine H57009. Retrieved November 1, 2018, from https://www.sigmaaldrich.com/catalog/product/aldrich/h57009

Sigma Aldrich. (n.d.-b). Acetic acid 695092. Retrieved November 1, 2018, from https://www.sigmaaldrich.com/catalog/product/sigald/695092

Sigma Aldrich. (n.d.-c). Bis(2-ethylhexyl) adipate 525197. Retrieved November 2, 2018, from https://www.sigmaaldrich.com/catalog/product/aldrich/525197

Sigma Aldrich. (n.d.-d). Butyric acid | Sigma-Aldrich. Retrieved November 1, 2018, from https://www.sigmaaldrich.com/catalog/substance/butyricacid881110792611?lang=en&region=US

Sigma Aldrich. (n.d.-e). L-Pyroglutamic acid | Sigma-Aldrich. Retrieved November 1, 2018, from https://www.sigmaaldrich.com/catalog/substance/lpyroglutamicacid129119879311?lang=en&region=US

Sigma Aldrich. (n.d.-f). Palmitic acid 800508. Retrieved November 2, 2018, from https://www.sigmaaldrich.com/catalog/product/mm/800508

Sigma Aldrich. (n.d.-g). Tropicamide Related Compound D 1699049. Retrieved November 1, 2018, from https://www.sigmaaldrich.com/catalog/product/usp/1699049

Singh, U. B., & Ahluwalia, A. (2013). Microalgae: A promising tool for carbon sequestration. *Mitigation and Adaptation Strategies for Global Change*, *18*. https://doi.org/10.1007/s11027-012-9393-3

Slade, R., & Bauen, A. (2013). Micro-algae cultivation for biofuels: Cost, energy balance, environmental impacts and future prospects. *Biomass and Bioenergy*, *53*, 29–38. https://doi.org/10.1016/j.biombioe.2012.12.019

Teri, G., Luo, L., & Savage, P. E. (2014). Hydrothermal Treatment of Protein, Polysaccharide, and Lipids Alone and in Mixtures. *Energy & Fuels*, *28*(12), 7501–7509. https://doi.org/10.1021/ef501760d

Tezuka, Y. (1989). The C:N:P ratio of Microcystis and Anabaena (blue-green algae) and its importance for nutrient regeneration by aerobic decomposition. *Japanese Journal of Limnology (Rikusuigaku Zasshi)*, *50*(2), 149–155. https://doi.org/10.3739/rikusui.50.149

Tian, C., Liu, Z., Zhang, Y., Li, B., Cao, W., Lu, H., … Zhang, T. (2015). Hydrothermal liquefaction of harvested high-ash low-lipid algal biomass from Dianchi Lake: Effects of operational parameters and relations of products. *Bioresource Technology*, *184*, 336–343. https://doi.org/10.1016/j.biortech.2014.10.093

TMLIA. (2016). EPA Approved: Red Cedar Implementation Plan. Retrieved from http://taintermenomin.mylaketown.com/TMDLImplementationPlan

TMLIA, WI DNR, & UW extension. (2013). Restoring Water Quality in Red Cedar River Basin: A Community's Guide. Retrieved from http://taintermenomin.mylaketown.com/Community-Guide

US EPA, O. (2018, February 22). A Plain English Guide to the EPA Part 503 Biosolids Rule [Reports and Assessments]. Retrieved July 18, 2018, from https://www.epa.gov/biosolids/plain-english-guide-epa-part-503-biosolids-rule

Valdez, P. J., Nelson, M. C., Wang, H. Y., Lin, X. N., & Savage, P. E. (2012). Hydrothermal liquefaction of Nannochloropsis sp.: Systematic study of process variables and analysis of the product fractions. *Biomass and Bioenergy*, *46*, 317–331. https://doi.org/10.1016/j.biombioe.2012.08.009

Valdez, P. J., Tocco, V. J., & Savage, P. E. (2014). A general kinetic model for the hydrothermal liquefaction of microalgae. *Bioresource Technology*, *163*, 123–127. https://doi.org/10.1016/j.biortech.2014.04.013

Vardon, D. R. (2012). *Hydrothermal Liquefaction for Energy Recovery from High-moisture Waste Biomass*. University of Illinois Urbana-Champaign. Retrieved from http://hdl.handle.net/2142/34327

Vardon, D. R., Sharma, B. K., Blazina, G. V., Rajagopalan, K., & Strathmann, T. J. (2012). Thermochemical conversion of raw and defatted algal biomass via hydrothermal liquefaction and slow pyrolysis. *Bioresource Technology*, *109*, 178–187. https://doi.org/10.1016/j.biortech.2012.01.008

Vardon, D. R., Sharma, B. K., Scott, J., Yu, G., Wang, Z., Schideman, L., … Strathmann, T. J. (2011). Chemical properties of biocrude oil from the hydrothermal liquefaction of Spirulina algae, swine manure, and digested anaerobic sludge. *Bioresource Technology*, *102*(17), 8295–8303. https://doi.org/10.1016/j.biortech.2011.06.041

Vargas-Moreno, J. M., Callejón-Ferre, A. J., Pérez-Alonso, J., & Velázquez-Martí, B. (2012). A review of the mathematical models for predicting the heating value of biomass materials.

Renewable and Sustainable Energy Reviews, *16*(5), 3065–3083. https://doi.org/10.1016/j.rser.2012.02.054

Veasey, M. (2015, April 1). Utah: Home of the Next Oil Sands Breakthrough? Retrieved September 2, 2018, from https://www.rigzone.com/news/oil_gas/a/149498/utah_home_of_the_next_oil_sands_breakthrough/

Wauquier, J.-P. (1995). *Petroleum Refining V1: Crude Oil, Petroleum Products, Process Flowsheets* (Vol. 1). Retrieved from http://archive.org/details/WauquierJeanPierre1995PetroleumRefiningV1CrudeOilPetroleumProductsProcessFlowsheets

WHO. (2003). Cyanobacterial toxins: Microcystin-LR in drinking-water. Background document for preparation of WHO Guidelines for drinking-water quality. Retrieved from http://www.who.int/water_sanitation_health/dwq/chemicals/cyanobactoxins.pdf?ua=1

WI DNR. (2018). *Trophic State Index Graph: Tainter Lake - Middle Basin - Site 2, Dunn County*. Retrieved from https://dnr.wi.gov/lakes/clmn/reports/tsigraph.aspx?stationid=173215

WQOW. (2016). Toxic Blue-Green Algae blooming in Wisconsin lakes. Retrieved August 16, 2018, from http://www.wqow.com/story/32421325/2016/07/Monday/toxic-blue-green-algae-blooming-in-wisconsin-lakes

Wu, H., Wei, G., Tan, X., Li, L., & Li, M. (2017). Species-dependent variation in sensitivity of *Microcystis* species to copper sulfate: implication in algal toxicity of copper and controls of blooms. *Scientific Reports*, *7*, 40393. https://doi.org/10.1038/srep40393

Yang, Y. F., Feng, C. P., Inamori, Y., & Maekawa, T. (2004). Analysis of energy conversion characteristics in liquefaction of algae. *Resources, Conservation and Recycling*, *43*(1), 21–33. https://doi.org/10.1016/j.resconrec.2004.03.003

Yin, S., Dolan, R., Harris, M., & Tan, Z. (2010). Subcritical hydrothermal liquefaction of cattle manure to bio-oil: Effects of conversion parameters on bio-oil yield and characterization of bio-oil. *Bioresource Technology*, *101*(10), 3657–3664. https://doi.org/10.1016/j.biortech.2009.12.058

Yu, G., Zhang, Y., Schideman, L., Funk, T., & Wang, Z. (2011). Distributions of carbon and nitrogen in the products from hydrothermal liquefaction of low-lipid microalgae. *Energy & Environmental Science*, *4*(11), 4587. https://doi.org/10.1039/c1ee01541a

Yuan, X., Shi, X., Zhang, D., Qiu, Y., Guo, R., & Wang, L. (2011). Biogas production and microcystin biodegradation in anaerobic digestion of blue algae. *Energy & Environmental Science*, *4*(4), 1511. https://doi.org/10.1039/c0ee00452a

Zhang, L., Lu, H., Zhang, Y., Li, B., Liu, Z., Duan, N., & Liu, M. (2016). Nutrient recovery and biomass production by cultivating Chlorella vulgaris from four types of post-hydrothermal liquefaction wastewater. *Journal of Applied Phycology*, *28*(2), 1031–1039. https://doi.org/10.1007/s10811-015-0640-3

Zhou, Y., Schideman, L., Yu, G., & Zhang, Y. (2013). A synergistic combination of algal wastewater treatment and hydrothermal biofuel production maximized by nutrient and carbon recycling. *Energy & Environmental Science*, *6*(12), 3765. https://doi.org/10.1039/c3ee24241b